**SYNTHESIS AND CHARACTERIZATION OF WATER DISPERSIBLE
CONJUGATED POLYMER NANOPARTICLES**

A THESIS

SUBMITTED TO THE DEPARTMENT OF CHEMISTRY AND THE

GRADUATE SCHOOL OF ENGINEERING AND SCIENCES

OF BILKENT UNIVERSITY

IN PARTIAL FULFILLMENT OF THE REQUIREMENTS

FOR THE DEGREE OF MASTER OF SCIENCE

By
VUSALA IBRAHIMOVA
DECEMBER 2011

I certify that I have read this thesis and in my opinion it is fully adequate, in scope and in quality, as a thesis of the degree of Master of Science

_____

Assoc. Prof. Dr Dönüş TUNCEL

I certify that I have read this thesis and in my opinion it is fully adequate, in scope and in quality, as a thesis of the degree of Master of Science

_____

Prof. Dr Engin Umut AKKAYA

I certify that I have read this thesis and in my opinion it is fully adequate, in scope and in quality, as a thesis of the degree of Master of Science

_____

Prof. Dr. Ahmet M. ÖNAL

I certify that I have read this thesis and in my opinion it is fully adequate, in scope and in quality, as a thesis of the degree of Master of Science

_____

Prof. Dr. Tuncer ÇAYKARA

I certify that I have read this thesis and in my opinion it is fully adequate, in scope and in quality, as a thesis of the degree of Master of Science

_____

Assoc. Prof. İhsan GÜRSEL

Approved for the Graduate School of Engineering and Sciences

_____

Prof. Dr Levent ONURAL

Director of Graduate School of Engineering and Sciences

ABSTRACT

SYNTHESIS AND CHARACTERIZATION OF WATER DISPERSIBLE
CONJUGATED POLYMER NANOPARTICLES

VUSALA IBRAHIMOVA

M. S. in Chemistry

Supervisor: Assoc. Prof. Dr. Dönüş Tuncel

December 2011

In this study, novel water dispersible conjugated polymer nanoparticles having various potential applications in the areas including biomedicine and photonics have been synthesized from blue, green and yellow light emitting conjugated polymers. Their sizes, morphology, surface charges and optical properties have been determined using various techniques. Cell viability of nanoparticles was tested in mesenchymal stem cells.

For the synthesis of nanoparticles, first the following polymers carrying a number of different functional groups and based on derivatives of fluorene and benzothiodiazole monomers are designed and synthesized using the Suzuki coupling reactions: Poly[(9,9-bis{propeny}fluorenyl-2,7-diyl)-co-(9,9-dihexyl-9H-fluorene)] (**P1**), poly[(9,9-bis{carboxymethylsulfonyl-propyl}fluorenyl-2,7-diyl)-co-(9,9-dihexyl-9H-fluorene) (**P2**), poly[(9,9- bis{propeny}fluorenyl-2,7-diyl))-co-(1,4-benzo-{2,1,3}-thiodiazole)] (**P3**), poly[(9,9- bis{carboxymethylsulfonyl-propyl}fluorenyl-2,7-diyl)-co(1,4-benzo-{2,1,3}-thiodiazole)]  (**P4**), poly[(9,9-bis{3-bromopropyl}fluorenyl-2,7-diyl)-co-(1,4-benzo-{2,1,3}-thiodiazole)] (**P5**), poly[(9,9-bis{3-azidopropyl}fluorenyl-2,7-diyl)-co-(benzothiadiazole)] (**P6**).

Polymers were characterized by using spectroscopic techniques such as ^{1}H-NMR, FT-IR, UV-Vis, Fluorescence spectrophotometer and Gel Permeation Chromatography (GPC).

Conjugated polymers carry functional groups on their side chains, such as azide and allyl groups that can be cross-linkable using UV light to form shape-persistent, stable nanoparticles. Nanoparticles were characterized by various techniques before and after UV-treatment. Their sizes and morphologies were determined by using dynamic light scattering measurements (DLS) and imaging techniques such as scanning electron microscopy (SEM) and atomic force microscopy (AFM). For optical characterization UV-vis, fluorescent spectroscopies and FT-IR were used.

CNPs affect on cells shows their nontoxic and biocompatible properties which give opportunity to use them in cell imaging.

**Keywords:** Conjugated Polymers, water dispersible nanoparticles, cross-linking, cell imaging.

ÖZET

SUDA DAĞILABİLİR IŞIYAN POLİMER NANOPARÇACIKLARININ SENTEZİ
VE KARAKTERİZASYONU


VUSALA IBRAHIMOVA

Kimya Bölümü Yüksek Lisans Tezi

Tez Yöneticisi: Doç. Dr. Dönüş Tuncel

Aralık 2011

Bu çalışmada, mavi, yeşil ve sarı ışıyan konjüge polimerlerden biyomedikal ve
fotonik alanında çeşitli potansiyel uygulamaları olan suda dağılabilir konjuge polimer
nanopartiküller sentezlendi. Bunların boyutları, morfolojisi, yüzey yükü ve optik
özellikleri çeşitli teknikler kullanılarak belirlenmiştir. Nanopartiküllerin hücre
canlılığı mezenkimal kök hücrelerinde test edilmiştir.


Nanoparçacıkların sentezi için ilk olarak çeşitli fonksiyonel grupları taşıyan aşağıdaki
fluorene ve benzothiodiazole monomerlerin türevleri olan polimerler tasarlanmış ve
Suzuki bağlantı reaksiyonları ile sentezlenmiştir:  Poli [(9,9-bis {propenil} florenil-2
,7-diyl)-co-(9,9-diheksil-9H-floren)] (P1), poli [(9,9-bis {karboksimetilsülfonil-
propil} fluorenil-2,7-dil)-ko-(9 ,9-diheksil-9H-floren) (P2), poli [(9,9 - bis {propenil}
 florenil-2 ,7-dil))-co-(1,4-benzo-{2,1,3} -tiyodiazol] (P3), poli [(9,9- bis
{karboksimetilsülfonil-propil} florenil-2 ,7-dil)-ko (1,4-benzo-{2,1,3}-tiyodiazol] (
P4), poli [(9,9-bis {3} bromopropil florenil-2 ,7-dil)-ko-(1,4-benzo-{2,1,3}-
tiyodiazol)] (P5), poli [(9,9-bis {3} azidopropil florenil-2 ,7-dil)-ko-(benzotiyazol)]
(P6). Polimerler ^{1}H-NMR, FT-IR, UV-Vis ve Floresans Spektrofotometre ve Jel
Geçirgenlik Kromatografisi (GPC) gibi teknikler kullanılarak karakterize edilmiştir.


Yan zincirlerinde azit ve alil gibi fonksiyonel grupları olan konjuge polimerler UV

ışığı kullanarak çapraz bağlanıp şekilleri kalıcı, istikrarlı nanopartiküller oluştururlar. Nanopartiküller UV ışını altında bekletilmeden önce ve sonra çeşitli teknikler kullanılarak karakterize edilmiştir. Bunların boyutları ve morfolojileri dinamik ışık saçılımı ölçümleri (DLS) ve taramalı elektron mikroskobu (SEM) ve atomik kuvvet mikroskobu (AFM) gibi görüntüleme yöntemleri kullanılarak belirlenmiştir. Optik karakterizasyon için UV-vis, flüoresan spektroskopileri ve FT-IR kullanılmıştır.

Konjuge polimer nanopartiküllerinin  toksik olmayan ve biyo-uyumlu özellikleri onların hücre görüntülemede kullanılmasına fırsat verir.


**Anahtar Kelimeler:** Konjuge Polimerler,  suda dağılabilir nanopartiküller, çapraz bağlanma

# ACKNOWLEDGEMENT

I would like to express my appreciation to my advisor Assoc. Prof. Dönüş Tuncel for her supervision and encouragement throughout the research.

I am thankful to Prof. Dr Engin Umut Akkaya, Prof. Dr. Ahmet M. Önal, Prof. Dr. Tuncer Çaykara and Assoc. Prof. İhsan Gürsel for reading my thesis.

I wish to thanks Assist. Prof. Akçalı Kamil Can and his student Ece Akhan from Molecular Biology and Genetics department of Bilkent University for their help in study with MSCs.

I would like to express sincere thanks to my group mates Dr. Eun Ju Park, Şeyma Ekiz, Müge Artar, Özlem Gezici, Özlem Ünal, Meltem Aygüler, Eda Koçak and Senem Avaz and other people who support and encourage me throughout my research.

Lastly, I am grateful to my parents and sisters for their supports.

I am dedicating my thesis to my grandfather Memmedov Esed who was devoted his life to teaching chemistry.

TABLE OF CONTENT

# LIST OF FIGURES

## LIST OF SCHEMES

**LIST OF TABLES**

## ABBREVATIONS

FT-IR                       Fourier Transform-Infrared

$^1$H-NMR                    Proton-Nuclear Magnetic Resonance

UV-Vis                       Ultraviolet- visible spectroscopy

PL                          Fluorescence spectroscopy

GPC                         Gel Permission Chromatography

DLS                         Dynamic Light Scattering

SEM                         Scanning Electron Microscopy

TEM                         Transmission Electron Microscopy

AFM                         Atomic Force Microscopy

CDCl3                       Deuterated chloroform

DMSO                        Dimethyl sulfoxide

TBAB                        Tetra-n-butylammoniumbromid

P1                          Poly[(9,9-bis{propeny}fluorenyl-2,7-diyl)-co-(9,9-dihexyl-
                            9H-fluorene)]

P2                          Poly[(9,9-bis{carboxymethylsulfonyl-propyl}fluorenyl-2,7
                            -diyl)-co-(9,9-dihexyl-9H-fluorene)

P3                          Poly[(9,9- bis{propeny}fluorenyl-2,7-diyl))-co-(1,4-benzo
                            -{2,1,3}-thiodiazole)]

P4                          Poly[(9,9- bis{carboxymethylsulfonyl-propyl}fluorenyl-2,7
                            -diyl)-co(1,4-benzo-{2,1,3}-thiodiazole)]

P5                          Poly[(9,9-bis{3-bromopropyl}fluorenyl-2,7-diyl)-co-(1,4-
                            benzo-{2,1,3}-thiodiazole)]

| | |
|---|---|
| P6 | Poly[(9,9-bis{3-azidopropyl}fluorenyl-2,7-diyl)-co-(benzothiadiazole)] |
| CNPs | Conjugated Polymer Nanoparticles |
| P1NPs | Poly[(9,9-bis{propeny}fluorenyl-2,7-diyl)-co-(9,9-dihexyl-9H-fluorene)] nanoparticles |
| P3NPs | Poly[(9,9- bis{propeny}fluorenyl-2,7-diyl))-co-(1,4-benzo-{2,1,3}-thiodiazole)] nanoparticles |
| P4NPs | Poly[(9,9- bis{carboxymethylsulfonyl-propyl}fluorenyl-2,7-diyl)-co(1,4-benzo-{2,1,3}-thiodiazole)]  nanoparticles |
| P5NPs | Poly[(9,9-bis{3-bromopropyl}fluorenyl-2,7-diyl)-co-(1,4-benzo-{2,1,3}-thiodiazole)] nanoparticles |
| P6NPs | Poly[(9,9-bis{3-azidopropyl}fluorenyl-2,7-diyl)-co-(benzothiadiazole)] nanoparticles |
| MTT | (3-(4,5-dimethyl-2-thiazolyl)-2,5-diphenyl-2H-tetrazolium bromide) |
| ELISA | enzyme-linked immunosorbent assay |
| MSCs | Mesenchymal Stem Cells |
| DMEM | Dulbecco's Modified Eagle Medium |
| FCS | Fetal Calf Serum |

**CHAPTER 1**

**INTRODUCTION**

**1.1 CONJUGATED POLYMERS**

 Conjugated polymers exhibit semi-conducting properties because of a delocalised $\pi$-electron system along the polymer backbone (Figure 1).[1] The extensive main-chain conjugation allows high charge-mobility along polymer chains; this in turn, influences the overall physical behaviour of the polymers. Overlap of $P_z$ orbitals leads to the formation of $\pi$ (bonding) and $\pi^*$ (antibonding) molecular orbitals, which are mainly highest occupied molecular orbitals (HOMO, valance band) and lowest unoccupied molecular orbitals (LUMO, conduction band), respectively. Depending on the structure of the conjugated polymers the band gap can vary approximately from 1.5 eV to 4 eV.[1-2]
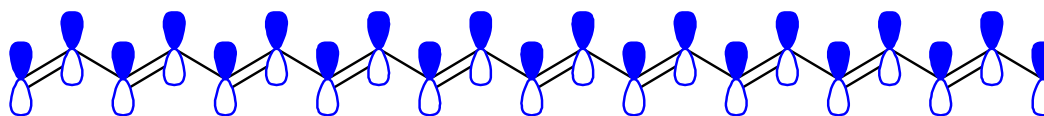


**Figure 1: $\pi$-**Conjugation system in polyacetylene. Overlap of $P_z$ orbitals leads to the formation of a delocalised pi-electron cloud above and below the plane of the sigma bonds, which form the structural framework.[2]

Although the first conductive polymer, polyacetylene, was first synthesized in 1958, a major breakthrough in this area was achieved by the discovery of the conductive properties of polyacteylene films upon a treatment with iodine (doping) in 1977 by H. Shirakawa.[3] Electrons are injected or removed (oxidation or reduction) to/from the polymers using appropriate reagents. These reagents are called as dopant and the process is known as doping. Polyacetylene had a very low conductivity before doping but its conductivity increased upon doping.

H. Shirakawa, A. G. MacDiarmid, and A. J. Heeger, were awarded with 2000 Nobel Prize in Chemistry because of this discovery.[2] Various conjugated polymers were

1

synthesized and their electrical conductivity properties were investigated after this discovery.

Conjugated polymers exhibit also photoluminescence properties.[4] When they are irradiated by a light with an appropriate wavelength, electrons at the ground state are excited and promoted to the excited state by absorbing photons. Excited electrons may return back to the ground state via several pathways as shown in Figuere 2 by a Jablonski diagram. Photons are given out upon returning to the ground state from singlet excited state; this is called fluorescence. Electrons may also first travel to the triplet state through intersystem crossing and relax back to ground state and this phenomenon is called phosphorescence.
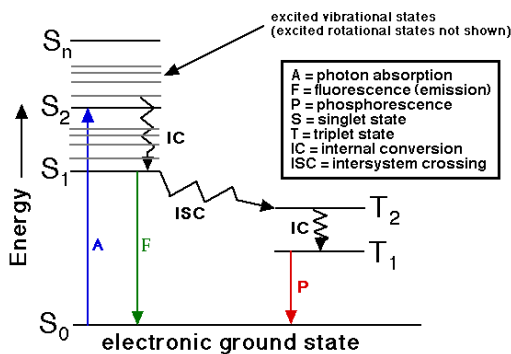


**Figure 2:** Jablonski diagram illustrates the photoluminescence event of a molecule.[4]

Another important property of conjugated polymers is electroluminescence, which was reported in 1990 at Cambridge University. [5-7] When electric current was applied to polymer thin film, the polymer emitted light showing electroluminescent properties. The wavelength of the emitted light can vary depending on the structure of the polymer. These polymers are called light emitting polymers and used in the fabrication of optoelectronic devices such as light emitting diodes, photovoltaic cells and solid state white lighting. Figure 3 shows the device configuration of photovoltaic and light emitting diodes.
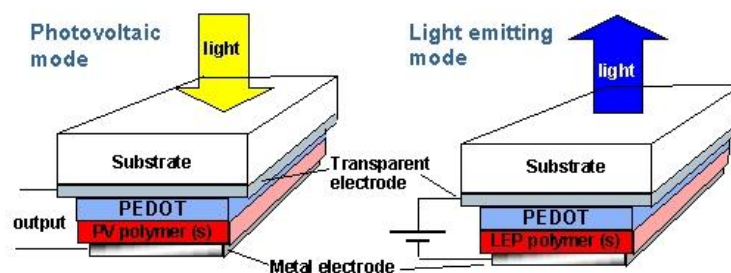
**Figure 3:** Schematic representation of photovoltaic diode and light emitting diode made from conjugated light emitting polymers.[8]

Conjugated polymers have wide application areas spanning from light emitting diodes, photovoltaic cells, field-effect transistor and sensor as well as new emerging areas such as artificial noses, artificial muscles and nanoelectromechanical systems.[9-10] Moreover, they are good chemical sensors that can be used in detection of ions (ionochromism) which is used to detect pollution rate in water, UV radiation (dual photochromism), and molecular recognition of chemical or biological materials (affinitychromism).[11]

## 1.2 Conjugated polymers based on fluorene derivatives

Fluorene-based conjugated polymers are getting increasing attention because they exhibit high optical and electroluminescent efficiencies.[12] Using polyfluorene derivatives it would be possible to obtain pure blue colour which is important for the full colour display. Moreover, they can be easily processed and have high thermal stability. These features are very important for the optoelectronic device fabrication. Polymers can be made soluble in desired solvents by attaching appropriate side chains to the 9th position of the fluorene by nucleophilic substitution reaction because of the acidic properties of protons of sp3 carbon in methylene bridge (Figure 4).[12]
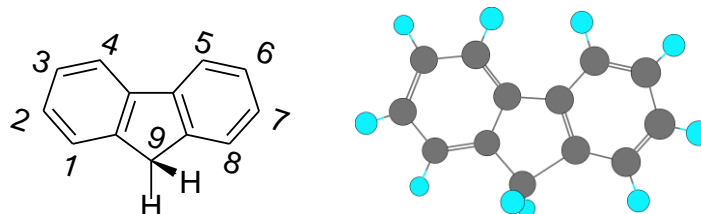


**Figure 4:** Chemical structure and 3D structure of the fluorene molecule

Fluorene-based conjugated polymers can be tuned to emit color across the entire visible range by copolymerizing fluorene with appropriate monomers as shown in Figure 5; this makes polyfluorene homo- and co-polymers attractive components for luminescent materials in organic light emitting diodes (OLEDs).
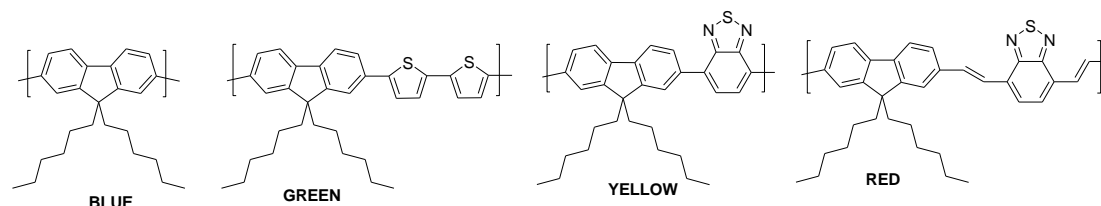


**Figure 5:** Fluorene based conjugated polymers

## 1.3 Synthesis methods of conjugated polymers

Early generation of conjugated polymers were mostly synthesized by electrochemical methods. However, the resulting polymers had solubility and processability problems. To this end, new synthetic methods were developed to obtain soluble polymers. The monomers were selected carefully in such a way to render solubility but to preserve the delocalized pi-conjugation of the polymer.

### 1.3.1   Synthesis of conjugated polymer by electrochemistry

Conjugated polymers could be produced in nonaqueous medium by using electrochemical polymerization.[13, 14] By using different electrolyte salt polypyrrole was produced as a film on Pt anode by electrolysis. Diaz and his coworkers produced polypyrrole by electrochemical polymerization in acetonitrile by using supporting electrolyte $Et_4NBF_4$. There were many studies about producing conjugated polymers by electrochemical polymerization and utilizing them in different areas of electronics due to semiconductive properties.[13, 14]

In electrochemical polymerization, as a result of reaction, conjugated polymers are deposited onto the electrode. This method is simple and provides to obtain nano- or

micrometer size polymeric surface. Set-up for electrochemical polymerization is shown in Figure 6.[15]
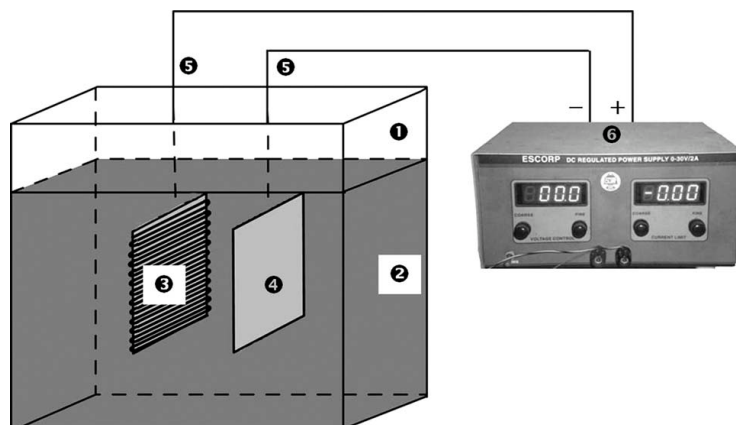


**Figure 6:** Schematic diagram of experimental set-up for electrochemical polymerization: 1) polymerization bath, 2) electrolyte solution, 3) anode, 4) cathode, 5) electrical wire, 6) power supply. Reprinted with permission from ref. 15 (Copyright Clearance Center ("CCC") 2011, John Wiley and Sons ("John Wiley and Sons"))

### 1.3.2 Synthesis of Conjugated Polymers via Wet Chemistry

In the history of science there were many scientist who developed new methods for carbon-carbon bond formation and received the Nobel prize for their invention like Grignard reaction (1912), the Diels-Alder reaction (1950), the Witting reaction (1979).[16] Very recently Richard F. Heck, Ei-ichi Negishi and Akira Suzuki were awarded with the Nobel Prize in Chemistry 2010 for palladium-catalyzed cross couplings in organic synthesis.[17] These reactions have also been applied widely in the conjugated polymer synthesis.

Heck reported in 1972 a new cross-coupling reaction by using aril, vinyl halides and olefins as coupling agents in the presence of Pd(0) and base. Scheme 1 shows the mechanism of Heck coupling reaction.[17-18]
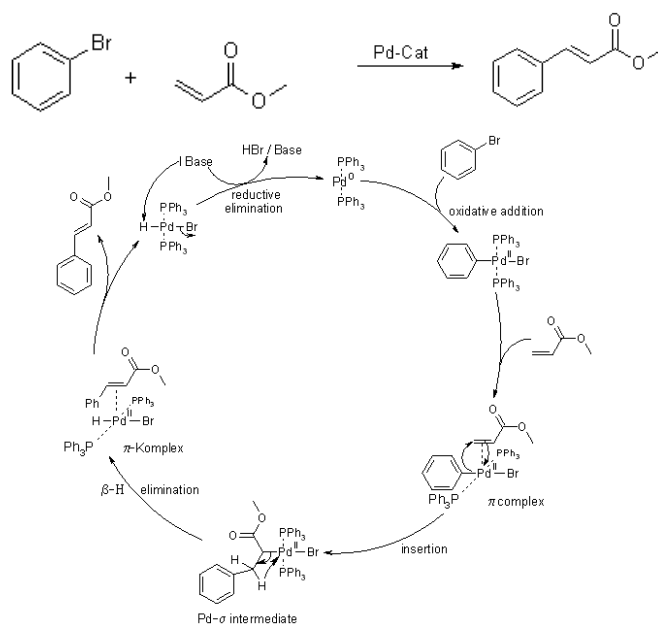
**Scheme 1**: Mechanism of Heck coupling reaction.[17-18]

In the Negishi coupling reaction, organozinc compounds are coupled with aryl, vinyl, benzyl or allyl halides in the presence of nickel or palladium catalysts to form C-C bond.[17]

Suzuki and co-workers developed palladium catalyzed cross coupling reaction and differently from others used organoborane compounds.[17, 19-20] Suzuki cross-coupling reaction is preferred in our synthesis due to its mild condition and commercially available coupling agents. Also, boronic acids are environmentally safer than other reagents which are used to made new C-C bond. Reaction mechanism of the Palladium catalyzed Suzuki cross-coupling reaction is shown in Scheme 2. Reaction mechanism has tree steps which are oxidative addition, trans-metallation and reductive elimination. Most important advantage of the Suzuki cross-coupling reaction is its tolerance for different functional groups. In the literature there are many examples to the Suzuki Cross-Coupling reaction.
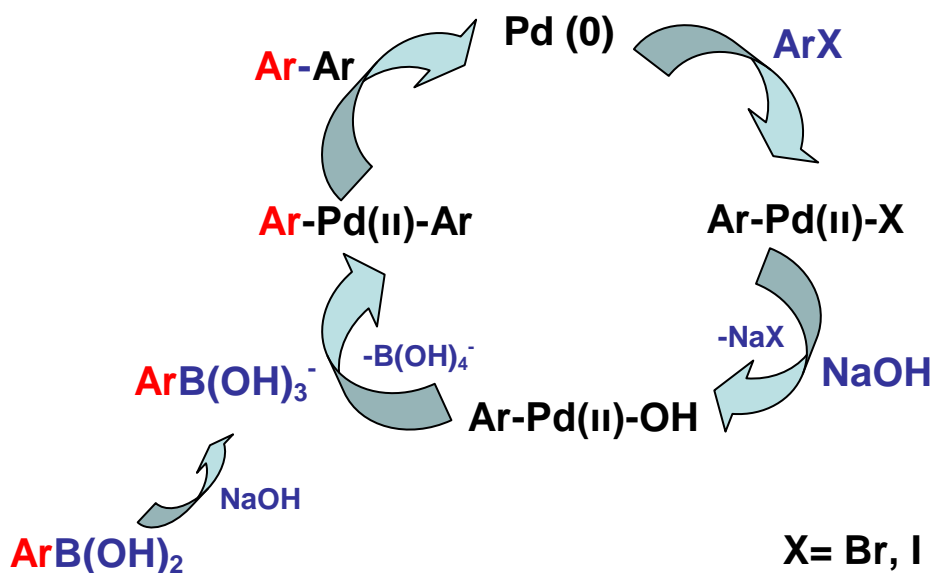
**Scheme 2:** Palladium catalyzed Suzuki Cross-coupling reaction mechanism. Adapted from ref. 19

In the synthesis of the conjugated polymers, other methods coupling reactions such as Stille, Yamamoto and Sonogashira coupling are used. In the Stille coupling reaction organotin compounds are coupled with organic halides, triflates, carbonyl chlorides in the presence of palladium catalyst (e.g. $Pd(PPh)_2Cl_2$) under nitrogen atmosphere. Reaction condition is mild and many functionalized conjugated polymers could be synthesized by Stille coupling. [21] Mechanism of the Stille cross- coupling reaction is illustrated in Scheme 3.
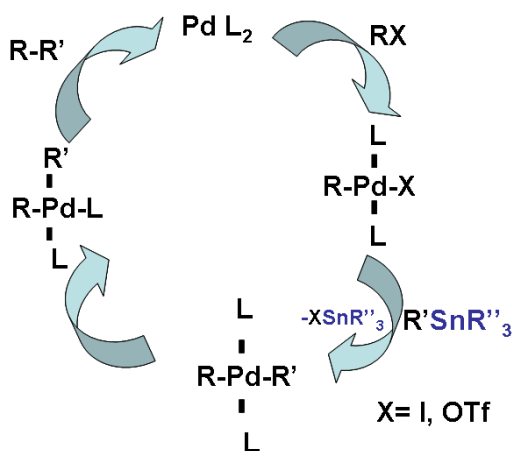


**Scheme 3:** Stille coupling reaction mechanism. Adapted from ref. 21

In the Yamamota reaction, aryl halides are coupled to form biaryl in the presence of Ni catalyst.[22] Sonogashira coupling is a palladium- copper catalyzed reaction which takes place between $sp^2$ carbons (aryl or vinyl halides) and sp- carbon centers of alkynes (Scheme 4).[23-24] Generally organic solvents like THF, DMF and toluene are used in this reaction. However, a stoichiometric amount of Cu(I) is required in Sonogashira coupling which is a drawback in the large scale synthesis.
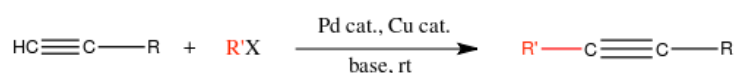


R' = Aryl, Vinyl
X = I, Br, Cl, OTf

**Scheme 4:** Reaction scheme for a Sonogashira coupling.

## 1.4 Water soluble conjugated polymers and their applications

Conjugated polymers with suitable side chains can be made soluble in various solvents. If hydrophilic or ionic side groups are attached, they can be soluble in water as well. Water soluble ionic conjugated polymers are called conjugated polyelectrolytes (CPE). Scheme 5 shows the cartoon representation of CPEs.[25]
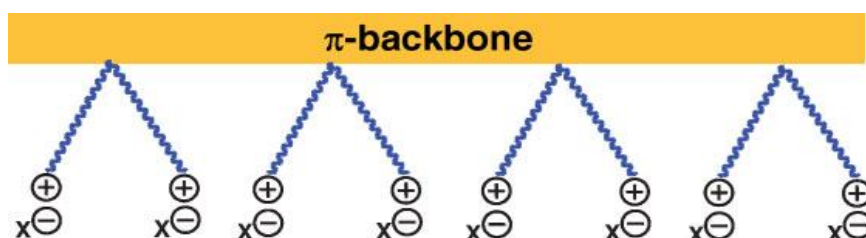


**Scheme 5:** Generalized structural components of a cationic CPE.[25]

Water soluble conjugated polymers have wide range of application areas that one of them is sensing. Conjugated polymers could be applied in preparation of electrochemical sensors and biosensors. Electrochemical sensors consist of analyte

and receptor and transducer as shown in figure 7. Recognising information by analyte and converting it into an electrical or optical signal gives fast and selective determination of different chemicals. [26]
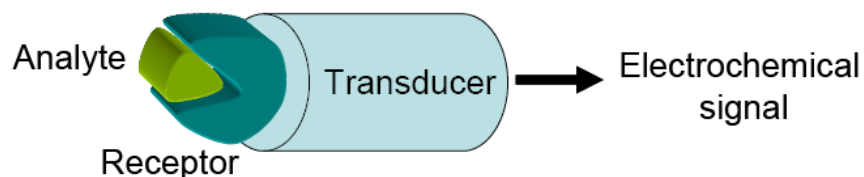
**Figure 7:** Schematic presentation of an electrochemical sensor.[26]

Receptor part of electrochemical sensors converts information into energy and transducer part converts it into signal. These systems generally used in medicine to detect some diseases or cancer cells, or to detect pollution rate in water and est.[26] M. Yu and et al. report about crown-ether substituted polyfluorene which is quench its fluorescence at the presence of $Pb^{2+}$. Due to this property it could be used in lead ion detection. Because of toxic effect to human, detection of $Pb^{2+}$ is important. Crown-ether-substituted polyfluorene was checked with different metal ions ($Ca^{2+}$, $Co^{2+}$, $Cu^{2+}$, $Fe^{2+}$, $Hg^{2+}$, $K^+$, $Li^+$, $Mg^{2+}$, $Mn^{2+}$, $Na^+$, $Zn^{2+}$, $Ba^{2+}$) and only shows selectivity toward $Pb^{2+}$ ions by making sandwich complex with $Pb^{2+}$ ions in aqueous environment.[27] There are many reports about using conjugated polymers for sensing different ions.[28-30]

Phosphonate group containing polyfluorene reported as chemosensor for metal ions by G. Zhou and coworkers. Phosphonate group in side chain of the polymer make it sensitive toward several metal ions, moreover, made polymer soluble in polar solvents. Sensing properties of polymer was examined in dichloromethane ($CH_2Cl_2$) by addition of different metal ions ($Li^+$, $Na^+$, $K^+$, $Ca^{2+}$, $Sr^{2+}$, $Cd^{2+}$, $Mn^{2+}$, $Fe^{2+}$, $Cu^{2+}$, $Co^{2+}$, $Ni^{2+}$, $Ag^{2+}$, $Zn^{2+}$, $Pb^{2+}$) and only $Fe^{3+}$ shows positive result. There observed 210-fold fluorescence quenching while addition of $Fe^{3+}$ metal ions.[28]

In biology, biosensors have special role in detection of some diseases in time. Diagnosis, monitoring of some biochemical compounds selectively requires sensitive biosensors. Water soluble conjugated polymer based electrochemical biosensors are mostly used analytical methods in medicine.[26] Schematic illustration of the biosensor shown in figure 8.
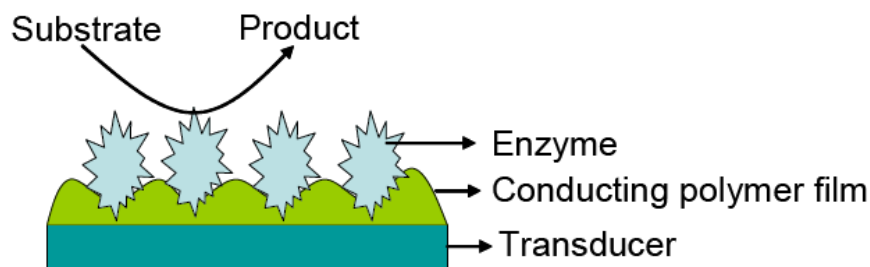


**Figure 8:** Schematic presentation of a biosensor [26]

In the literature many biosensors such as DNA biosensors, $O_2$ biosensor [31], glucose oxidase/polypyrrole biosensor[32] were reported. DNA biosensor was reported by A. Gambhir and coworkers. Biosensor was prepared by fabrication of DNA to polypyrrole/polyvinyl sulphonate film to detect DNA hybridizatioin.[33] Christopher A. Traina and et al. designed synthesis of monofuctionalized fluorene based water soluble conjugated polymer with photoluminescence quantum efficiency of 80% which is used in biosensing and imaging applications by using biotin-streptavidin complex formation. Probe-analyte interactions was determined by FRET detection which is observed in conjugation of Streptavidin-Alexa Fluor-488 to biotinylated polymer. and observation of blue fluorescence while binding of biotinylated polymer to streptavidin coated beads as shown in figure 9.[34]
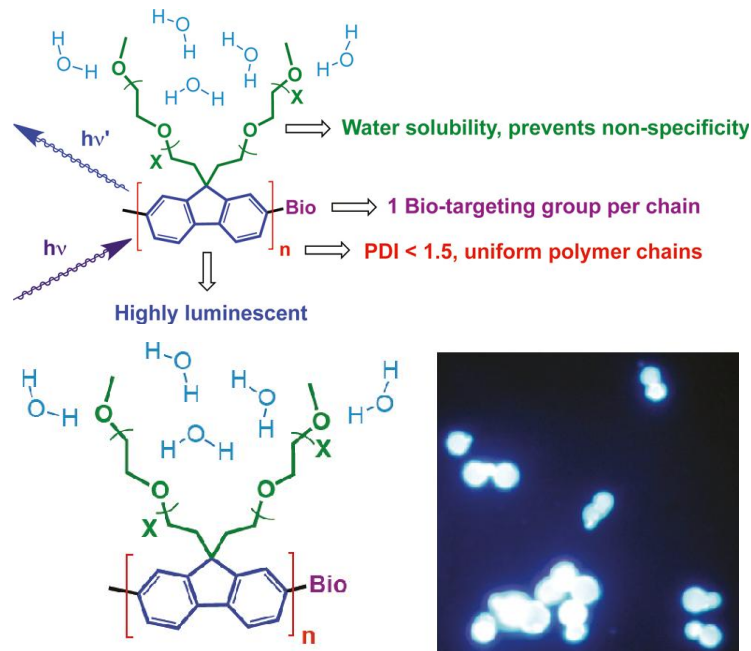
**Figure 9:** Water soluble biotin monofunctionalized poly(fluorene) polymer and polymer bounded agarose beads. Reprinted with permission from ref. 15 (Copyright 2011 The American Chemical Society)

## 1.5 Conjugated polymer nanoparticles preparation methods and applications

Making conjugated polymers water soluble is not so efficient so that polymer can aggregate and quantum yield of polymer may decrease. This process is undesired and time consuming. Second method to make these polymers soluble in water is converting them into nanoparticles. In the literature there are many examples for conjugated polymer nanoparticles. However, the examples are mostly limited to highly hydrophobic conjugated polymers carrying no functional groups to be further modified. Another drawback preventing the exploitation of CPNs is the mechanical instability of these nanoparticles. To this end, the development of CPNs which can be mechanically stable in water as well as in organic solvents and the surface functionalization of these nanoparticles could be highly valuable for many applications. Conjugated polymer nanoparticles could be synthesized through miniemulsion or reprecipitation methods. In miniemulsion method polymer is

11

dissolved in water immiscible solvent and then solution is injected into aqueous solution of surfactant, mixture is stirred and solvent is evaporated. In order to keep stable the formed nanoparticles some stabilizers is added in the dispersion.[35] The illustration of this process is shown in Figure 10.
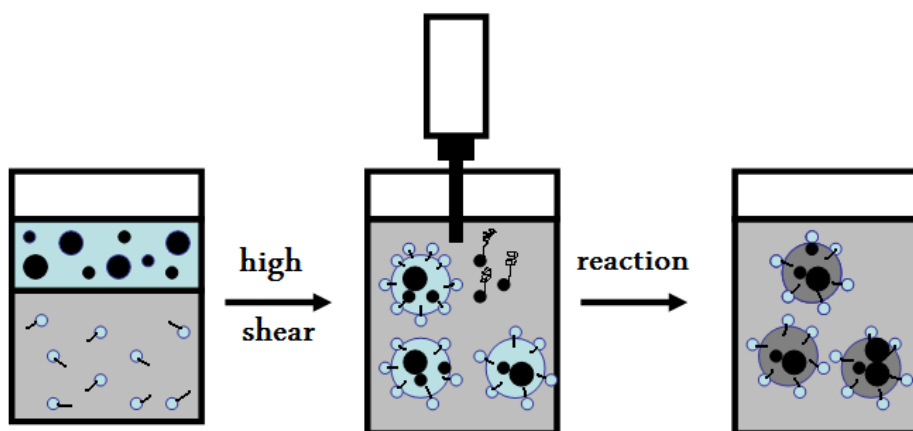


**Figure 10:** The preparation of nanoparticles using the miniemulsion method. Adapted from. Adapted from ref. 35

In reprecipitation method, polymer is dissolved in THF or other water miscible solvent and dropped into deionised pure water by stirring and than solution was ultrasonicated and solvent was removed in order to obtain stable spherical nanoparticles. This process mechanism is shown in Figure 11. Owing to hydrophobic effect polymer nanoparticles become spherical. Also, in this method we don't need to use any additives like surfactant or stabilizers and we can control the particles size.[35]
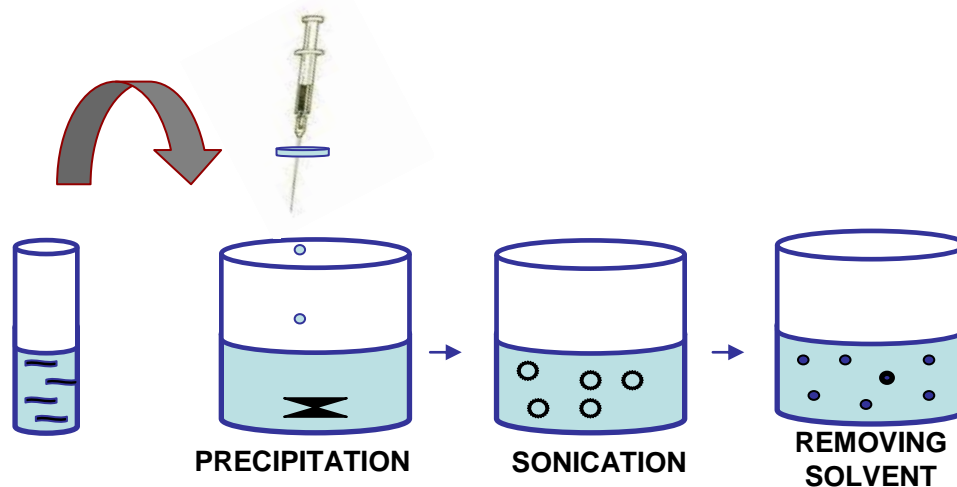
**Figure 11:** Preparation of conjugated polymer nanoparticles via reprecipitation method

In reprecipitation method, when polymer solution is added into ''poor solvent'' polymer-organic solvent interaction still favorable during sonication. Organic solvent was removed by evaporation. Organic solvent is more volatile than water so first organic solvent is evaporated and during evaporation polymer- organic solvent interaction is weakened and polymer- polymer interaction became more favorable and due to minimized contact area with unwanted poor solvent particles become spherical.

Conjugated polymer nanoparticles have a wide range of application areas because of their electrooptical properties. Thanks to their high quantum efficiency, thermal stability and processability nanoparticles can be used as organic light emitting diodes[36], actuators for biomedical applications[37], bioimaging agent.[35] Conjugated polymer nanoparticles are getting increasing attention because of their wide range applications spanning from biomedical field to optoelectronics.[35] They offer high brightness, improved photostability and high fluorescent quantum yield comparing to conventional dyes.[38]

Water dispersible conjugated polymer nanoparticles (CPNPs) can be used as a dispersant to disperse vertically aligned multi-walled carbon nanotubes (MWCNTs)

due to their well dispersion property in water and unique optical properties for MWCNTs can be created by CPNPs.[39] Image of dispersed MWCNTs with CPNPs is shown in figure 12.
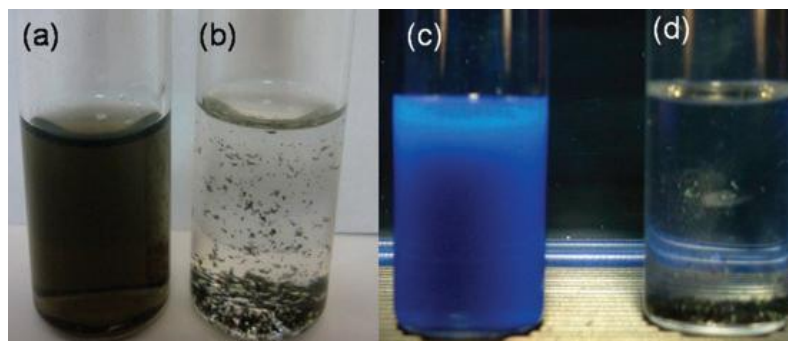


**Figure 12:** Images of CPN (40 nm-sized)–CNT with 0.2 : 1 CPN to CNT mass ratio (a, c) and CNT–water dispersion (b, d) under ambient (a, b) and UV-light irradiation (c, d). Reprinted with permission from ref. 39 (Copyright 2010, Royal Society of Chemistry)

Moreover, in optoelectronic colour tuneable CPNPs can be synthesized in order to generate white light that can be used in light emitting diodes (LED).[40] Azide group containing conjugated polymer was used in this study. After preparation of nanoparticles with reprecipitation method, nanoparticles were irradiated with UV light in order to obtain cross-linked nanoparticles to achieve further stability and at the same time by controlling irradiation time colour of nanoparticles can be tuned. Preparation of cross-linkable, colour tuneable, water dispersible azide group containing conjugated polymer nanoparticles is shown in figure 13.
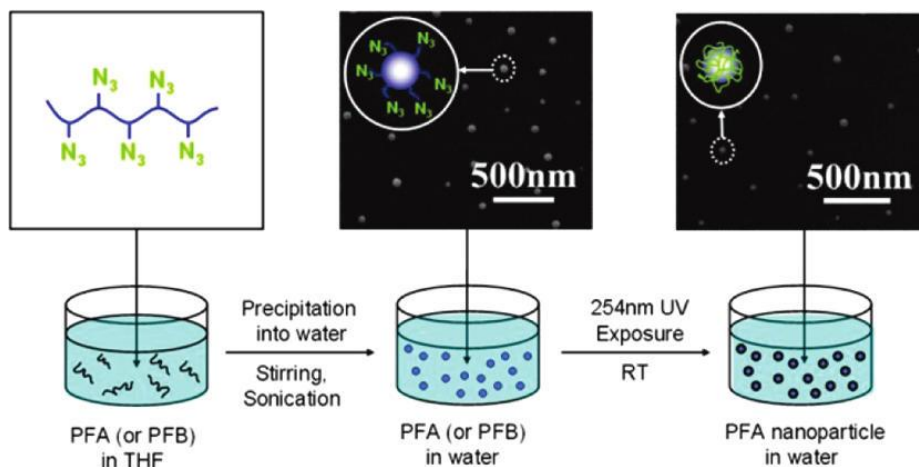
**Figure 13:** Cartoon representation of the conjugated polymer nanoparticle preparation. Reprinted with permission from ref. 40 (Copyright 2011 The American Chemical Society)

Furthermore, white light emitting single copolymer could be synthesized by using blue, green, red chromophores.[41] Polymer LEDs get increasing attention since it first discovered in 1989[42] due to lower production cost, high flexibility, lower operating voltage, tuneable optical and electrical properties and fastest response time and even now commercially produced.[43]

Conjugated polymer nanoparticles have an important role in medicine and biology so they can be used for drug and gene delivery, fluorescent biological labels, tumor destruction via heating, tissue engineering, probing of DNA structure, bio detection of pathogens and detection of proteins.[44] Light emitting conjugated polymer nanoparticles can be used in optical detection technique due to their optical properties like high quantum yield, photostability etc. Owing to low toxicity, long lifetime and high fluorescent quantum yield CPNPs efficient than QDs. Differently from QDs, hydrophobic conjugated polymer nanoparticles can be well dispersed in pure water without using different additives. Due to high chromophore density and signal brightness conjugated polymer nanoparticles can be used in vivo bioimaging similar to QDs[45] but moreover have not any cytotoxic effect on leaving organisms. Typically all living cell's size is around 10 μm which allow using nanoparticles in

15

vivo application. Nanoparticles could be made from inorganic materials (metals like Au, Ag or semiconductors Cd) and organic materials like polymer. Due to processability conjugated polymers are mostly preferred in optoelectronic and in biology. Some CPNs which have different functional groups (–COOH, -OH,-N$_3$, -SH etc.) can be used as a drug container but this particles should be biodegradable as well. Also, carboxylic group containing nanoparticles can be linked with different oligonucleotide sequences. Due to high reactivity of carboxylic group containing nanoparticles, they can combine to enzyme, proteins, antibody, antigen and nucleic acids at room temperature easily.[46] In addition; functional group containing nanoparticles can be used in cell separation, nucleic acid separation and immunity detection. By using carbodiimide chemistry, amine containing antibody attached onto light emitting carboxylic group containing nanoparticles which is used in detection of bacterial pathogens.[47]

Temperature sensing is important in cells to separate healthy cells from other cells (cancer, malignant cells) within tissues. Fangmoa et al. have prepared ratiometric optical temperature sensors by attaching temperature sensitive dye (rhodamine B, RhB) to two different fluorene based semiconducting polymer dots (Pdots). Pdot-RhB nanoparticles were prepared by blending PS-RhB (PS polystyrene) with semiconducting polymer while Pdots formation in order to make well splitting of PS-RhB into the Pdot matrix. These size tunable (20-160 nm) Pdot-RhB nanoparticles are well with measuring physiologically relevant temperatures and could be used as fluorescent probe for cellular imaging which also shows well cellular uptake by HeLa cells without any additives.[48] Similar to this study conjugated polymer nanoparticles were used to detect rhodamine-labeled peptides which is used for protein kinase enzymes that allows quantitative monitoring of phosphorylation of peptide by fluorescence quenching and FRET which were done by Moon and coworkers. Monitoring of phosphorylation is important in order to prevent some diseases like cancer, diabetes and inflammation which are results of uncontrolled functions of certain protein kinases. In this study metal ion chelating iminodoacetic acids containing conjugated polymer was used for selective detection of phosphopeptides.[49]

Nanoparticle based ion sensors have prepared by Yang-Hsiang Chan and his coworkers which can quantitatively detect most important metal ions copper and iron. Sensor based on fluorescence quenching by the aggregation of carboxyl functionalized fluorene and benzothiodiazole based semiconductive polymer dots at the presence of copper and iron ions were prepared. Similar to Pdot-RhB preparation in this study PS-COOH is added into semiconductive polymer matrix in order to prepare carboxyl group containing Pdots. Chelating interaction between $Cu^{2+}$ and $Fe^{2+}$ and carboxylic groups in the surface of Pdots (21nm) cause aggregation (500nm) of particles in the solution which is quench the fluorescence by forming 2:1 (carboxylic moiety Pdot: $Cu^{+2}$) sandwich complex and can be redispersed by ethylenediaminetetraacetic acid (EDTA) and fluorescence can be restored again.[50] This type of particles could be used as targeting agent, probes for cell labeling or imaging as well. McNeill and et al. were designed $\pi$-Conjugated polymer nanoparticles which were functionalized with carboxylic group containing polymer and surface of particles further functionalized with ethylene glycol in order to achieve biocompatibility and use these nanoparticles to target biomolecules.[51] Biological multi-target imaging study was performed by fluorescent nanoparticles based on self-assembly of conjugated amphiphilic oligomers in water by Katja Petkau, Adrien Kaeser and coworkers. The amphiphilic oligomers were pre-functionalized with ligands (mannose) and with azide to allow post-functionalization via copper catalyzed click chemistry. Mannose group can specifically bind to FimH receptor of E. Coli bacteria and FRET was observed while post-functionalization with dye labeled protein ConA-AF633( concanavalin A-AlexaFluor633) which gives an opportunity to use them in biology and medicine for imaging purposes.[52] Magnetically responsive semiconducting polymer nanoparticles also could be synthesized to increase efficiency and versatility of application areas. Philip Howes, Mark Green and coworkers have designed magnetin-fluorescent semiconductor polymer nanoparticles (MF-SPNs) which are encapsulated in phospholipid micelles to control size and size distribution that could be used in MRI studies and fluorescent imaging. In this study iron oxide nanoparticles and SPNs are encapsulated in PEG-phospholipids where PEG increases circulation lifetime of materials, makes it biocompatible and decreases

17

toxicity. MRI study showed that MF-SPNs have transverse magnetization in MR and it has linear relationship with iron oxide concentration. Imaging study was performed by SH-SY5Y neuroblastoma cells show that it has uniform distribution throughout the cell and internalize in cytoplasm. Cell viability test for 48h shows that MF-SPNs do not effect growth of the cells and do not have toxic effect.[53] Green and coworkers have prepared SPNs encapsulated phospholipid micelles without iron oxide and apply it in imaging SH-SY5Y neuroblastoma cells and live HeLa cells. Fluorescent lifetime measurement shows that nanoparticles have shorter lifetime than QDs in cells. In order to apply wide range of cell types, biomolecules can be conjugated onto nanoparticles so in this study bovine serum albumin (BSA) was conjugated to carboxyl functionalized SPNs via carbodiimide chemistry.[54] Bioorthogonal labeled by click chemistry semiconducting polymer with 0.28 quantum yield dots were prepared by Jin and coworkers for cell imaging. QDs are mostly preferred probe in this area however it is not possible to use copper catalyzed click chemistry for them due to fluorescence quenching. However, Pdot shows no significant change in fluorescence intensity while using azide-alkyne cycloaddition click chemistry and they shows thousand –fold faster emission rate than QDs. To functionalized Pdots poly(styrene-co-maleic anhydride) were added to the solution while nanoparticles formation and maleic anhydride hydrolyze in aqueous environment to generate carboxylic group at the surface of 15 nm size Pdots. Azide group containing PEG was attached to carboxylic group via EDC coupling of amine and carboxylic groups. In order to control specific binding in the presence of copper Pdots mixed with alkyne-Alexa 594 and fluorescence quenching was observed due to fluorescence resonance energy transfer (FRET) while binding. After, allyl-Pdots were used to image azidohomoalanin (AHA) and N-azidoacetylgalactosamine (GalNAz) proteins in cell. First MCF-7 cells treated with azidohomoalanin (AHA) and N-azidoacetylgalactosamine (GalNAz) proteins and than treated with allyl-Pdots in the presence of Cu(I) and fluorescence was observer due to specific binding of Pdots to protein. This bright, specific protein labeling by using copper catalyzed click chemistry we can visualize various cellular processes.[55] CPNs can be used in deep tissue imaging due to high two photon absorption cross section. Color tunable CPNs

were synthesized by emulsion polymerization via Sonogashira coupling by Mecking et al in 60-120 nm size. Their color can be tuned from blue to orange by using dyes to demonstrate two-photon excitation microscopy in the NIR region. Cellular uptake was controlled by live HeLa cells and results show that particles accumulate in the cytosol and do not have any toxic effect. Illumination over 500s shows that CPNs stable toward bleaching.[56] Due to limited fluorescent probes for two-photon (2P) imaging studies there is a need for exploration of new types of materials to image tissue sensitively. Because of high brightness conjugated polymer nanoparticles could be best solution in this area because high brightness and exhibiting large 2P cross-section and photostability of particles can minimize back-grounds autofluorescence of tissue. Nur Aida Abdul Rahim and et al. was synthesized 8nm CNPs for two-photon imaging in endothelial cells in tissue mode. In order to create ionic environment in CNPs solution and prevent aggregation tartaric acid was added to solution. Moreover, strong interaction between ions lowers interaction between polymer chains and causes small particle formation and increases storage time up to three month at room temperature. The 2P action cross-section of CPNs was measured between 1000 and 11000 GM in 730 nm. Lifetime and photobleaching studies show that lifetime of CPNs are 10-50 times faster than QDs and bleaching rate of CNPs virtually identical to QD525. So that these particles could be used to understand immune-cell trafficking in animal models and monitor implanted-stem-cell migration due to long-term imaging properties.[57]

## 1.6 Aim of the Thesis

Our aim in this project was to synthesized novel light emitting conjugated polymers and converting them into water dispersible nanoparticles and applies them in cell imaging.

In this study six different fluorene based fluorescent polymers namely poly[(9,9-bis{propeny}fluorenyl-2,7-diyl)-co-(9,9-dihexyl-9H-fluorene)] (**P1**), poly[(9,9-bis{carboxymethylsulfonyl-propyl}fluorenyl-2,7-diyl)-co-(9,9-dihexyl-9H-fluorene) (**P2**), poly[(9,9- bis{propeny}fluorenyl-2,7-diyl))-co-(1,4-benzo-{2,1,3}-thiodiazole)] (**P3**), poly[(9,9- bis{carboxymethylsulfonyl-propyl}fluorenyl-2,7-diyl)-co(1,4-benzo-{2,1,3}-thiodiazole)]  (**P4**), poly[(9,9-bis{3-bromopropyl}fluorenyl-2,7-diyl)-co-(1,4-benzo-{2,1,3}-thiodiazole)] (**P5**), poly[(9,9-bis{3-azidopropyl}fluorenyl-2,7-diyl)-co-(benzothiadiazole)] (**P6**) were synthesized by using 2, 7-dibromo-9,9-bis-(dibromopropane)-9H-fluorene **M1** and 2, 7-dibromo-9,9-bis-(propenyl)-9H-fluorene **M2** according to Suzuki Coupling reaction**.**

Nanoparticles of P1, P3, P4, P5 and P6 were prepared by using reprecipitation method. Due to hydrophilic environment hydrophobic polymers form spherical particles.
Pure polymer nanoparticles (P1NPs and P3NPs) were mechanically modified by using [2+2] photochemical cycloaddition reaction.

In final step cytotoxicity of P3NPs and P4NPs were characterised by MTT assay. General scheme of the thesis work is illustrated in figure 14.
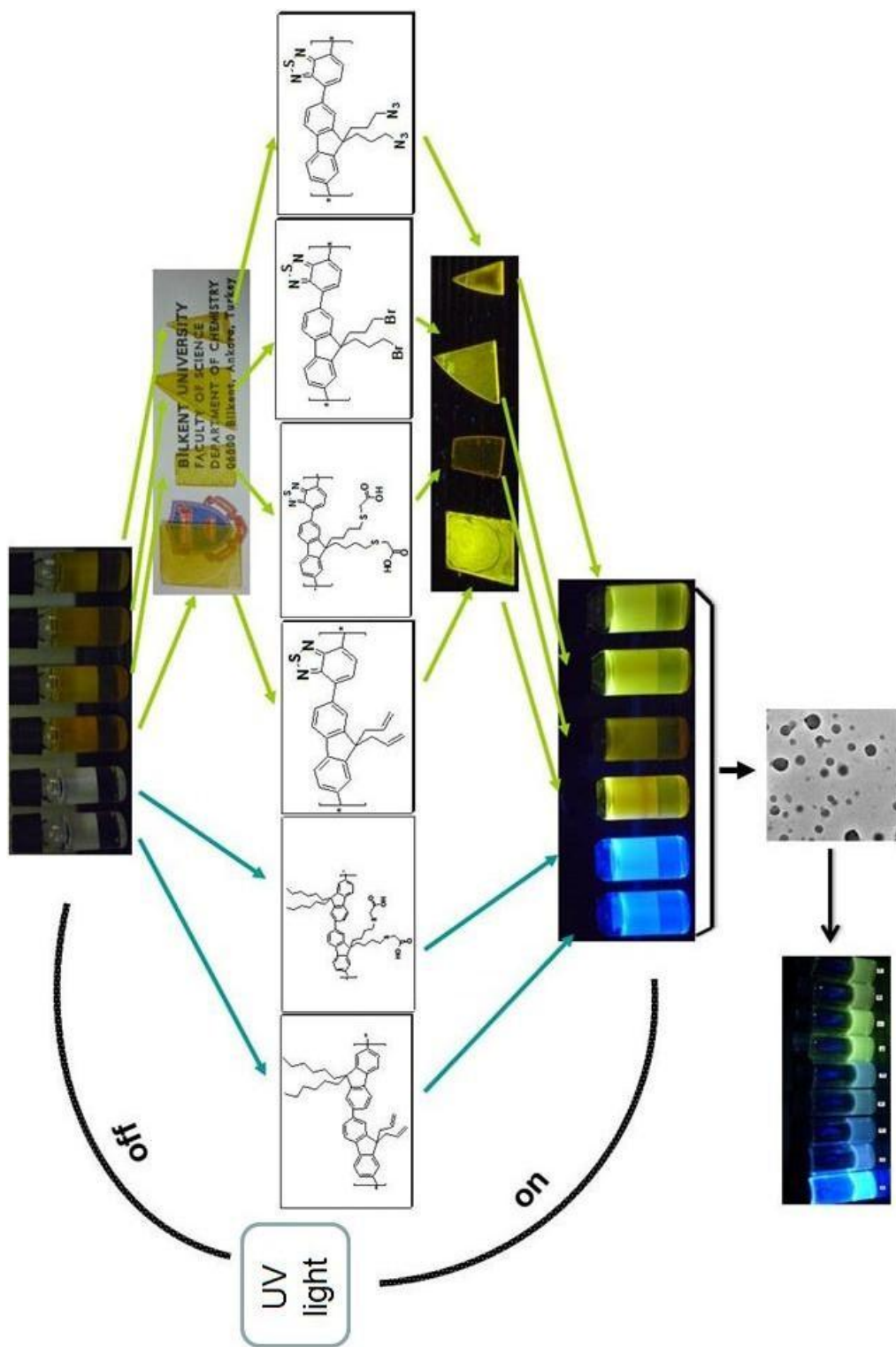
**Figure 14:** General scheme of the Thesis work

**CHAPTER 2**

**RESULTS AND DISCUSSION**

This chapter consists of three sections. In the first section of this chapter, synthesis of monomers, their purification steps, polymer synthesis and their characterizations are discussed. In the second section, preparation of nanoparticles, their modification and characterizations are discussed. In the final section, MTT assay test result is discussed. These experiments show nontoxic nature of **CNPs** and may open a new window in the nanomedicine for cell imaging, drug delivery and monitoring movement of drug, and biosensing.

## 2.1 Synthesis and characterization of monomers and polymers

For the synthesis of nanoparticles, first the following polymers shown in Scheme 6 carrying a number of different functional groups and based on derivatives of fluorene and benzothiodiazole monomers were designed and synthesized using the Suzuki coupling reactions.
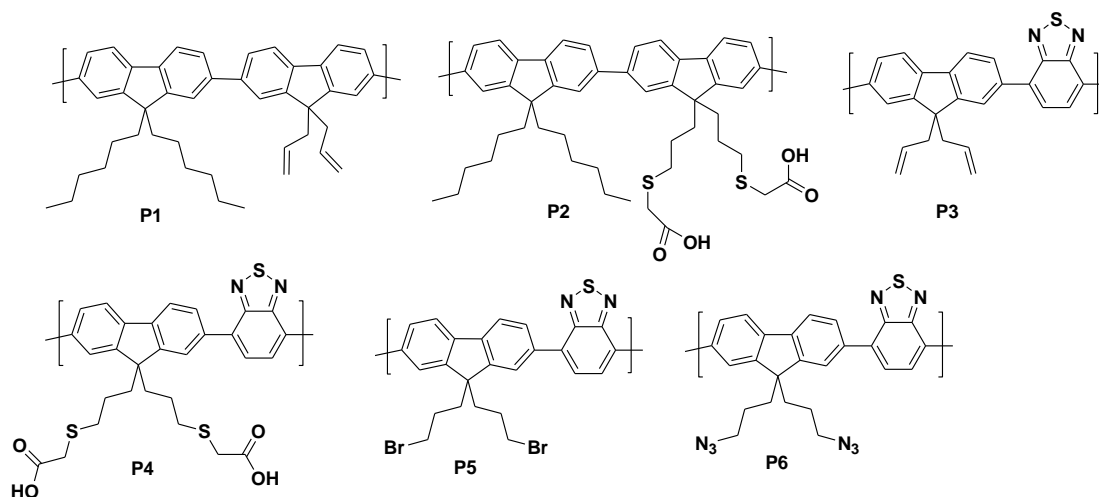


**Scheme 6:** Poly[(9,9-bis{propeny}fluorenyl-2,7-diyl)-co-(9,9-dihexyl-9H-fluorene)] (**P1**), poly[(9,9-bis{carboxymethylsulfonyl-propyl}fluorenyl-2,7-diyl)-co-(9,9-dihexyl-9H-fluorene) (**P2**), poly[(9,9- bis{propeny}fluorenyl-2,7-diyl))-co-(1,4-benzo-{2,1,3}-thiodiazole)] (**P3**), poly[(9,9- bis{carboxymethylsulfonyl-propyl}fluorenyl-2,7-diyl)-co(1,4-benzo-{2,1,3}-thiodiazole)]  (**P4**), poly[(9,9-bis{3-bromopropyl}fluorenyl-2,7-diyl)-co-(1,4-benzo-{2,1,3}-thiodiazole)] (**P5**), poly[(9,9-bis{3-azidopropyl}fluorenyl-2,7-diyl)-co-(benzothiadiazole)] (**P6**).

These polymers carry functional groups on their side chains, such as azide and allyl groups that can be cross-linkable using UV light to form shape-persistent, stable nanoparticles. Moreover, these functional groups can also be converted into other functional groups for desired applications.

In polymerization reaction, step growth cross-coupling reaction was used in order to form new C-C bond. Due to mild condition and availability of coupling agents like boronic acids, Suzuki cross-coupling reaction was performed. Moreover, boronic

acids or esters are environmentally friendly and final products are nontoxic materials as compared to other C-C bond formation reactions. [58]

### 2.1.1 Synthesis and charaterisation of monomer 2, 7-dibromo-9,9-bis-(dibromopropane)-9H-fluorene (M1)

To synthesize conjugated polymers two monomers based on fluorene were synthesized by a nucleophilic substitution reaction. Fluorene-based monomer was selected because of its easy modification at the 9th position. Moreover they can be polymerized using co-monomers to obtain light emitting polymers with various emission wavelengths.

2,7-dibromo-9,9-bis-(dibromopropane)-9H-fluorene (M1) was synthesised according to reaction Scheme 7. The synthesis involves the use of commercially available 1,3-dibromopropane and 2,7-dibromofluorene. Using very strong basic condition, first C9 protons in fluorene were abstracted and by a nucleophilic substitution reaction side chains were added. After work up, the product was purified by column chromatography to obtain white powders in 67% yield.
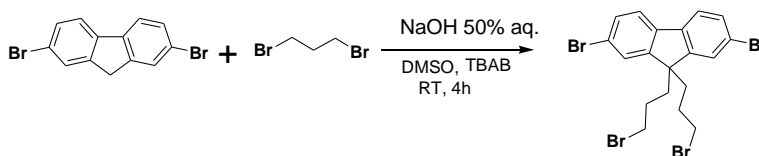


**Scheme 7:** Synthesis mechanism of monomer 2, 7-dibromo-9,9-bis-(dibromopropane)-9H-fluorene **M1**

After the synthesis, monomer **M1** was characterized with ^{1}H-NMR spectroscopy. ^{1}H-NMR spectrum is shown in figure 15.

^{1}H-NMR spectrum of 2, 7-dibromo-9,9-bis-(dibromopropane)-9H-fluorene monomer showed multiplet at 7.53 ppm due to protons in aromatic ring, triplet at 3,14 ppm due to –$CH_2$ protons near bromine were deshielded because of the electronegative bromine atoms. Protons in –$CH_2$ at position b show triplet at 2.17 ppm and at 1.16 ppm multiplet observed for the methylene protons near aromatic ring.
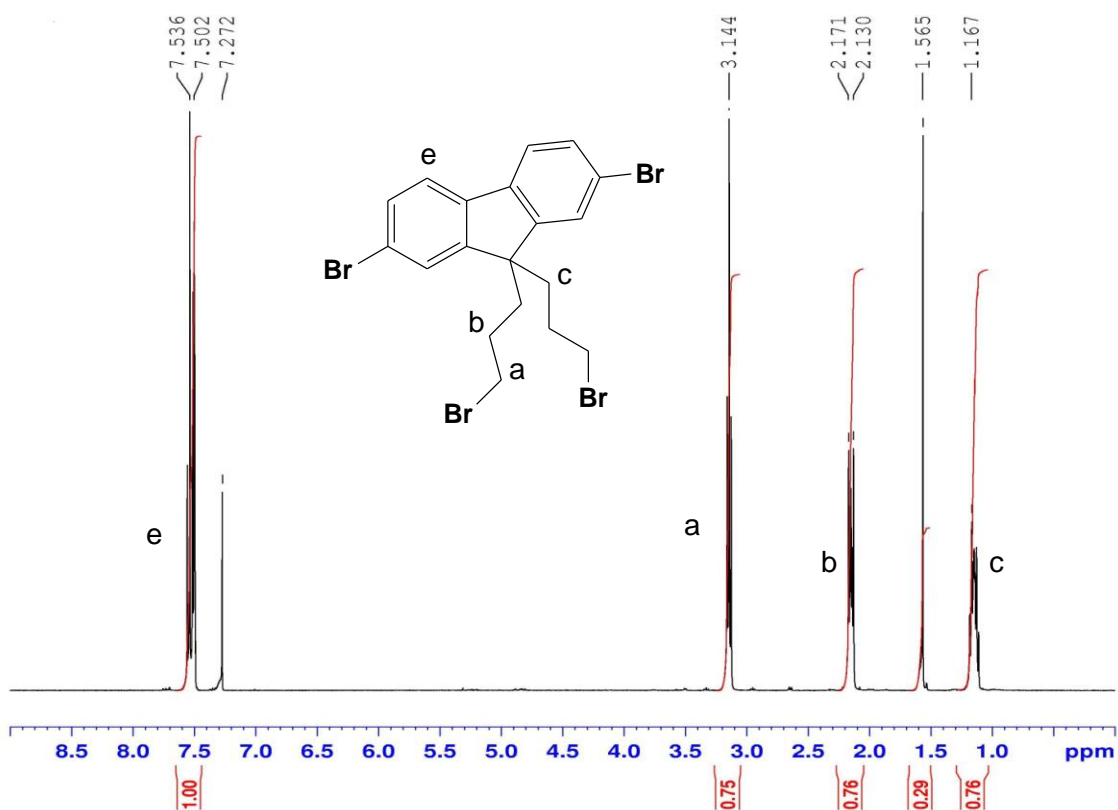
**Figure 15:** $^1$H-NMR spectrum of 2, 7-dibromo-9,9-bis-(dibromopropane)-9H-fluorene (**M1**) (400 MHz, CDCl$_3$, 25$^0$C).

### 2.1.2 Synthesis and characterization of monomer 2, 7-dibromo-9,9-bis-(propenyl)-9H-fluorene (M2)

**M2** was synthesized according to reaction Scheme 8. In this synthesis, first 2,7-dibromofluorene was treated with strong base to abstract the protons at the 9$^{th}$ position and then excess allylbromide was added. After purification by column chromatography the product was obtained in 89 % yield.

The reasons of synthesizing allyl group containing monomer are as follows: First these groups can be cross-linked under light through light triggered 2+2 cycloaddition; second they can be cross-linked using dithiol species through thiol-ene chemistry and third they can be converted into other functional groups for example by treating with mercaptoacetic acid carboxylic groups can be installed.
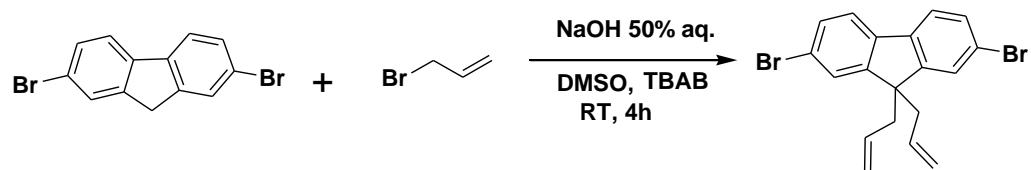
**Scheme 8:** Synthesis mechanism of monomer 2, 7-dibromo-9,9-bis-(propenyl)-9H-fluorene (**M2)**

$^1$H-NMR spectum of the monomer 2, 7-dibromo-9,9-bis-(propenyl)-9H-fluorene is shown in Figure 16.
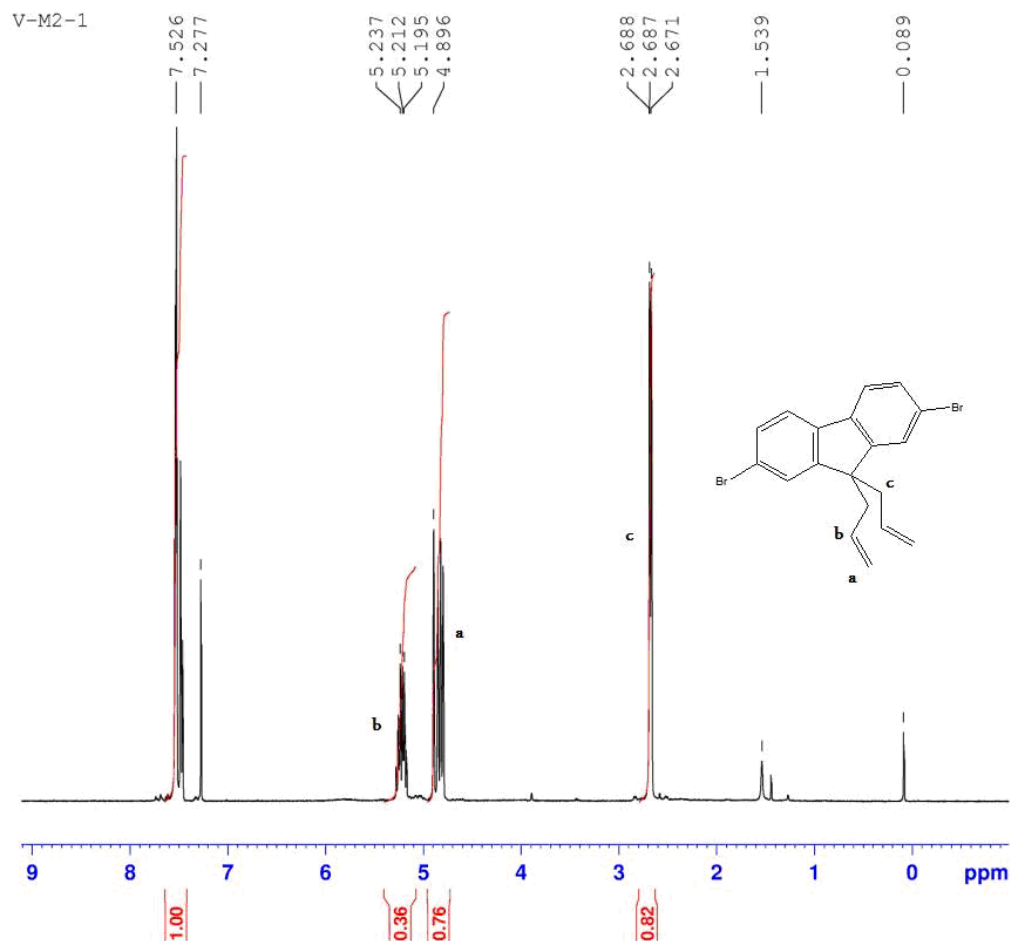


**Figure 16:** $^1$H-NMR spectrum of monomer 2, 7-dibromo-9,9-bis-(propenyl)-9H-fluorene (**M2)** (400 MHz, CDCl$_3$, 25$^0$C).

^{1}H-NMR spectrum of monomer 2, 7-dibromo-9,9-bis-(propenyl)-9H-fluorene showed multiplet at 7.53 ppm due to aromatic protons and multiplet at 5.21 and 4.89 ppm – CH protons. Also, triplet at 2.68 ppm was observed due to alkyl protons near aromatic ring.

## 2.1.3 Synthesis and characterization of poly[(9,9-bis{propenyl}-9H-fluorene)-co-(9,9-dihexyl-9H-fluorene)] (P1)

**P1** was synthesized as shown in the Scheme 9. **M2** and boronic ester 9,9-dihexylfluorene-2,7-bis(trimethyleneborate) were coupled using Suzuki coupling reaction conditions. Purification was done by precipitation of **P1** solution in THF into cold methanol. Yellow powders were obtained in 60% yield.
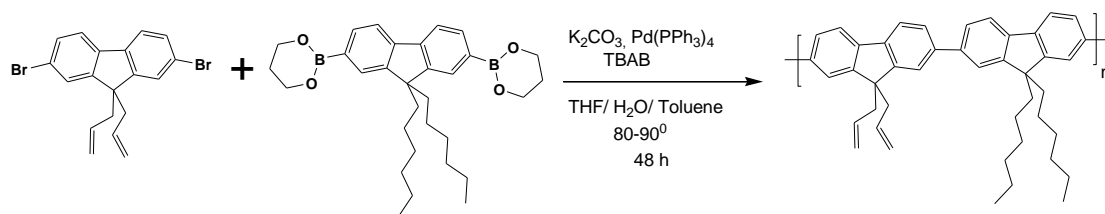


**Scheme 9:** Polymerization reaction of the polymer poly[(9,9-bis{propeny}fluorenyl-2,7-diyl)-co-(9,9-dihexyl-9H-fluorene)] (**P1**) (400 MHz, CDCl$_3$, 25$^0$C).

Characterization of polymers was done by ^{1}H-NMR, UV-Vis, fluorescence and FT-IR spectroscopy. ^{1}H-NMR spectrum of the polymer poly[(9,9-{propenyl}-9H-fluorene)-co-(9,9-dihexyl-9H-fluorene)] is shown in Figure 17.
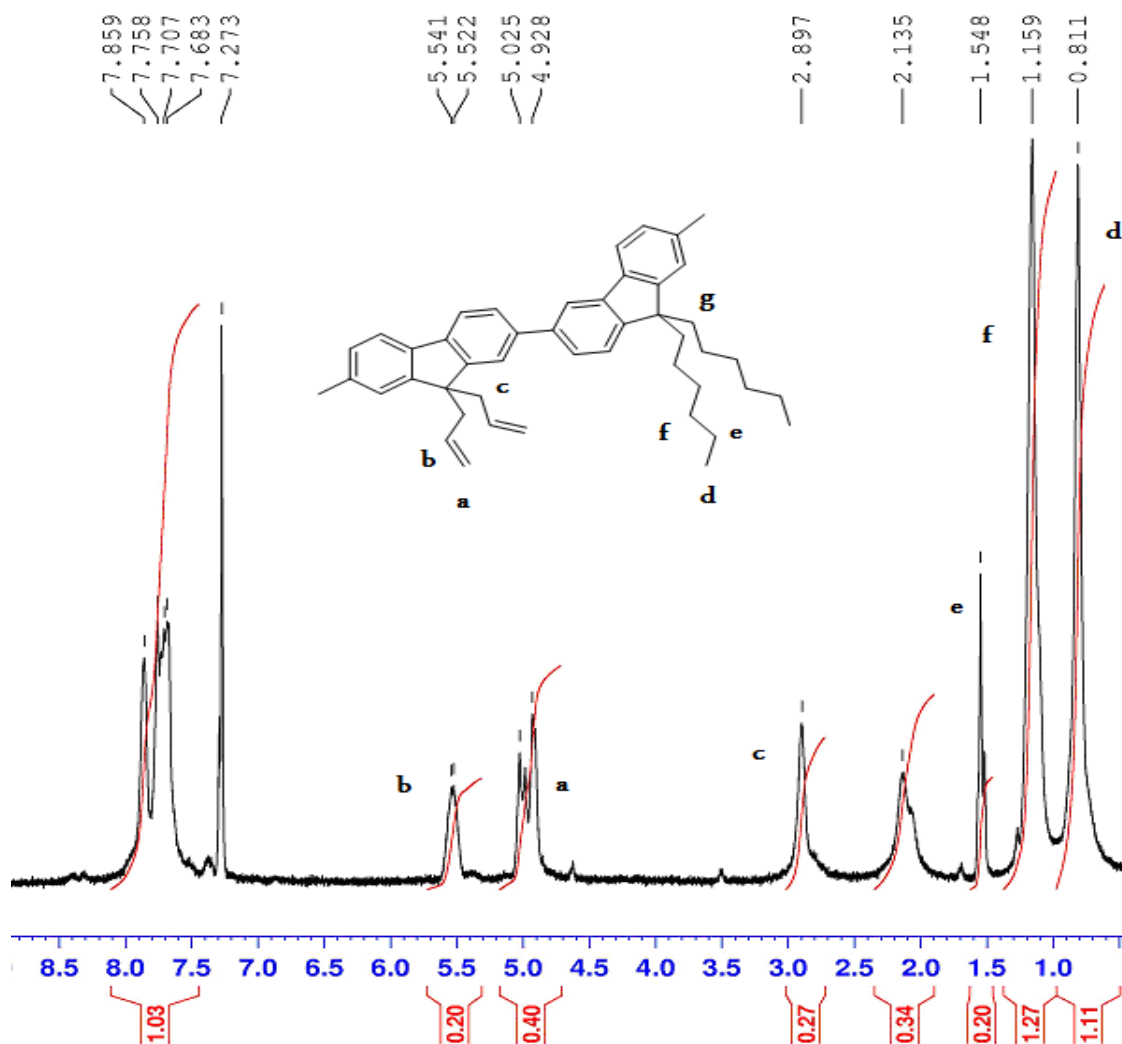
**Figure 17:** $^1$H-NMR spectrum of the polymer poly[(9,9-bis{propenyl}-9H-fluorene)-co-(9,9-dihexyl-9H-fluorene)] (**P1**) (400 MHz, CDCl$_3$, 25$^0$C).

In $^1$H-NMR spectrum of **P1** polymer, multiplet was observed in 7.85 ppm due to aromatic protons and at 5.54 ppm quartet was observed due to –CH protons. Triplet at 5.02 ppm observed due to –CH$_2$ protons at the end of side chain and multiplets at 2.89, 1.54, 1.15 and 0.8 ppm due to protons of alkyl chain. FT-IR spectrum of **P1** polymer is shown in figure 18. In the spectrum aromatic Ph-H stretching band was observed at 3023 cm$^{-1}$ and aliphatic –C-H stretching at 2928 cm$^{-1}$. A weak peak at 1609 cm$^{-1}$ was observed due to C=C stretching of benzene rings and characteristic peak of R-CH=CH$_2$ observed at 919 cm$^{-1}$ due to out- of - plane C-H bendings.

For optical characterization UV-vis and fluorescence spectroscopy were performed in THF. Absorption and emission spectra of the polymer **P1** are shown in Figure 19. As can be seen from spectra, maximum absorption band at 383 nm and fluorescence maximum band at 418 and 439 nm were observed, respectively.

### 2.1.4 Synthesis and characterization of poly[(9,9-bis{carboxymethylsulfonyl-propyl}fluorenyl-2,7-diyl)-co-(9,9-dihexyl-9H-fluorene) (P2)

Thiol-ene click chemistry was used in the synthesis of **P2** (Scheme 10). Polymer **P1** was disolved in chloroform and treated with mercaptoacetic acid under Ar gas and stirred about 48h at room temperature. Solvent was evaporated by rotary evaporator and dissolved in THF and precipitated into water to remove the excess acid. Yellow powder was collected via filtration and dried under vacuum.
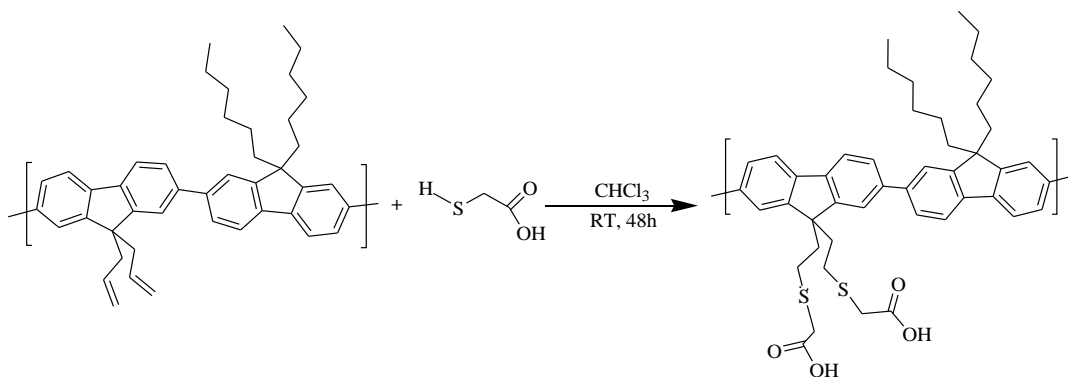


**Scheme 10:** Synthesis of **P2** through thiol-ene click chemistry.

Successful functionalization of **P1** to **P2** polymer was confirmed by FT-IR spectroscopy. FT-IR spectrum is shown in Figure 18. After functionalization a sharp peak for –C=O group at 1705 cm$^{-1}$ was observed.
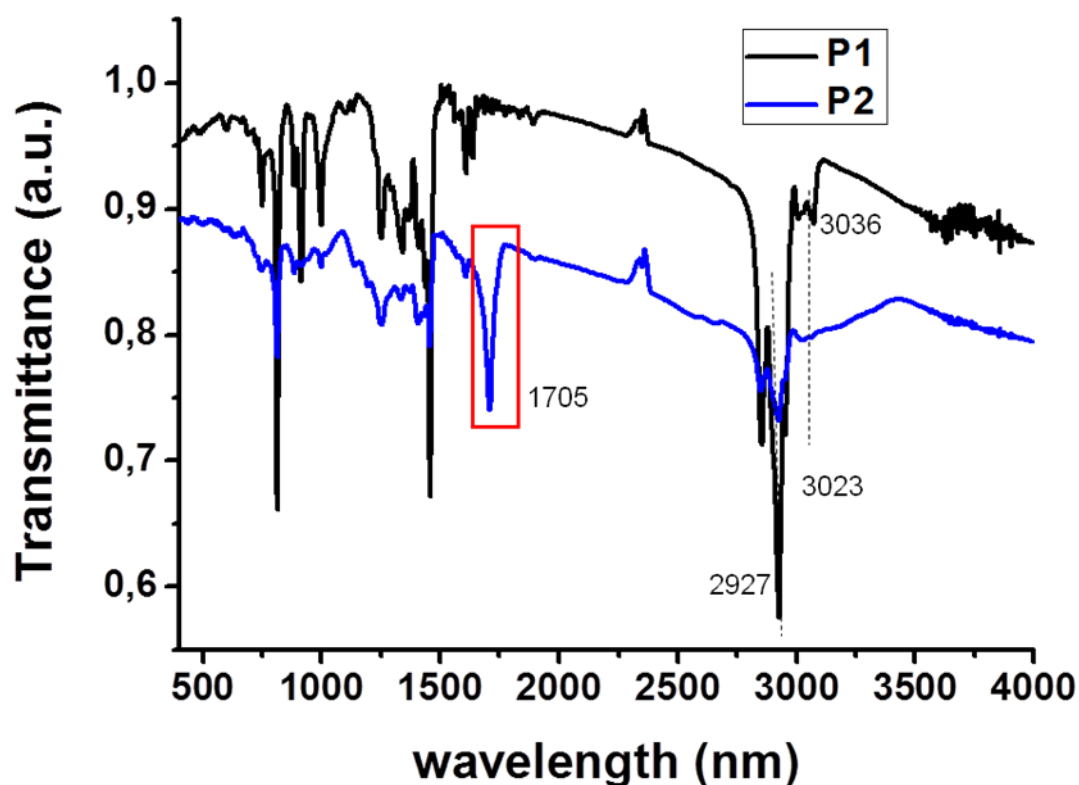
**Figure 18:** FT-IR spectra of the polymer poly[(9,9-bis{propenyl}-9H-fluorene)-co-(9,9-dihexyl-9H-fluorene)] (**P1**) and poly[(9,9-bis{carboxymethylsulfonyl-propyl}fluorenyl-2,7-diyl)-co-(9,9-dihexyl-9H-fluorene) (**P2**).

Optical characterization of **P2** was performed by UV-Vis and fluorescence spectroscopy and compared with the optical data of **P1** polymer in order to see whether there are any changes in optical properties of **P1**. Absorption and emission spectra of polymer **P2** are shown in figure 19. From spectra we observed absorption band at 384 nm which is similar to **P1** polymer, only 1 nm red shifting was observed and in the emission spectrum peaks are seen at 421, 440 nm which are 3 and 1 nm red-shifted due to the addition of hydrophilic group to the side chain of the polymer.
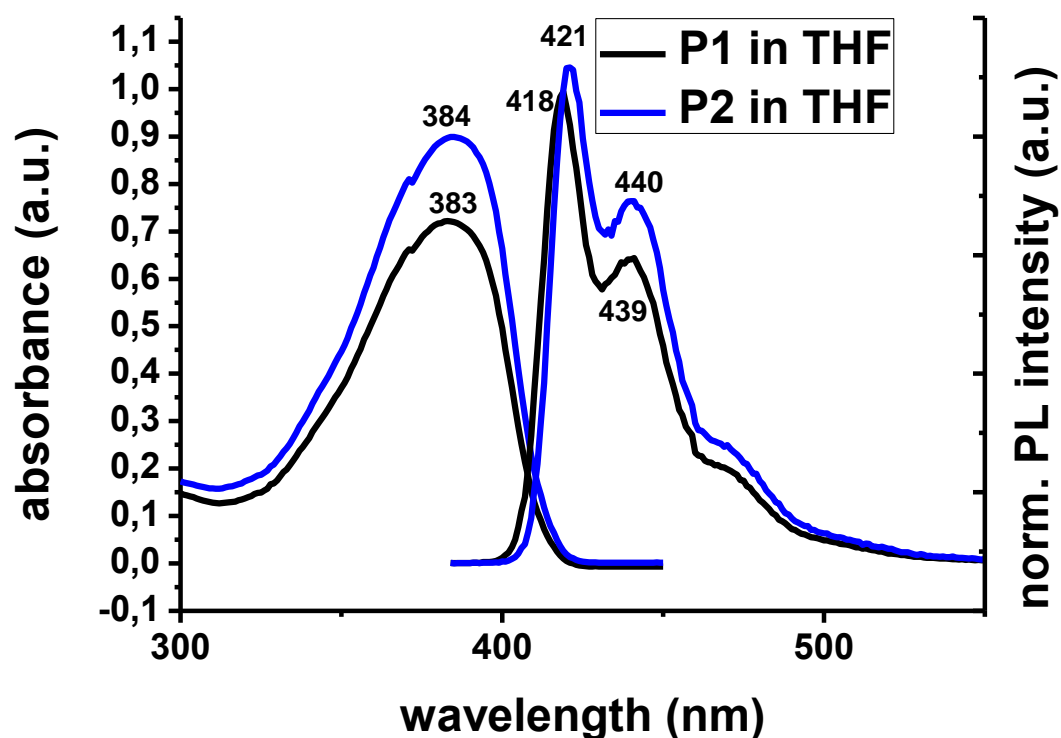
**Figure 19:** UV-Vis and PL spectra of the polymer poly[(9,9- bis{propenyl}-9H-fluorene)-co-(9,9-dihexyl-9H-fluorene)] (**P1**) ($\lambda_{ex}$=383nm) and poly[(9,9-bis{carboxymethylsulfonyl-propyl}fluorenyl-2,7-diyl)-co-(9,9-dihexyl-9H-fluorene) (**P2**) ($\lambda_{ex}$=384nm).

## 2.1.5 Synthesis and characterization of polymer poly[(9,9-bis{propenyl}-9H-fluorene)-co-(benzothiadiazole)] (P3)

**P3** was synthesized as shown in the Scheme 11. Monomer **M2** and 2,1,3-benzothiadiazole-4,7-bis (boronic acid pinocol ester) were coupled using Suzuki coupling reaction conditions. Purification was done by precipitation of **P3** solution in THF into cold methanol. Orange powder was obtained in 47% yield.
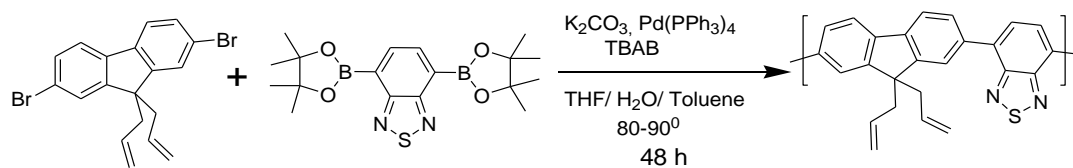
**Scheme 11:** Polymerization reaction of poly[(9,9- bis{propeny}fluorenyl-2,7-diyl))-co-(1,4-benzo-{2,1,3}-thiodiazole)] (**P3**).

Characterizations of polymer was done by ^{1}H-NMR spectrometry, UV-Vis spectroscopy, fluorescence spectroscopy, and FT-IR spectroscopy.

^{1}H-NMR spectrum of the polymer poly[(9,9- bis{propeny}fluorenyl-2,7-diyl))-co-(1,4-benzo-{2,1,3}-thiodiazole)] is shown in figure 20. In ^{1}H-NMR spectrum of **P3** polymer, multiplet was observed at 7.53 ppm due to aromatic protons and at 5.24 ppm a multiplet was observed due to –CH protons. Another multiplet at 4.86 ppm was observed due to –CH$_2$ protons at the end of side chain and triplet at 2.64 ppm due to protons of –CH$_2$ labelled as *c*.
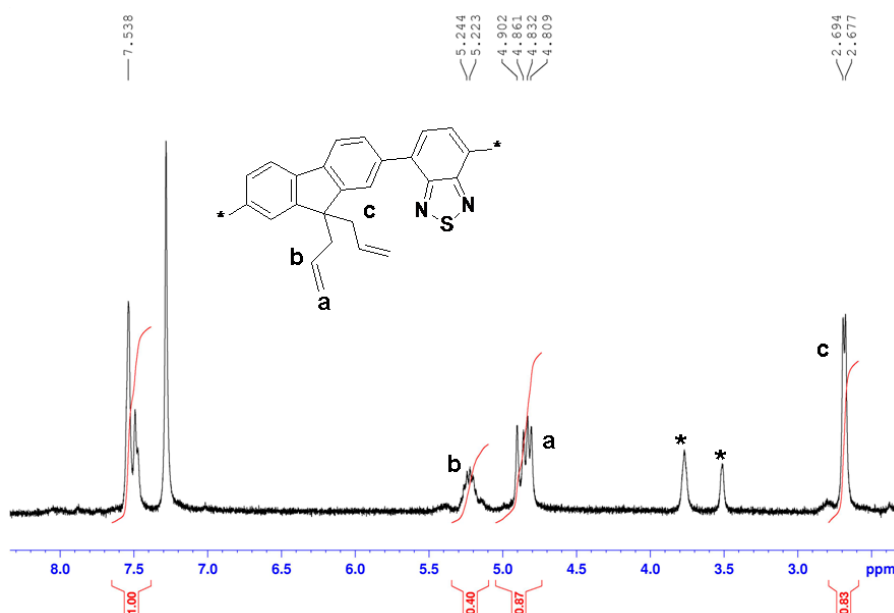


**Figure 20:** ^{1}H-NMR spectrum of the polymer poly[(9,9-bis{propenyl}-9H-fluorene)-co-(benzothiadiazole)] (**P3**). *Denotes for impurities in solvent. (400 MHz, CDCl$_3$, 25$^0$C).

FT-IR spectrum of the polymer **P3** is shown in figure 21. FT-IR spectrum shows a peak at 3074 cm$^{-1}$ for Ph-*H* stretching and characteristic peak of R-CH=CH$_2$ was observed at 910 cm$^{-1}$ due to out- of - plane C-H bendings**.** Peaks are observed at 1461 cm$^{-1}$, 2918 cm$^{-1}$ and 1609 cm$^{-1}$ for –C=N stretching in benzothiadiazole moiety and aliphatic –C-H stretching, C=C stretching of benzene rings, respectively. Absorption and emission properties of polymer **P3** was performed in THF and their spectra are shown in Figure 22 along with P4 polymer. Maximum absorption bands at 317 and 447 nm and fluorescence maximum band at 537 nm were observed, respectively.

### 2.1.6 Synthesis and characterization of polymer poly[(9,9-bis{carboxymethylsulfonyl-propyl}fluorenyl-2,7-diyl)-co(1,4-benzo-{2,1,3}-thiodiazole)] (P4)

Thiol-ene click chemistry was used in the synthesis of **P4** (Scheme 12). Polymer poly[(9,9- bis{propeny}fluorenyl-2,7-diyl))-co-(1,4-benzo-{2,1,3}-thiodiazole)] was disolved in chloroform and treated with mercaptoacetic acid under Ar gas and stirred about 48h at room temperature. Solvent was evaporated in rotary evaporator and dissolved in THF and precipitated into water to remove the excess acid. Orange powder was collected via ultracentrifugation at 2500 rpm and dried under vacuum.
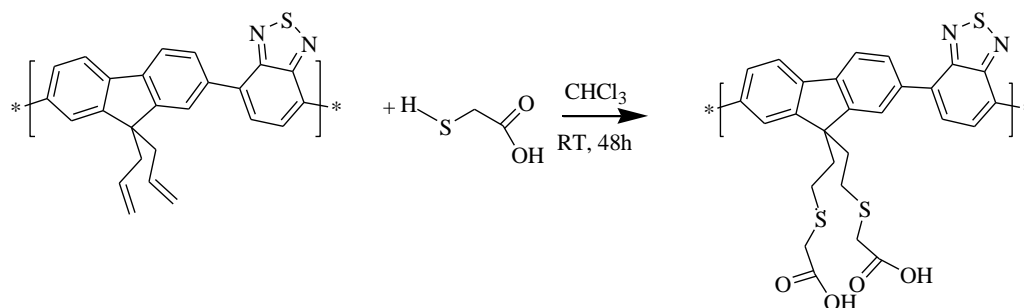


**Scheme 12:** Synthesis of poly[(9,9- bis{carboxymethylsulfonyl-propyl}fluorenyl-2,7-diyl)-co(1,4-benzo-{2,1,3}-thiodiazole)] (**P4**)

Successful functionalization of poly[(9,9- bis{propeny}fluorenyl-2,7-diyl))-co-(1,4-benzo-{2,1,3}-thiodiazole)] (**P3)** to **P4** polymer was confirmed by FT-IR

33

spectroscopy. FT-IR spectrum shown in Figure 21. After functionalization a sharp peak at 1713 cm$^{-1}$ was observed due to C=O stretching.



**Figure 21:** FT-IR spectra of the polymer poly[(9,9- bis{propeny}fluorenyl-2,7-diyl))-co-(1,4-benzo-{2,1,3}-thiodiazole)] (**P3**) and poly[(9,9- bis{carboxymethylsulfonyl-propyl}fluorenyl-2,7-diyl)-co(1,4-benzo-{2,1,3}-thiodiazole)]  (**P4)**

Optical characterization of **P4** was performed by UV-Vis and fluorescence spectroscopy and compared with optical data of **P3** polymer in order to see whether there are any changes in the optical properties of **P3**. Absorption and emission spectra of polymer poly[(9,9- bis{carboxymethylsulfonyl-propyl}fluorenyl-2,7-diyl)-co(1,4-benzo-{2,1,3}-thiodiazole)]  (**P4)** is shown in figure 22. From the spectra we observed absorption band at 318 and 449 nm which is similar to **P3** polymer, only 1, 2 nm red shifting was observed and in the emission spectrum peaks are seen at 541

34

nm which are 4 nm red-shifted due to the addition of hydrophilic group to the side chain of the polymer.



**Figure 22:** Absorption and emission spectra of poly[(9,9- bis{propeny}fluorenyl-2,7-diyl))-co-(1,4-benzo-{2,1,3}-thiodiazole)] (**P3**) ($\lambda_{ex}$=447nm)  and poly[(9,9-bis{carboxymethylsulfonyl-propyl}fluorenyl-2,7-diyl)-co(1,4-benzo-{2,1,3}-thiodiazole)]  (**P4**) ($\lambda_{ex}$=449nm)  polymers.

## 2.1.7    Synthesis    and    characterization    of    polymer    poly[(9,9-bis{3-bromopropyl}fluorenyl-2,7-diyl)-co-(1,4-benzo-{2,1,3}-thiodiazole)] (**P5**)

**P5** was synthesized as shown in the Scheme 13. **M1** and 2,1,3-benzothiadiazole-4,7-bis (boronic acid pinocol ester) were coupled using Suzuki coupling reaction conditons. Purification was done by precipitation of **P5** solution in THF into cold methanol and water mixture. Orange powder was obtained by centrifugation in 56% yield.
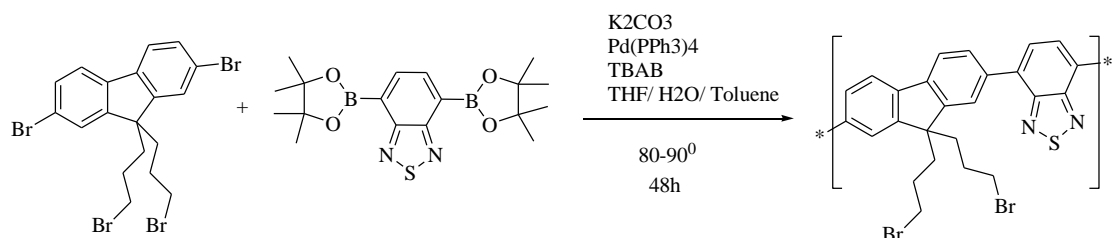
**Scheme 13:** Synthesis mechanism of poly[(9,9-bis{3-bromopropyl}fluorenyl-2,7-diyl)-co-(1,4-benzo-{2,1,3}-thiodiazole)] (**P5**)

Characterization of polymer **P5** was done by ^{1}H-NMR, UV-Vis, fluorescence and FT-IR spectroscopy. ^{1}H-NMR spectrum of the polymer **P5** is shown in Figure 23. In ^{1}H-NMR spectrum aromatic protons due to fluorene and benzothiadiazole appeared at 7.5-8.1 ppm and quartet coming from the methylene protons near bromine atom was observed at 3.26 ppm because of the electron withdrawing effect of bromine atom. Another quartet was observed at 2.41 ppm due to methylene protons near fluorene ring. Multiplet at 1.25 ppm is observed due to aliphatic protons in side chain of the polymer.
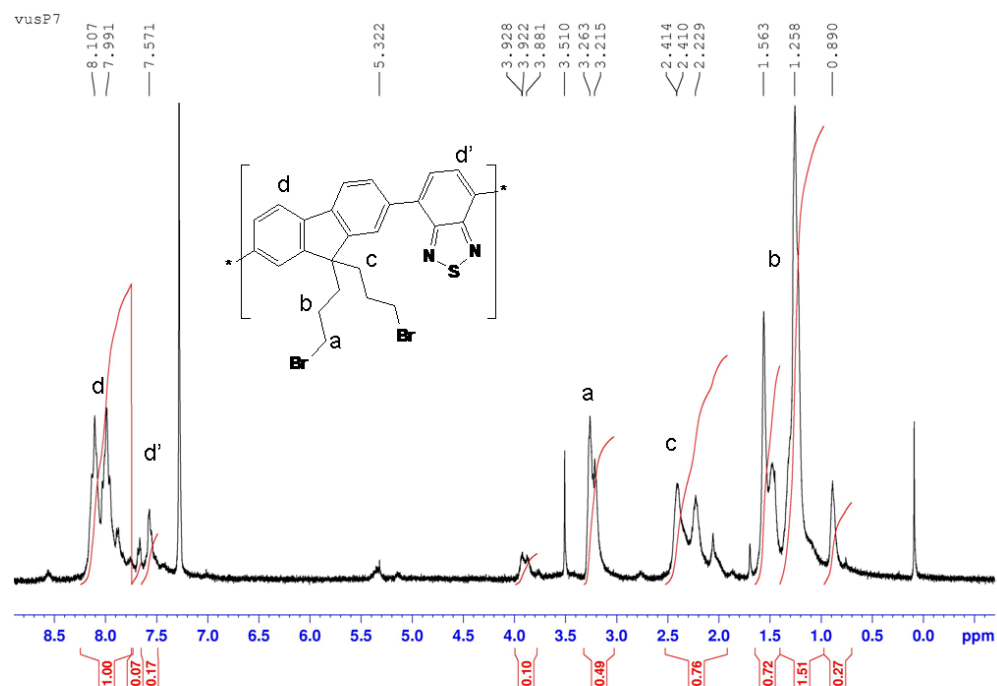
**Figure 23:** ^{1}H-NMR spectrum of the polymer poly[(9,9-dibromopropane-9H-fluorene)-co-(benzothiadiazole)] (**P5**) (400 MHz, CDCl$_3$, 25$^0$C).

FT-IR spectrum of **P5** polymer is shown in figure 24. In spectra aromatic carbon hydrogen stretching band observed at 3033 cm^{-1} and aliphatic –C-H stretching at 2918 cm^{-1}. A weak peak due to C=C bond was observed at 1597 cm^{-1}.

For optical characterization UV-vis and fluorescence spectroscopy were performed in THF. Absorption and emission spectra of the polymer **P5** are shown in Figure 25. As can be seen from spectra, maximum absorption band at 318 and 440 nm and fluorescence maximum band at 535 nm were observed, respectively.

**2.1.8 Synthesis and characterization of polymer poly[(9,9-bis{3-azidopropyl}fluorenyl-2,7-diyl)-co-(benzothiadiazole)] (P6)**

Polymer **P5** was used in the synthesis of **P6**, bromine group of the **P5** converted to azide group by using nucleophilic reaction in the presence of NaN$_3$. **P5** and NaN$_3$ were dissolved in small amount of DMF and refluxed at $60^0$ C about 24h. The reaction scheme of **P6** is shown in Scheme 14. Reaction mixture precipitated into pure water to purify **P6** and orange brown-orange powder was collected via filtration and centrifugation.
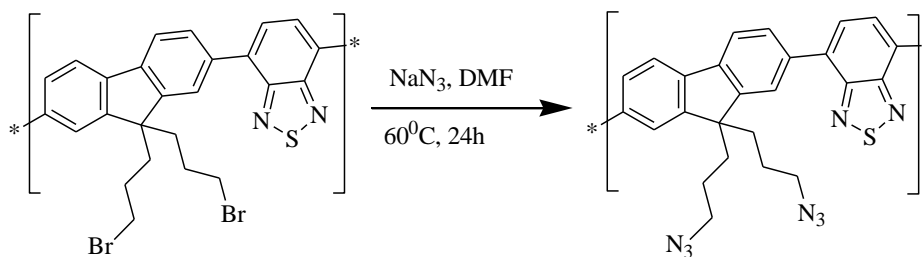


**Scheme 14:** The synthesis of poly[(9,9-bis{3-azidopropyl}fluorenyl-2,7-diyl)-co-(benzothiadiazole)] (**P6**).

Characterization of polymer **P6** was done by ^{1}H-NMR, UV-Vis, fluorescence and FT-IR spectroscopy. ^{1}H-NMR spectrum of the polymer **P6** is shown in Figure 26. In ^{1}H-NMR spectrum aromatic protons due to fluorene and benzothiadiazole appeared at 7.5-8.1 ppm and quartet coming from the methylene protons near bromine atom was observed at 3.21 ppm because of the electron withdrawing effect of azide group. Another quartet was observed at 2.40 ppm due to methylene protons near fluorene ring. Multiplet at 1.25 ppm is observed due to aliphatic protons in side chain of the polymer.
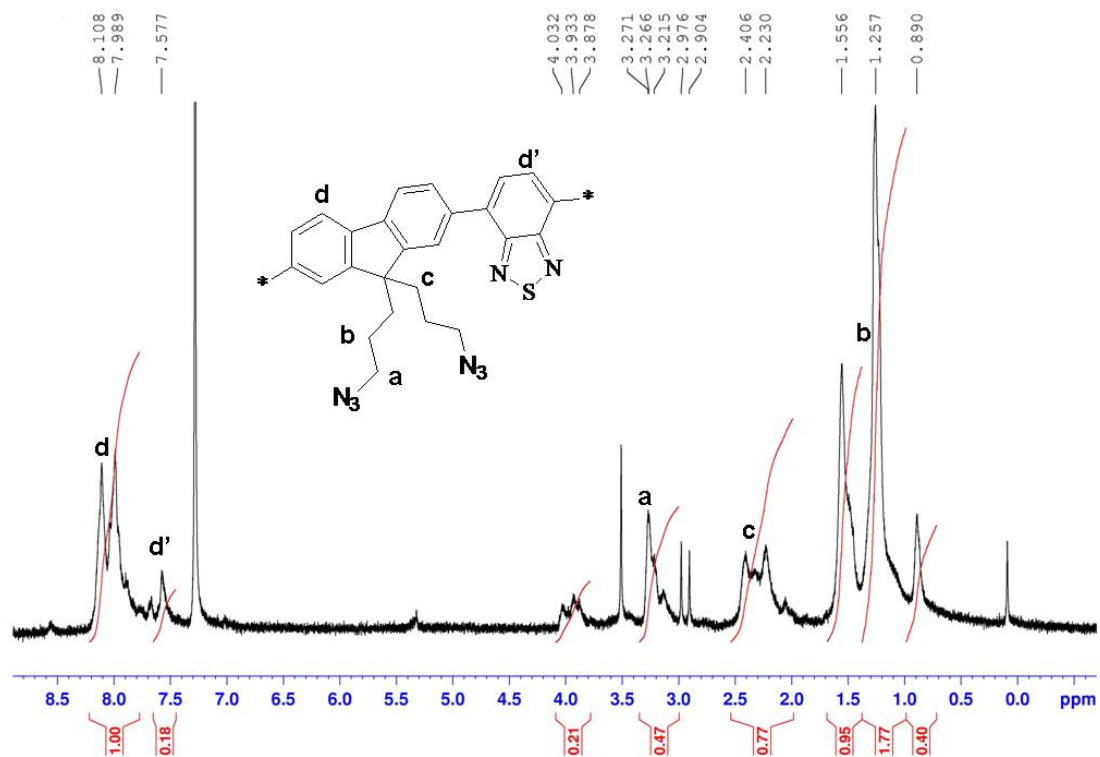
**Figure 26:** ^{1}H-NMR spectrum of the polymer poly[(9,9-bis{3-azidopropyl}fluorenyl-2,7-diyl)-co-(benzothiadiazole)] (**P6**) (400 MHz, CDCl$_3$, 25$^0$C).

Successful functionalization of **P5** to poly[(9,9-bis{3-azidopropyl}fluorenyl-2,7-diyl)-co-(benzothiadiazole)] (**P6**) polymer was confirmed by FT-IR spectroscopy, as well (figure 24). After functionalization a sharp carbon-azide stretching peak at 2088 cm$^{-1}$ was observed.
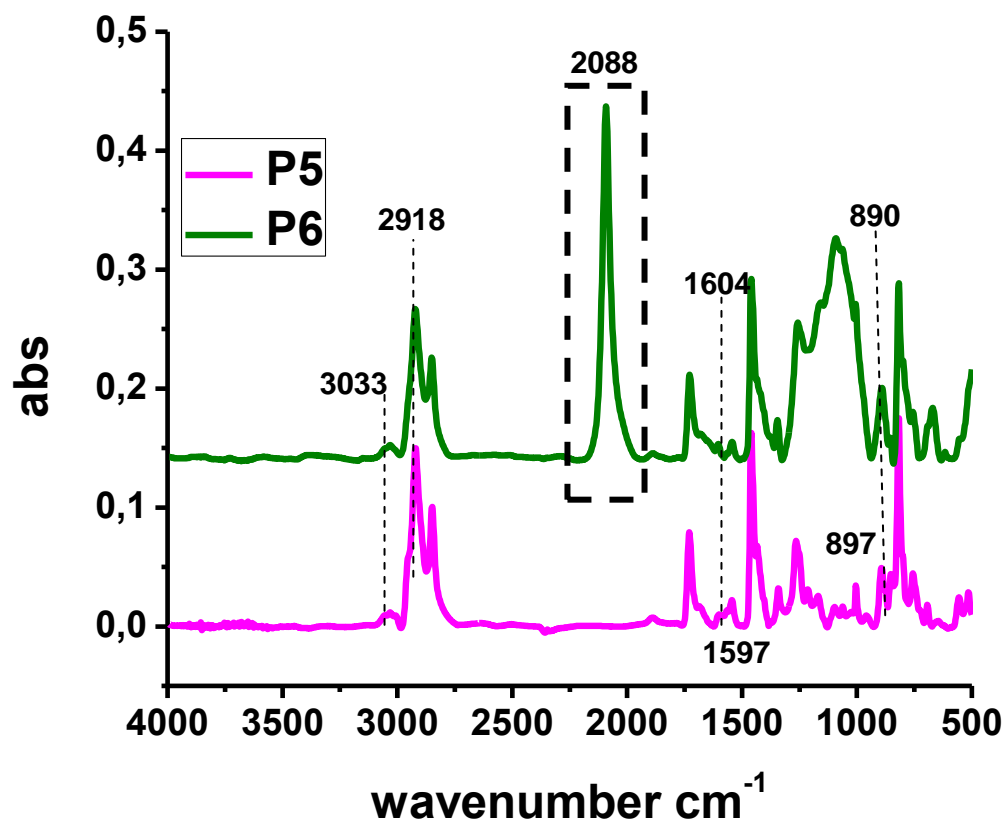
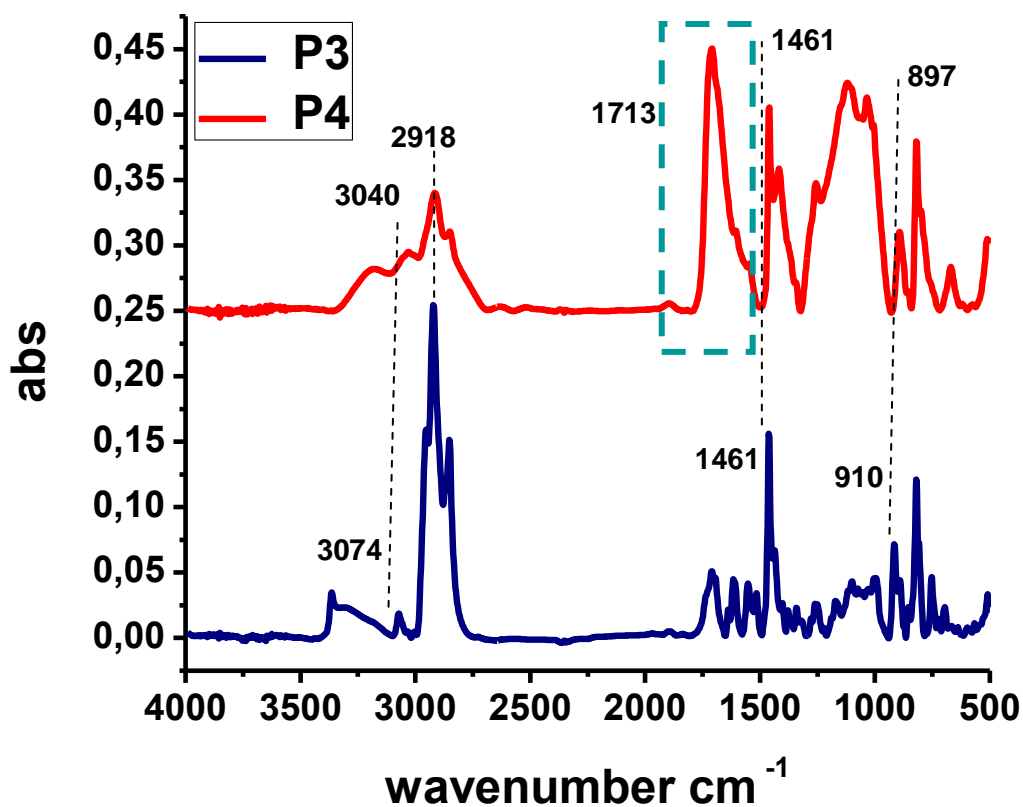**Figure 24:** FT-IR spectra of poly[(9,9-bis{3-bromopropyl}fluorenyl-2,7-diyl)-co-(1,4-benzo-{2,1,3}-thiodiazole)] (**P5**) and poly[(9,9-bis{3-azidopropyl}fluorenyl-2,7-diyl)-co-(benzothiadiazole)] (**P6**) polymers.
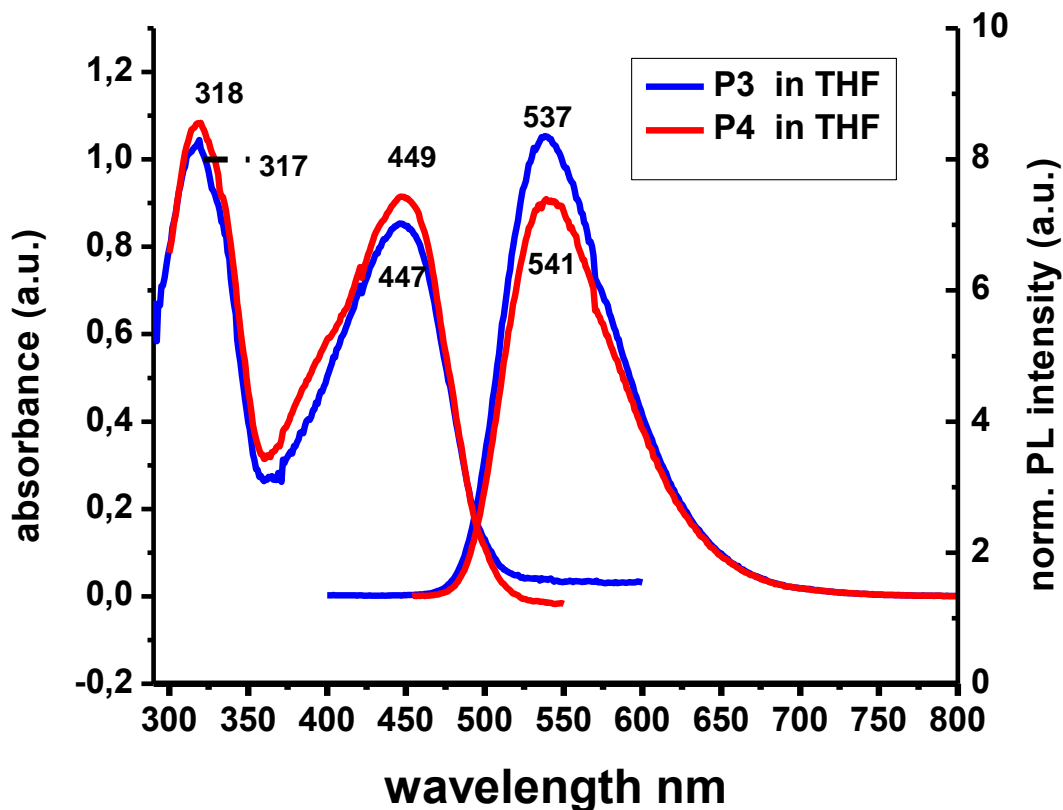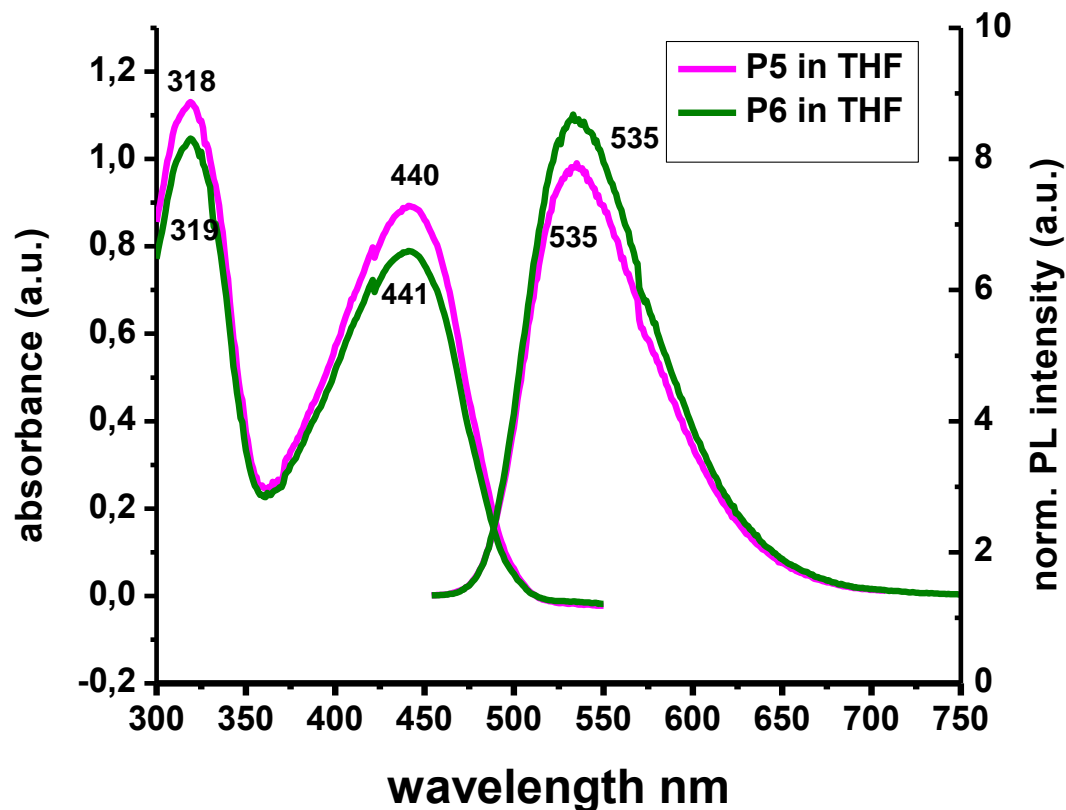
**Figure 25:** Absorption and emission spectra of polymer poly[(9,9-bis{3-bromopropyl}fluorenyl-2,7-diyl)-co-(1,4-benzo-{2,1,3}-thiodiazole)] (**P5**) ($\lambda_{ex}$=440nm)  and poly[(9,9-bis{3-azidopropyl}fluorenyl-2,7-diyl)-co-(benzothiadiazole)]  (**P6**) ($\lambda_{ex}$=441nm).

Optical characterization of **P6** was performed by UV-Vis and fluorescence spectroscopy and compared with the optical data of **P5** polymer in order to see whether there are any changes in optical properties of **P5**. Absorption and emission spectra of polymer **P6** are shown in figure 25. From spectra we observed absorption band at 319 and 441 nm which is similar to **P5** polymer, only 1 nm red shifting was observed and in the emission spectrum peaks are seen at 535 nm which are the same with **P5** polymer.

## 2.2 Synthesis of Water Dispersible Conjugated polymer nanoparticles (CPNs)

In the synthesis of CPNs, reprecipitation method was used. In this method basically the polymer solution in a good solvent (e.g. THF) is injected into a rapidly stirring poor solvent (e.g. $H_2O$). Hydrophobic polymer chains tend to avoid from water molecules by folding as nanoparticles and after the removal of THF, water-dispersible spherical nanoparticles are obtained. In order to confer stability and shape persistency in the nanoparticles, the allyl or azides groups of polymer chains were lightly cross-linked under UV-light either through decomposition of azide into reactive nitrene species or through 2+2 cycloaddition. The nanoparticles have been characterized by spectroscopic (UV-Vis, Fluorescent), imaging (SEM, TEM) and dynamic light scattering/zeta potential for their optical properties (absorbance, emission, fluorescent quantum yields), their morphology and sizes/stability, respectively.

## 2.2.1 Synthesis and characterization of poly[(9,9-bis{propenyl}-9H-fluorene)-co-(9,9-dihexyl-9H-fluorene)] nanoparticles P1NPs

**P1** was dissolved in THF and stirred for 1h. The resulting solution was filtered with syringe filter and injected into rapidly stirring excess water. The mixture was stirred further 1 h. THF was removed under reduced pressure to obtain nanoparticle dispersion in water. The volume was concentrated under reduced pressure to yield a clear solution. Size of the particles (28 nm) was measured by dynamic light scattering (DLS) as shown in figure 27.
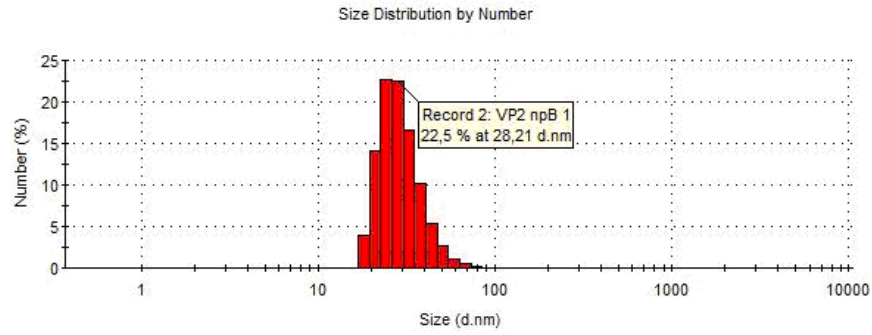
**Figure 27:** Size distributions by number of **P1NPs** nanoparticles

Morphological characterization of **P1NPs** was performed with SEM and AFM. Topographical image of in figure 28 shows that nanoparticles have spherical shape.
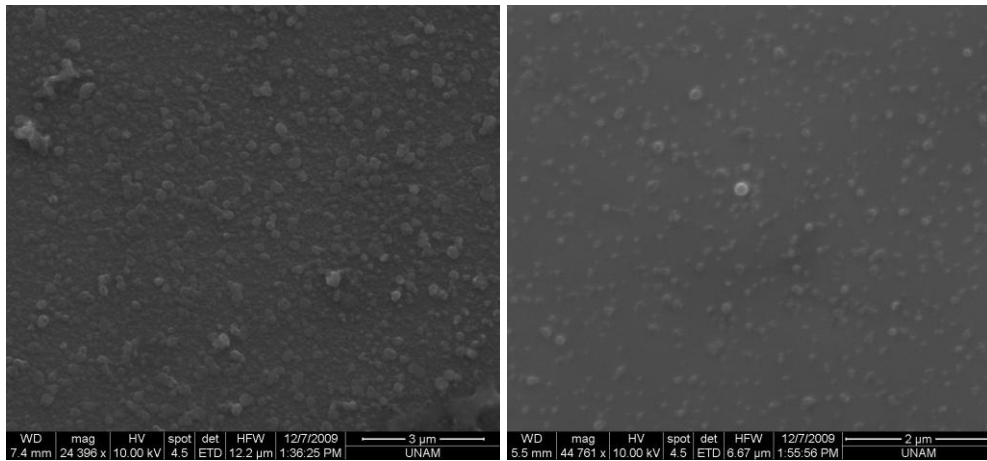


**Figure 28:** SEM images of **P1NPs**

Atomic force microscopy results also show that **P1NPs** have spherical morphology (Figure 29).
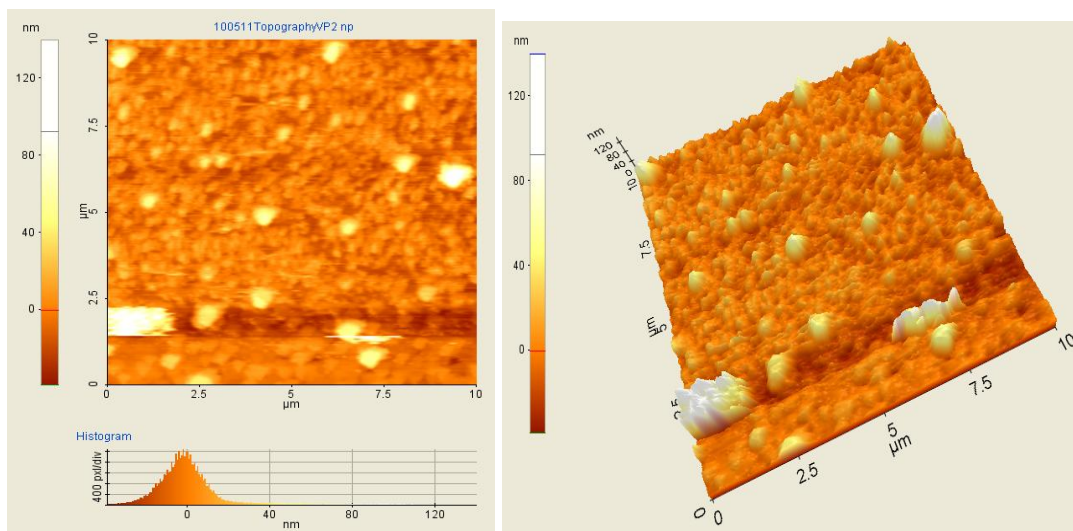
**Figure 29:** Topographical AFM images of **P1NPs**

Absorption and emission of nanoparticles were determined by UV-Vis and Fluorescent spectroscopies; nanoparticles absorb at 385 nm which is 2 nm red shifted compared with **P1** polymer while excitation with 385 nm light gives blue fluorescence with maximum at 425 and 450 nm which are 7 and 11 nm red shifted compared to polymer solution in THF due to nanoparticle formation.

In order to make this **P1NPs** stable, network was created around the nanoparticles by cross-linking of allyl groups by [2+2] cycloaddition reaction and as a result core-shell structure was obtained. Cross-linking was performed by irradiating nanoparticle solution by 254 nm UV light about 15 min, 30 min, 1h, 2h, 3h, 4h, 5h timescale. UV-Vis spectra are shown in figure 30.
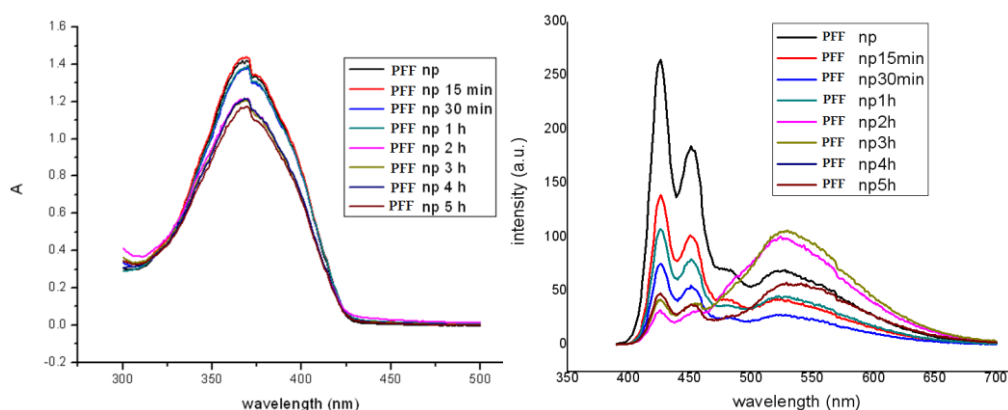
**Figure 30:** Absorption and emission spectra of the cross-linked **P1NPs** (PFF) nanoparticles under 254 nm UV light

In the absorption spectra small changes were observed while in the emission spectra intensity of emission peak in the blue region 400-450 nm decreased while the intensity of a peak at green region 450-650 nm increased. From figure 30 we can see clearly the changes in the emission colour of the nanoparticles from blue to green. The origin of the green emission in polyfluorene-based conjugated polymer has been investigated extensively and in general attributed to aggregate/excimer formation or keto defects.[55,56] However, recently it was shown that cross-linking *via* azide decomposition in the absence of oxygen which is required for the keto defect formation could still cause the emergence of the green emission band.[54] There are no significant changes observed in the UV-Vis spectra of nanoparticles upon UV-exposure while the emission spectra change; this suggest that the defects must be in minute quantity and have low molar absorptivity not to be seen in the UV-Vis spectrum. These defects might have a low lying energy state that can act as a energy trap like in the fluorenone containing polymers;[55, 56] consequently cross-linking most likely facilitates the excitation energy migration and energy transfer to the energy traps because the rotational freedom of polymer chains is greatly reduced upon cross-linking. In this way, core-shell type of nanostructures in which blue emitting core and green-yellow emitting shell can be obtained.
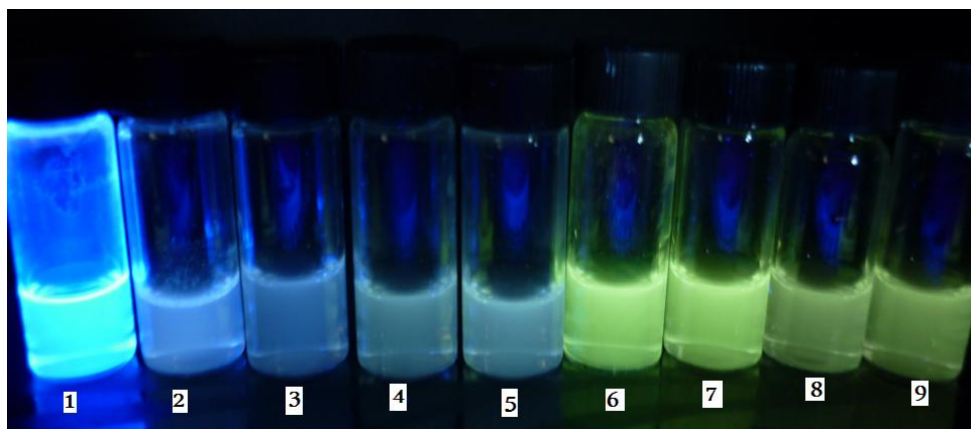
**Figure 31:** P1NPs polymer nanoparticles treated under 254nm UV light over varying time scale for crosslinking of allyl groups through 2+2 cycloaddition (**1: P1** polymer solution in THF, **2: P1NPs** in water, **3:** 15 min cross-linked nanoparticles (CLNPs), **4:** 30 min CLNPs, **5:** 1 h CLNPs, **6:** 2 h CLNPs, **7:** 3 h CLNP, **8:** 4 h CLNPs, **9:** 5 h CLNPs)

Figure 31 shows the photos of P1NPs polymer nanoparticles treated under 254 nm UV light over varying time scale for crosslinking of allyl groups through 2+2 cycloaddition. Size distributions of cross-linked **P1NPs** were measured and compared; no changes in the sizes of nanoparticles were observed indicating the stability of nanoparticles during photochemical cross-linking.
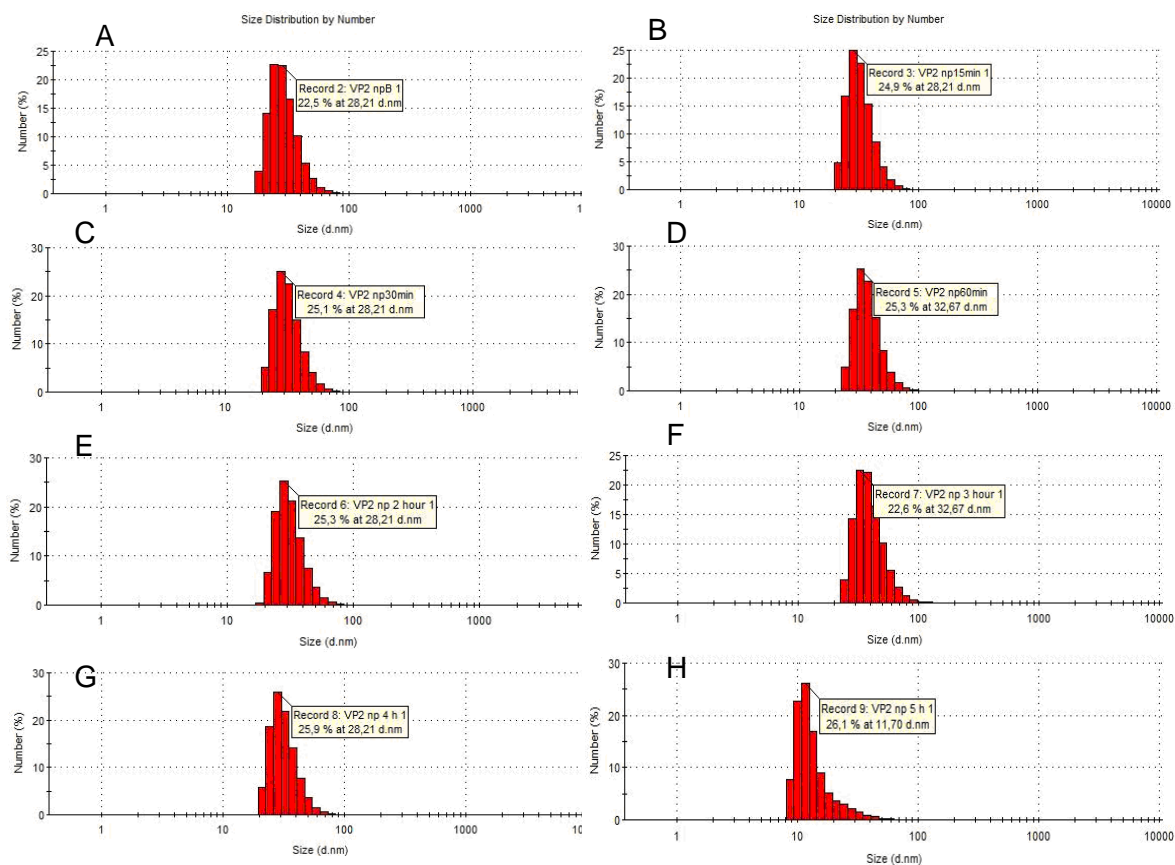
**Figure 32:** Size distribution histograms of A- **P1NPs** in water, B- 15 min cross-linked, C- 30 min, D-1 h cross-linked, E- 2 h, F-3 h, G-4 h and H- 5 h cross-linked **P1NPs** polymer nanoparticles

## 2.2.2 Synthesis and characterization of poly[(9,9- bis{propeny}fluorenyl-2,7-diyl))-co-(1,4-benzo-{2,1,3}-thiodiazole)] nanoparticles P3NPs

**P3** polymer was used in **P3NPs** polymer nanoparticles synthesis. **P3** was dissolved in THF and stirred for 1h. The resulting solution was filtered with syringe filter and injected into rapidly stirring excess water. The mixture was stirred further 1 h. THF was removed under reduced pressure to obtain nanoparticle dispersion in water. The volume was concentrated under reduced pressure to yield a clear solution. Average size was measured as 58 nm by dynamic light scattering as shown in figure 33. To provide quantitative information about stability of nanoparticles in the solution, zeta potential measurement was applied. The zeta potential value for **P3NPs** was

measured as -32 eV, which indicates the formation of stable nanoparticle dispersion caused by the repulsion between the nanoparticles.
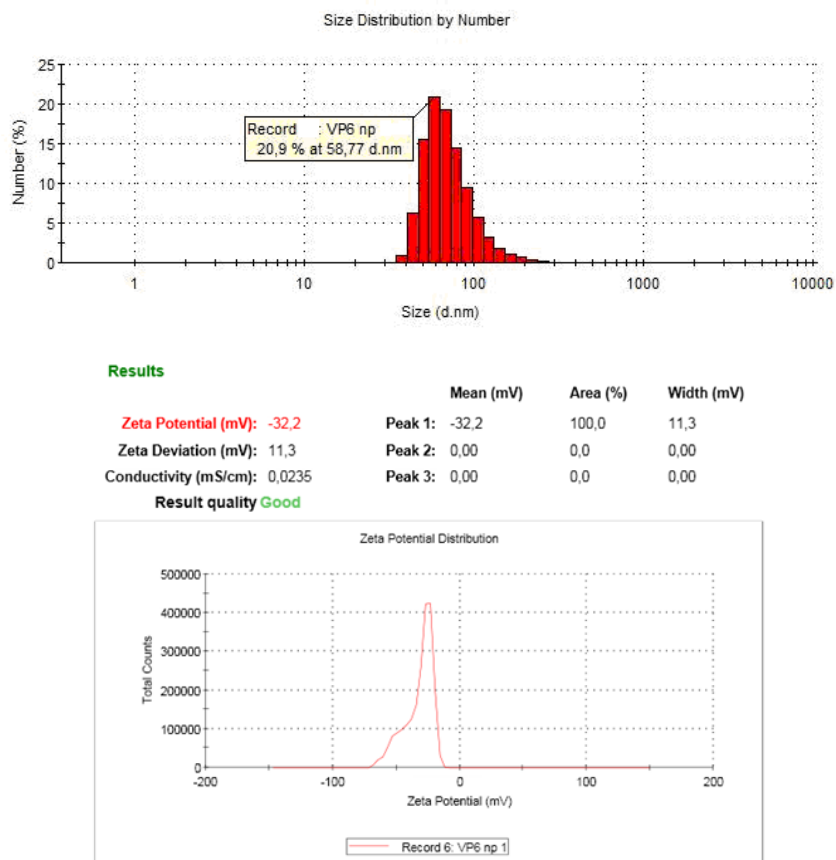


**Figure 33:** DLS and zeta potencial results of the **P3NPs**

Morphological analysis of **P3NPs** polymer nanoparticles was done by SEM, TEM and AFM imaging techniques. TEM results of the **P3NPs** nanoparticles are shown in figure 34.
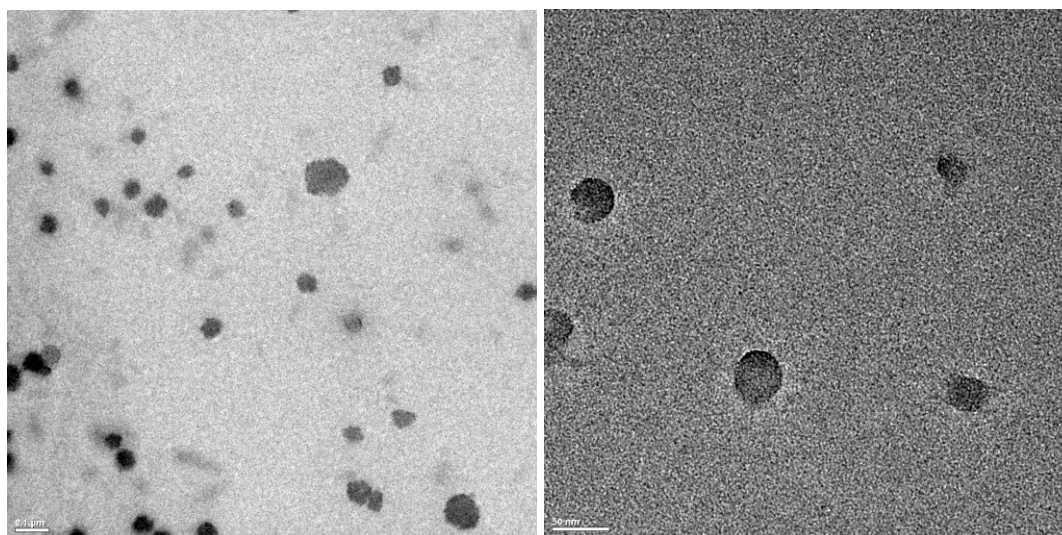
**Figure 34:** TEM images of **P3NPs**

AFM images of **P3NPs** show that particles have spherical shape as shown in figure 35.
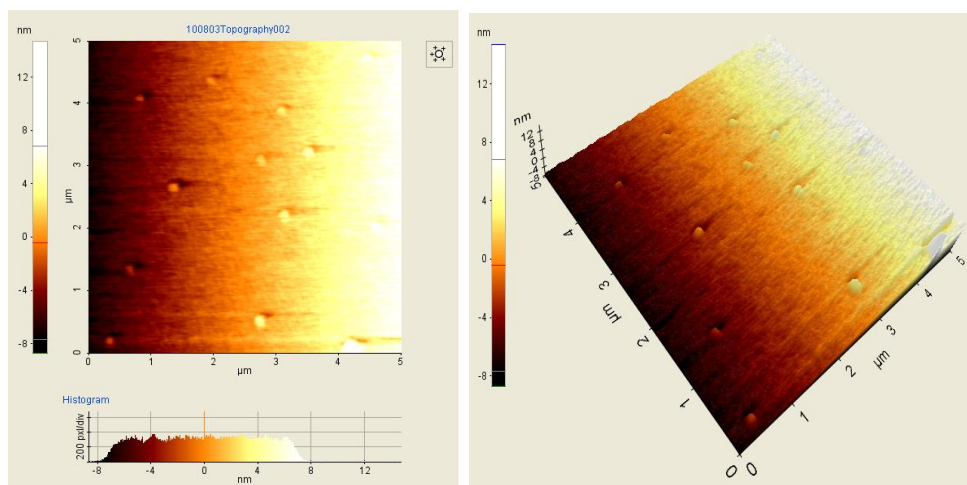


**Figure 35:** AFM topography images of **P3NPs**

Optical characterization of **P3NPs** was performed with UV-Vis and fluorescence spectroscopy and compared with **P3** polymer in THF and in solid state (Figure 36). Maximum absorption peaks were observed at 317, 447 nm for polymer in THF; these are almost the same for P3NPs in water but approximately 10 and 25 nm red shifted for the film of P3. However, when **P3NPs** were excited with 447 nm light, green-yellow emission band at 550 nm was observed which was 13 nm red shifted

compared to the emission band of **P3** in THF. If the emission wavelengths of **P3NPs** compared with the emission wavelength of **P3** film, it can be seen that only there is 8 nm differences between them (550 nm for **P3NPs** water dispersion and 558 nm for P3 film) indicating that optical properties of nanoparticles resembles to polymer's solid state properties.
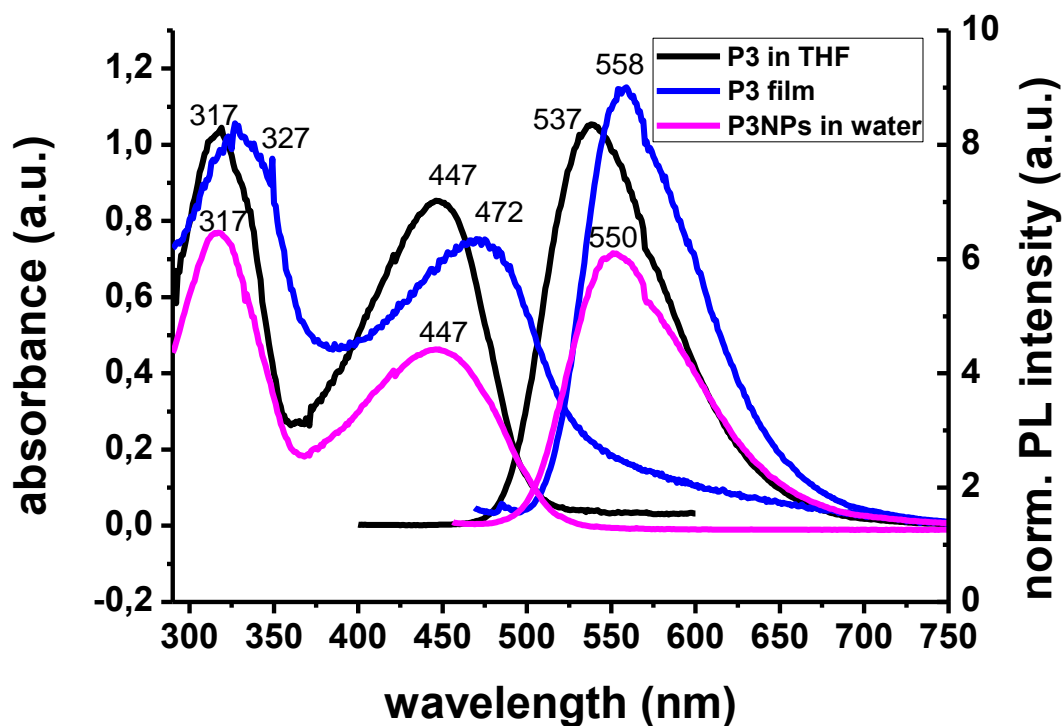


**Figure 36:** Absorption and emission spectra of the **P3**($\lambda_{ex}$=447nm) in THF, **P3**($\lambda_{ex}$=472nm) film and **P3NPs**($\lambda_{ex}$=447nm).

After characterization of **P3NPs** nanoparticles were cross-linked using 254 nm UV light about 15 min, 30 min, 1h, 2h, 3h, 5h timescale with [2+2] cycloaddition reaction. After treatment all samples were compared to determine stability of nanoparticles. Differently from **P1NPs**, **P3NPs** shows extreme photostability. Even after 5 h irradiation with 254nm UV light in absorption and emission only small decrease in intensity was observed. Absorbance and emission spectra is shown in figure 37.
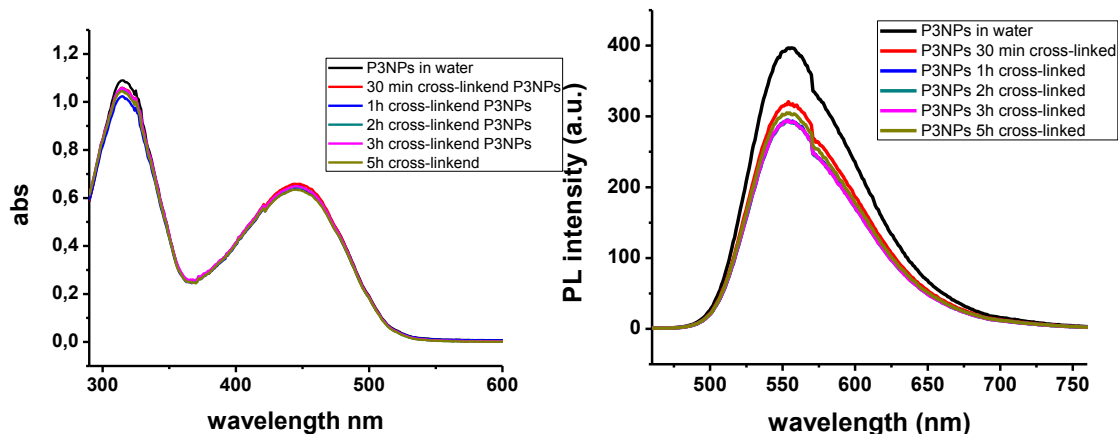
**Figure 37:** Absorbance and emission spectra of **P3NPs** ($\lambda_{ex}$=447nm)

From figure 36 it can be seen even that after 5 h there is no change in the emission colour. To determine the sizes of cross-linked **P3NPs** nanoparticles, DLS measurements were done. Size distribution of **P3NPs** after 15 min, 30 min, 1 h, 2 h, 3 h, 5 h UV-treatment are shown in figure 38. From the histograms it can be seen that no significant changes occurred in the sizes of nanoparticles upon UV-triggered cross-linking.
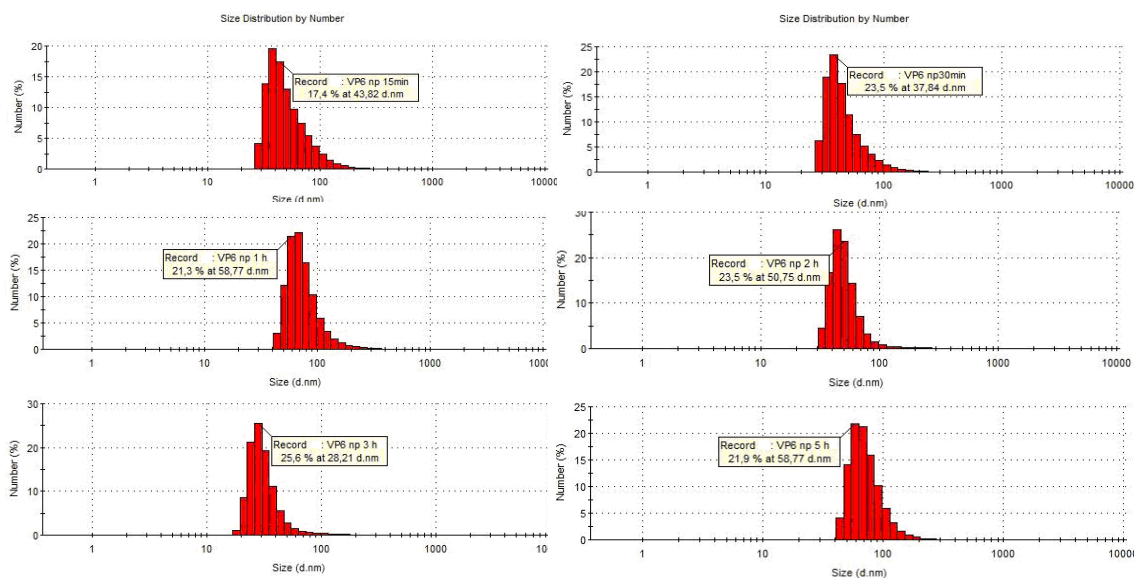


**Figure 38:** Size distribution histograms of A-15 min, B-30 min, C-1 h, D-2 h, E-3 h, F-5 h UV-treatment of **P3NPs** dispersion in water.

### 2.2.3 Synthesis and characterization of P4NPs

In the preparation of **P4NPs**, **P4** polymer was used. **P4** was dissolved in THF and stirred for 1h. The resulting solution was filtered with syringe filter and injected into rapidly stirring excess water. The mixture was stirred further 1 h. THF was removed under reduced pressure to obtain nanoparticle dispersion in water. The volume was concentrated under reduced pressure to yield a clear solution. Size of particles (20 nm) was measured by dynamic light scattering as shown in Figure 39. Due to hydrophilic carboxylic groups on the side chain of the polymer backbone, small particles were obtained compare with other polymer nanoparticles. Zeta potential of **P4NPs** (-57 eV) was measured by applying 150 V electric field.

**Size Distribution by Number**

**Results**

|  | | Mean (mV) | Area (%) | Width (mV) |
|---|---|---|---|---|
| Zeta Potential (mV): -57,9 | Peak 1: | -57,9 | 100,0 | 7,85 |
| Zeta Deviation (mV): 7,85 | Peak 2: | 0,00 | 0,0 | 0,00 |
| Conductivity (mS/cm): 0,0181 | Peak 3: | 0,00 | 0,0 | 0,00 |
| **Result quality** Good | | | | |

**Zeta Potential Distribution**

Record 3: VP6a np 1
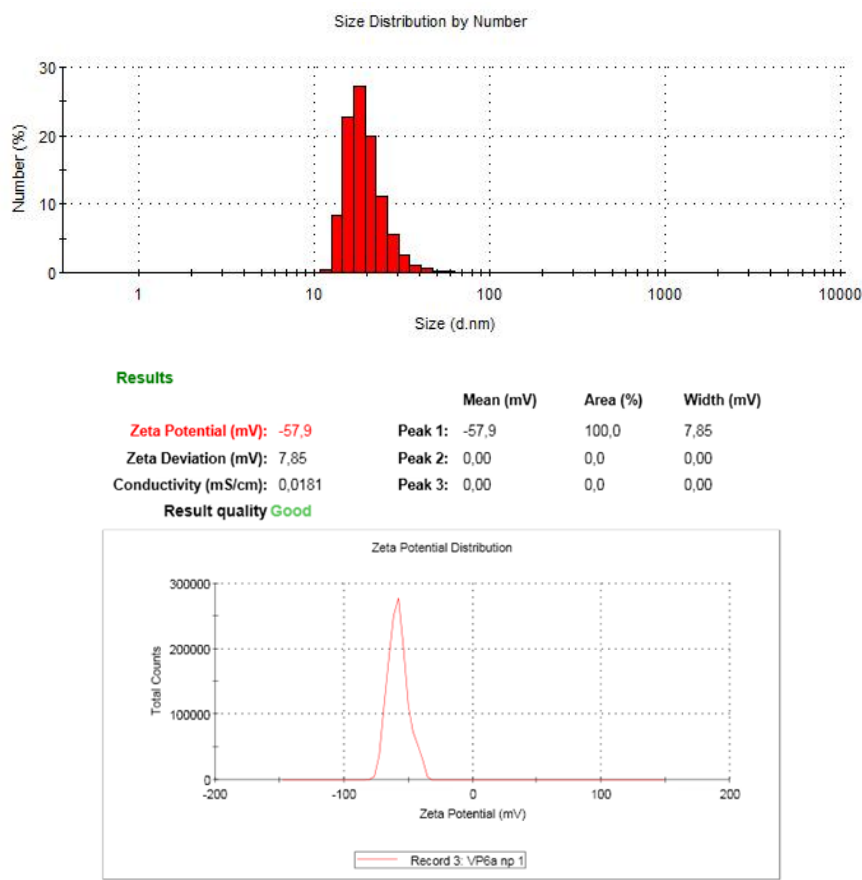
**Figure 39:** DLS and zeta potential result of **P4NPs**

A transmission electron microscopy result also shows same results (Figure 40). However, while drying particles form aggregate but in water they form very stable dispersion.
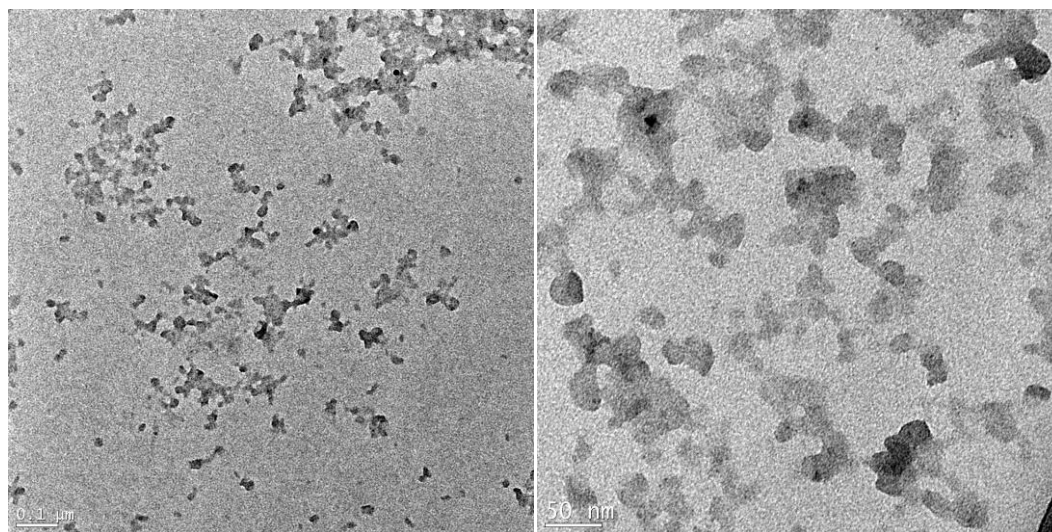


**Figure 40:** TEM images of **P4NPs**

After morphological characterization by TEM, optical properties were studied. Absorption and emission data of the **P4NPs** were compared with **P4** polymer in THF and as a film as shown in Figure 41.
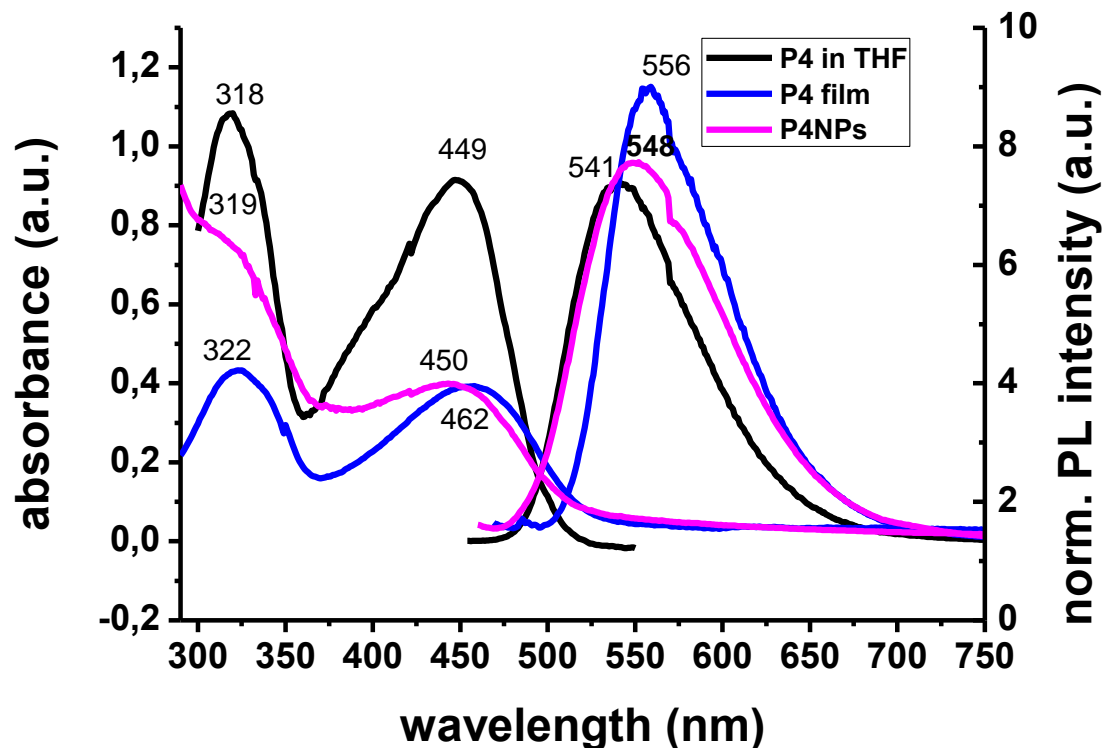
**Figure 41:** Absorption and emission spectra of the **P4** ($\lambda_{ex}$=449nm) polymer in THF,
**P4** film ($\lambda_{ex}$=462nm) and **P4NPs** in water ($\lambda_{ex}$=450nm)

**P4NPs** have two absorption peaks at 319 and 450 nm which are similar to the case of
P4 in THF but P4 film gives two absorption peaks which are red-shifted 3 and 13 nm
compared to P4 in THF. Emission peaks were observed at 541, 548 and 556 for P4 in
THF, P4NPs in water and P4 film, respectively.

**2.2.4 Synthesis and characterization of poly[(9,9-bis{3-bromopropyl}fluorenyl-
2,7-diyl)-co-(1,4-benzo-{2,1,3}-thiodiazole)] nanoparticles P5NPs**

In **P5NPs** preparation **P5** polymer was used. **P5** was dissolved in THF and stirred for
1h. The resulting solution was filtered with syringe filter and injected into rapidly
stirring excess water. The mixture was stirred further 1 h. THF was removed under
reduced pressure to obtain nanoparticle dispersion in water. The volume was

54

concentrated under reduced pressure to yield a clear solution. Size of the particles (68 nm) and zeta potential (-28 eV) were measured by dynamic light scattering and Zeta sizer as shown in Figure 42.
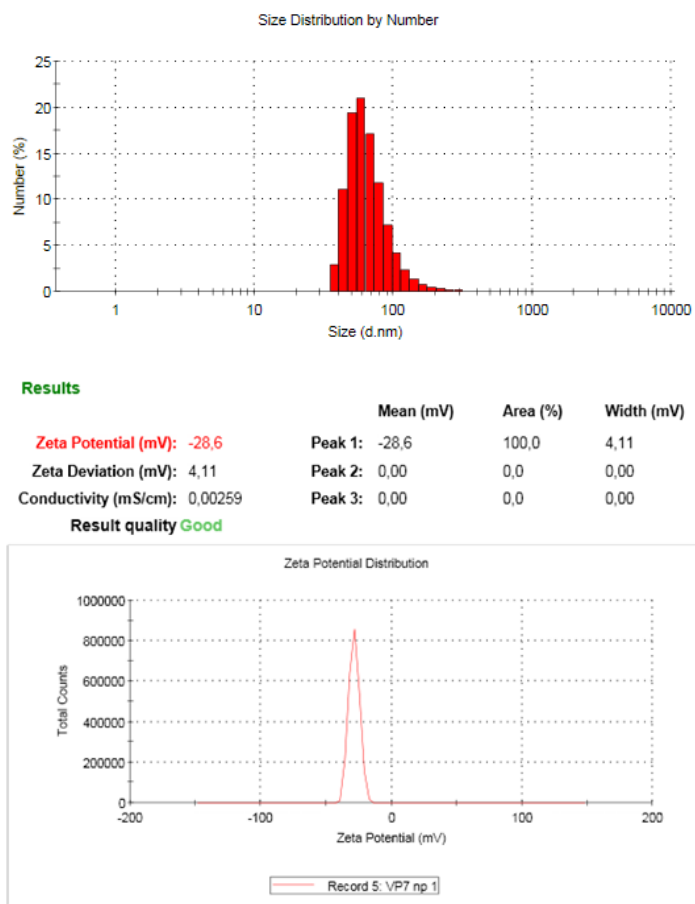


**Figure 42:** DLS and zeta potential results of the **P5NPs**

TEM image shows that nanoparticles have spherical shape and well dispersed (figure 43).
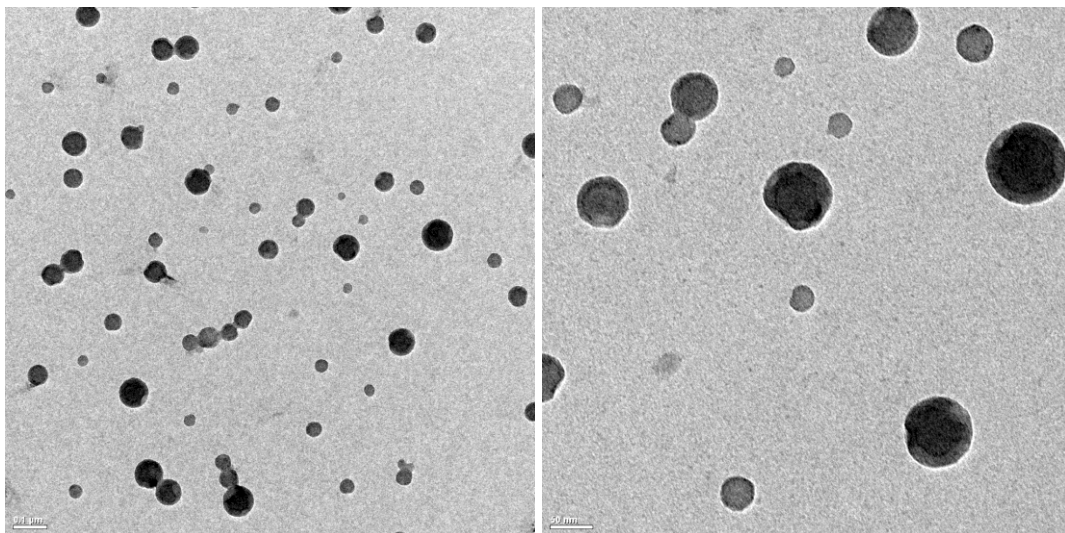
**Figure 43:** TEM images of the **P5NPs**

**P5NPs** have two absorption peaks at 324 and 463 nm which are 6 and 23 nm red-shifted compared to P4 in THF but P4 film gives two absorption peaks which are red-shifted 3 and 13 nm compared to P4 in THF. Emission peaks were observed at 541, 548 and 556 for P4 in THF, P4NPs in water and P4 film, respectively.

The absorption spectrum of **P5NPs** shows maximum absorbance at 324, 463 nm which are 6 and 23 nm red shifted compared with **P5** polymer in THF. When nanoparticles were excited with 463 nm light, yellow-green fluorescence with maximum at 546 nm which is 13 nm red shifted compared with **P5** polymer in THF and in solid state 25 nm red shift was observed as shown in figure 44.
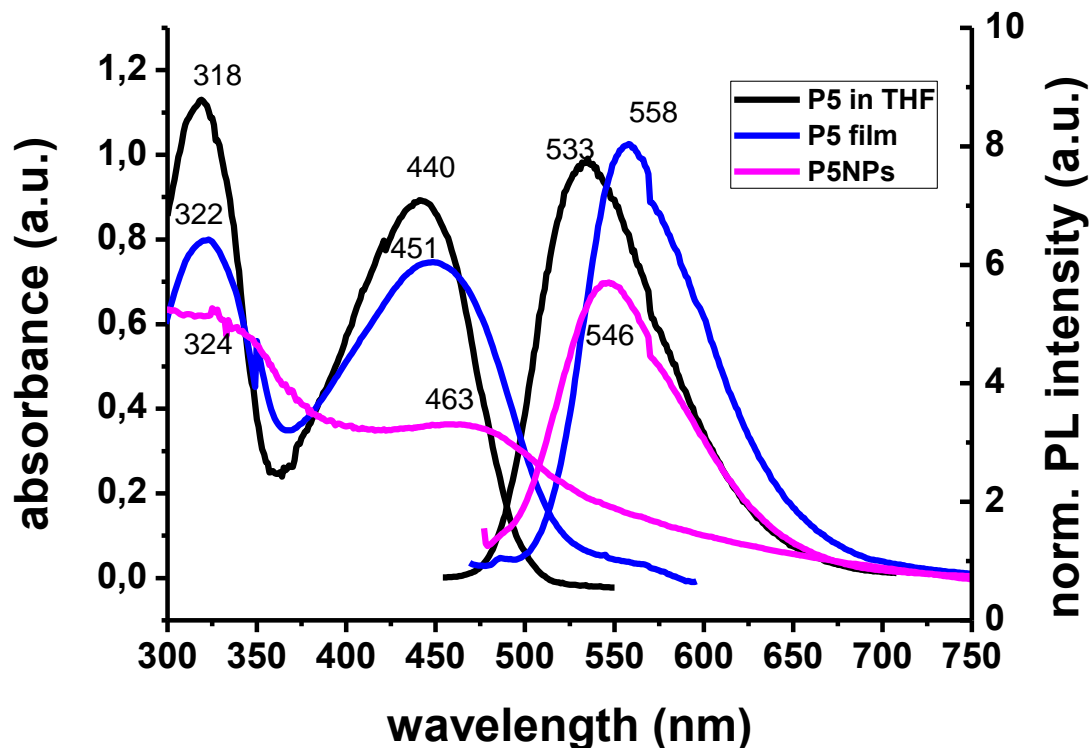
**Figure 44:** Absorption and emission spectra of the poly[(9,9-bis{3-bromopropyl}fluorenyl-2,7-diyl)-co-(1,4-benzo-{2,1,3}-thiodiazole)] **P5** ($\lambda_{ex}$=440nm) polymer in THF, in solid state ($\lambda_{ex}$=451nm)  and **P5NPs** in water ($\lambda_{ex}$=463nm)

## 2.2.5 Synthesis and characterization of poly[(9,9-bis{3-azidopropyl}fluorenyl-2,7-diyl)-co-(benzothiadiazole)] nanoparticles P6NPs

In **P6NPs** preparation **P6** polymer was used. **P6** was dissolved in THF and stirred for 1h. The resulting solution was filtered with syringe filter and injected into rapidly stirring excess water. The mixture was stirred further 1 h. THF was removed under reduced pressure to obtain nanoparticle dispersion in water. The volume was concentrated under reduced pressure to yield a clear solution. Size of particles (118 nm) and zeta potencial (-40 eV) was measured by dynamic light scattering as shown in figure 45.
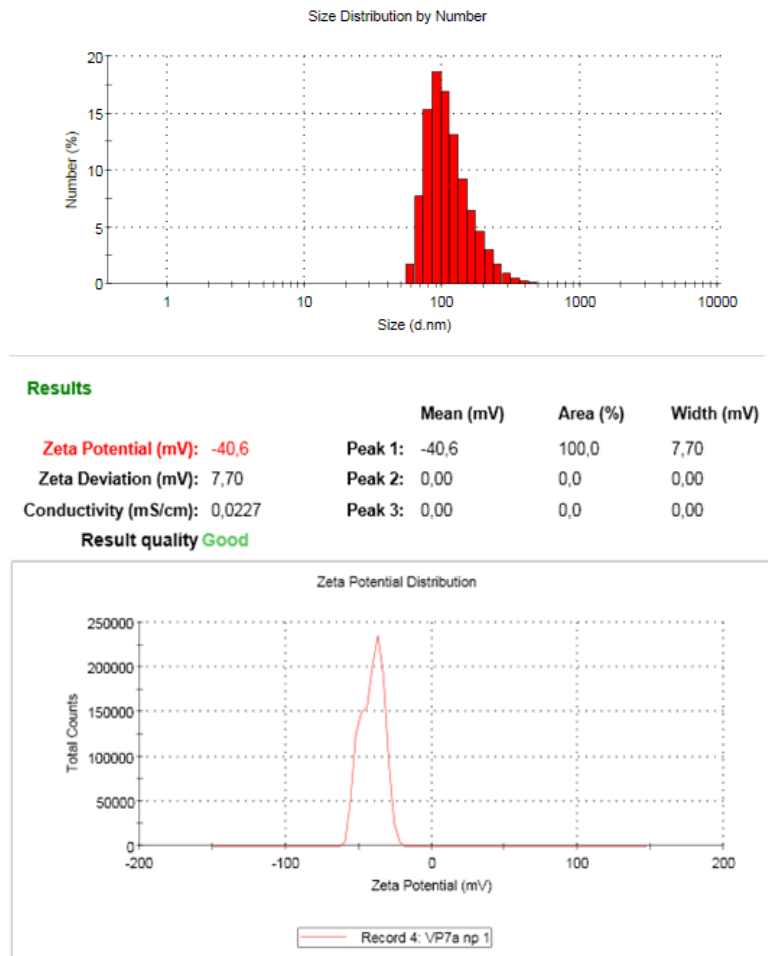
**Figure 45:** DLS and zeta potential results of the **P6NPs**

Morphology of **P6NPs** was characterized with transmission electron microscopy as shown in figure 46. **P6NPs** nanoparticles have spherical shape and well dispersed and there was not observed aggregation in the sample while drying.
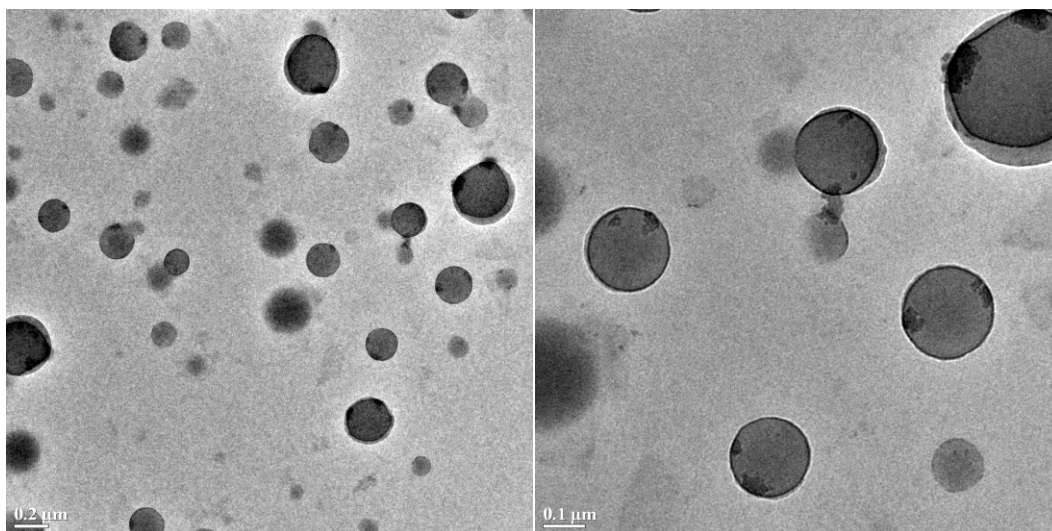
**Figure 46:** TEM images of the **P6NPs**

Optical properties of **P6NPs** were characterized with UV-Vis and fluorescence spectroscopy and compared with **P6** polymer in THF and **P6** polymer film as shown in Figure 47.
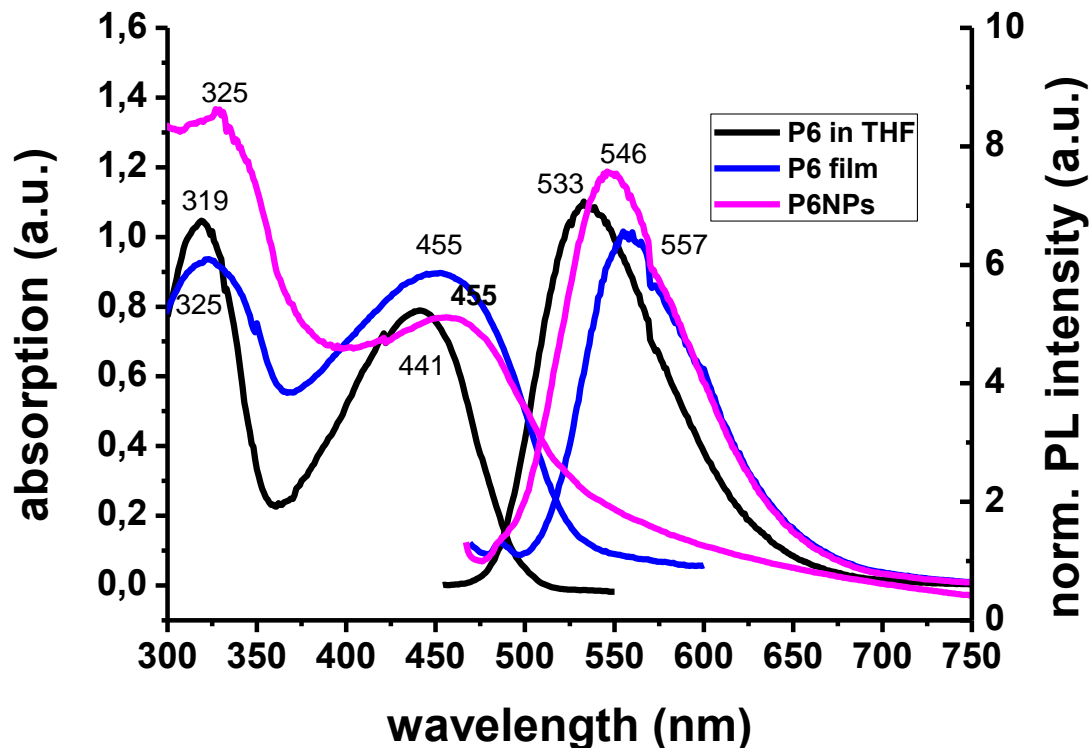
**Figure 47:** Absorption and emission spectra of the poly[(9,9-bis{3-azidopropyl}fluorenyl-2,7-diyl)-co-(benzothiadiazole)] (**P6**) polymer in THF($\lambda_{ex}$=441nm), in solid state ($\lambda_{ex}$=455nm) and **P6NPs** in water ($\lambda_{ex}$=455nm)

In the preparation of **P6** film, drop casting technique was used. For this purpose, 1 mg **P6** polymer was dissolved in 1 ml THF and dropped onto quartz substrate and dried at room temperature. **P6NPs** absorb light at the same wavelengths as **P6** film (325, 455 nm) which are 6 and 14 nm red shifted compared with **P6** solution in THF. In the emission spectra, maximum emission peaks for **P6NPs and P6 film** were observed at 546 nm, 557 nm respectively which were 13 and 24 nm red-shifted compared to the emission peak of **P6** in THF.

## 2.3 Cell viability test

The effect of CNPs on the proliferation of MSCs was performed by MTT assay which is shown in Figure 48. For this purposes, 104 MSCs cells were seeded into each 96-well cell culture plates and incubated in medium containing polymer nanoparticles at the concentrations 40 µg/ml to for 24h. At the end of the incubation period MTT assay was performed according to Cell Proliferation KitI (Roche)'s manufacturer protocol.

The 96 –well plate was read by an enzyme-linked immunosorbent assay (ELISA) reader between 550 and 600 nm for absorbance density values to determine the cell viability.
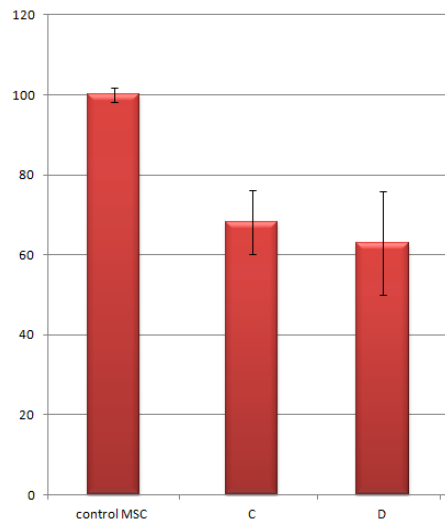


**Figure 48:** MTT assay result of C (**P3NPs**) and D (**P4NPs**)

According to the results P3NPs show 70% and P4NPs show 65% viability. Due to low toxicity, biocompatibility and fluorescent properties CPNPs can be used as imaging agent in cell imaging.

# CHAPTER 3

## CONCLUSION

In this thesis, novel water dispersible conjugated polymer nanoparticles having various potential applications in the areas including biomedicine and photonics have been synthesized from blue, green and yellow light emitting conjugated polymers. Their sizes, morphology, surface charges and optical properties have been determined using various techniques.

For the synthesis of nanoparticles, first the following polymers carrying a number of different functional groups and based on derivatives of fluorene and benzothiodiazole monomers are designed and synthesized using the Suzuki coupling reactions: Poly[(9,9-bis{propeny}fluorenyl-2,7-diyl)-co-(9,9-dihexyl-9H-fluorene)] (**P1**), poly[(9,9-bis{carboxymethylsulfonyl-propyl}fluorenyl-2,7-diyl)-co-(9,9-dihexyl-9H-fluoreny) (**P2**), poly[(9,9- bis{propeny}fluorenyl-2,7-diyl))-co-(1,4-benzo-{2,1,3}-thiodiazole)] (**P3**), poly[(9,9- bis{carboxymethylsulfonyl-propyl}fluorenyl-2,7-diyl)-co(1,4-benzo-{2,1,3}-thiodiazole)] (**P4**), poly[(9,9-bis{3-bromopropyl}fluorenyl-2,7-diyl)-co-(1,4-benzo-{2,1,3}-thiodiazole)] (**P5**), poly[(9,9-bis{3-azidopropyl}fluorenyl-2,7-diyl)-co-(benzothiadiazole)] (**P6**).

Polymers were characterized by using spectroscopic techniques such as $^1$H-NMR, FT-IR, UV-Vis and Fluorescence spectrophotometer and Gel Permeation Chromatography (GPC).

Conjugated polymers carry functional groups on their side chains, such as azide and allyl groups that can be cross-linkable using UV light to form shape-persistent, stable nanoparticles. Nanoparticles were characterized by various techniques before and after UV-treatment. Their sizes and morphologies were determined by using dynamic light scattering measurements (DLS) and imaging techniques such as scanning electron microscopy (SEM) and atomic force microscopy (AFM). For optical characterization UV-vis, fluorescent spectroscopies and FT-IR were used.

The Table 1 summarizes the optical properties (absorption, emission wavelengths and fluorescent quantum yields) of polymers and their nanoparticle dispersions in water

as well the sizes and zeta potential values of nanoparticle dispersions in water measured by dynamic light scattering and zetasizer.

Preliminary results of cell assay studies of these nanoparticles show that these nanoparticles were uptaken in the cells and do not exhibit cyctotoxic effects.

*Table 1:* Maximum absorption $\lambda_{abs}$ and emission $\lambda_{em}$ wavelengths and fluorescent quantum yield of polymers in THF and nanoparticle dispersions in water, dynamic light scattering (DLS), polydispersity index and zeta potential measurements

| | $\lambda_{abs}$[nm] | $\lambda_{em}$ [nm] | $\Phi_f$ (%) | DLS diameter (mean) (nm) | polydipersity index | zeta potential (mean) (eV) |
|---|---|---|---|---|---|---|
| **P1** | 383 | 418, 439 | 74 | | | |
| **P2** | 384 | 421, 440 | | | | |
| **P3** | 317, 447 | 537 | 69 | | | |
| **P4** | 318, 449 | 541 | 40 | | | |
| **P5** | 318, 440 | 535 | 17 | | | |
| **P6** | 319, 441 | 535 | 83 | | | |
| **P1NPs** | 385 | 425,450 | | 28 | 0.223 | |
| **P3NPs** | 317, 447 | 550 | 26 | 58 | 0.238 | -32.2 |
| **P4NPs** | 319, 450 | 548 | 14 | 20 | 0.293 | -57.9 |
| **P5NPs** | 324, 463 | 546 | 0.5 | 68 | 0.294 | -28.6 |
| **P6NPs** | 325, 455 | 546 | 26 | 118 | 0.138 | - 40.6 |

# CHAPTER 4

# EXPERIMENTAL SECTION

All of the reagents were merchandised from the Sigma-Aldrich Chemical Co. and were used as received. 2, 7-dibromo-9,9-bis-(dibromopropane)-9H-fluorene and 2, 7-dibromo-9,9-bis-(propenyl)-9H-fluorene were synthesized according to procedure shown in part one. For purification of monomers column chromatography was performed by using silica gel (Kieselgel 60, 0.063-0.200 mm) and thin layer chromatography (TLC) was used on silica gel plates (Kiselgel 60 F254, 1 mm) in order to monitor separation of side products. Final products were characterized by $^1$H-NMR. After synthesis polymers they were characterized by $^1$H-NMR, FT-IR and optical properties characterized by UV-Vis and PL spectroscopy methods and fluorescent quantum yield was calculated and molecular weight if polymers determined via Gel-permeation chromatography (GPC, Agilent 1200) were used. In order to disperse polymer in water polymers converted into nanoparticles and for characterization of nanoparticles different techniques were used. Morphological characterization was done by scanning electron microscope (SEM, Quanta 200 FEG SEM) and transmission electron microscope (TEM, FEI Tecnai G2 F30). Sizes of nanoparticles were measured by Dynamic light scattering (DLS, Zetasizer Nano-ZS) which is as light source is laser (wavelength 633 nm) and time-dependent autocorrelation function of the scattered light intensity was measured at an angle of $90^0$. For optical characterization UV-vis spectrophotometer (CARY UV-VIS) and fluorescent spectrophotometer (CARY Eclipse Fluorescent Spectrophotometer) equipped with a xenon-lamp excitation source were used. For structural characterization $^1$H-NMR nuclear magnetic resonance (NMR, Bruker Avance III 400 MHz spectrometer) and FT-IR (BRUKER OPTIK GmbH, TENSOR) were used. To investigate structural change while nanoparticle formation, nanoparticles dispersions were concentrated to increase the number of particles per unit area and made film by dropcasting onto silicon substrate and IR spectra were recorded. To prepare nanoparticles Milli-Q water (18.2 MΩ) was used and after preparation of

nanoparticles dispersion was dialyzed with regenerated cellulose tubular membrane (Cell Sep T3, MWCO: 12.000-14.000, Dry cylinder diameter: 21.0 mm, flat with: 33 nm, length: 30 m, vol/cm: 3.47 ml).

## 4.1 Synthesis of 2, 7-dibromo-9,9-bis-(bromopropyl)-9H-fluorene (M1)

2,7-dibromofluorene (3.0 g, 9.25 mmol) and tetrabutylammoniumbromide (0.6 g, 1.85 mmol) were dried under vacuum 30 min. Degassed DMSO (15 ml), 50% (w/w) NaOH (15 ml), 1,3-dibromopropene (13 ml, 90 mmol) were added into the mixture respectively and stirred under argon gas for two hour at room temperature. After two hours, Argon gas was removed and tertiary-butyl methyl ether (125 ml) and deionized water (50 ml) were added into the mixture and stirred 15 min. Then mixture was washed with deionized water (50 ml), 2N HCl (50 ml), brine solution (50 ml) and deionized water (50 ml) respectively. After extraction, t-butyl methyl ether was evaporated by rotary evaparator and the monomer was obtained. For the purification of the product, silica-packed column chromatography was used and cyclohexane and chloroform mixture (80:20) was used as the eluent. For more purification, the product was dissolved in $CHCl_3$, precipitated into cold methanol, filtered and dried under vacuum.

**Yield:** 1.8 g, 34 %

**1H-NMR** (400 MHz, $CDCl^3$): δ 7.53 (m, 6 H, Ar-H, $^3J$=9.6 Hz), 3.14 (t, 4H, $CH_2Br$, $^3J$=6.4 Hz ), 2.17 (t, 4H, $CH_2$), 1.16 ( m, 4H, $CH_2$)
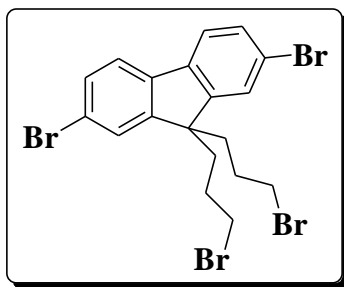


**Scheme 15:** 2, 7-dibromo-9,9-bis-(dibromopropane)-9H-fluorene (**M1**)

**4.2 Synthesis of 2, 7-dibromo-9,9-bis-(propenyl)-9H-fluorene (M2)**

2,7-dibromofluorene (3.0 g, 9.25 mmol) and phase transfer catalyst tetrabutylammoniumbromide (0.6 g, 1.85 mmol) were dried under vacuum for 30 min. DMSO was degassed under argon gas and than DMSO (15 ml), 50% (w/w) NaOH (15 ml), 3-bromo-1-propene (16 ml, 90 mmol) were added into the mixture respectively and stirred under argon gas for two hour at room temperature. After two hours, argon gas was removed and tertiary-butyl methyl ether (125 ml) and deionized water (50 ml) were added into the mixture and stirred 15 min. Then mixture was washed with deionized water (50 ml), 2N HCl (50 ml), brine solution (50 ml) and deionized water (50 ml) respectively. After extraction, t-butyl methyl ether was evaporated by rotary evaporator and the monomer was obtained. To purify product it was dissolved in $CHCl_3$, precipitated into cold methanol and white crystals was obtained. Then crystals was filtered and dried under vacuum.

**Yield:** 2.6 g, 69 %

**1H-NMR** (400 MHz, $CDCl_3$): δ 7.52 (m, 6 H, Ar-H, $^3J=8$), 5.21 (m, 2H, CH), 4.89 (m, 2H, CH), 2.68 (t, 4H, $CH_2$, $^3J=4$).
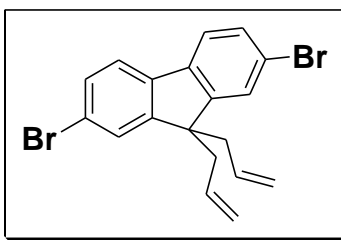


**Scheme 16:** 2, 7-dibromo-9,9-bis-(propenyl)-9H-fluorene (**M2**)

**4.3 Synthesis of poly[(9,9-bis{propenyl}-9H-fluorene)-co-(9,9-dihexyl-9H-fluorene)] (P1)**

2,7-dibromo-9,9-bis-(propenyl)-9H-fluorene (1 g, 0.00296 mmol), 9,9-dihexylfluorene-2,7-bis(trimethyleneborate) (0.4906 g, 0.00296 mmol) and $K_2CO_3$ (4.09 g, 0.0296 mmol) are dried under vacuum while THF, $H_2O$ and Toluene are degassed under Argon about 15 min. Then mixture suspended into THF (10 ml),

water (10 ml) and Toluene (10 ml). Then, catalyst tetrakis (triphenylphosphine) palladium (0) (Pd(PPh$_3$)$_4$ ) was added quickly and they were stirred under Argon gas for 48 hours at 80-90$^o$ C. After 3 hours phase transfer catalyst tetra-n-butylammoniumbromid (TBAB) was added. In order for the reaction to occur at 80 $^o$ C, the temperature of the oil bath was maintained at 90 $^o$ C. At the end of the reaction, there were two phases; one was brown organic layer and the other was colourless and transparent water phase. The solvents of the mixture were evaporated and dissolve in chloroform very excess and dropped into cold methanol (100 ml). Almost, the entire product precipitated in methanol. Then, the product was tried to be collected via filtration and than washed with deionised water to remove the base. The colour of the product was light yellow in the form of precipitate in methanol. Precipitating into cold methanol process was performed twice in order to obtain more pure product. The product, which is light yellow, was transferred into a vial and dried under vacuum. Yield: 0.9 g ( 60%)

**$^1$H-NMR** (400MHz, CDCl$_3$, 25°C), δH 7.85 (m, 8H, Ar H), 5.54 (q, 2H, CH), 5.02 (t, 4H, CH$_2$), 2.89 (m, 4H, CH$_2$), 1.54 (q, 4H, CH$_2$), 1.15 (m, 4H, CH$_2$), 0.81 (m, 6H, CH$_3$)

**IR** (KBr, pellet, υmax(cm$^{-1}$)): 3023 (-CH, w), 2928 (-CH, s), 919 (C=C-, w)

GPC: M$_n$= 7.01 x 10$^3$ M$_w$= 9.02 x 10$^3$ (THF solvent, Polystyrene as standard)

λ$_{abs}$= 383nm, λ$_{em}$= 418, 439 nm (in THF)
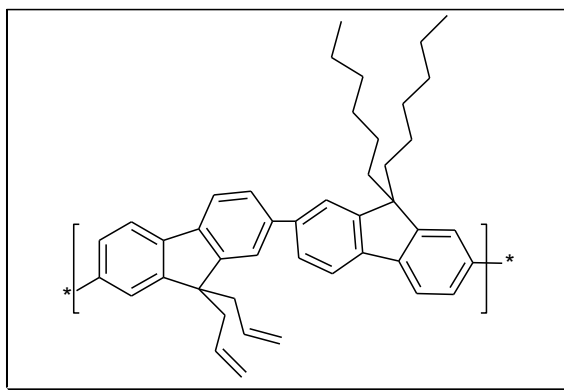


**Scheme 17:** Poly[(9,9-bis{propenyl}-9H-fluorene)-co-(9,9-dihexyl-9H-fluorene)]

(**P1**)

## 4.4 Synthesis of poly[(9,9-bis{carboxymethylsulfonyl-propyl}fluorenyl-2,7-diyl)-co-(9,9-dihexyl-9H-fluorene) (P2)

Poly[(9,9-bis{propenyl}-9H-fluorene)-co-(9,9-dihexyl-9H-fluorene)] (200 mg, 0.374 mmol) was treated with thioglycolic acid (0.163 ml, 1.87 mmol) in chloroform under Argon for 24 h. After the reaction was over, the mixture was precipitated into water. Yellow precipitates were collected by centrifugation and the precipitation was repeated twice to get rid off the excess amount of thioglycolic acid. The yellow precipitates were dried under vacuum.

Yield: 180 mg, 90%

**IR** (KBr, pellet, $\upsilon$max(cm$^{-1}$)): 3036 (-CH, w), 2928 (-CH, s), 1458 (C=C-, w), 1705 (C=O, s).

$\lambda_{abs}$= 384nm, $\lambda_{em}$= 421, 440 nm (in THF)
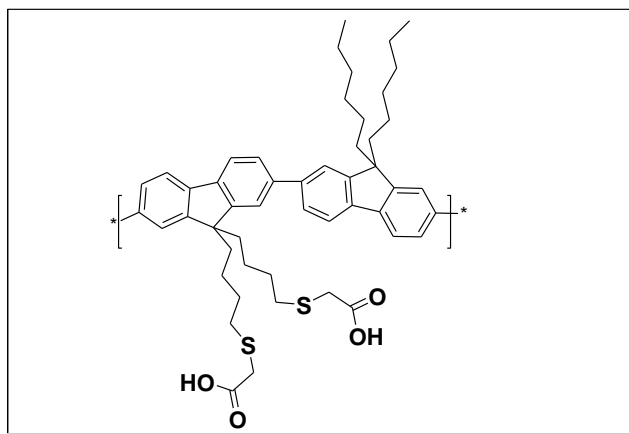


**Scheme 18:** poly[(9,9-bis{carboxymethylsulfonyl-propyl}fluorenyl-2,7-diyl)-co-(9,9-dihexyl-9H-fluorene) (**P2**)

## 4.5 Synthesis of poly[(9,9- bis{propeny}fluorenyl-2,7-diyl))-co-(1,4-benzo-{2,1,3}-thiodiazole)] (P3)

2,7-dibromo-9,9-bis-(propenyl)-9H-fluorene (300 mg, 0.000887 mmol), 2,1,3-benzothiadiazole-4,7-bis (boronic acid pinocol ester) (300 mg, 0.000887 mmol) and

K$_2$CO$_3$ (1.23 g, 0.00887 mmol) were dried under vacuum while THF, H$_2$O and toluene are degassed under Argon about 15 min. Then mixture suspended into THF (10 ml), water (10 ml) and toluene (10 ml). Then, catalyst tetrakis (triphenylphosphine) palladium (0) (Pd (PPh$_3$)$_4$) (68 mg) was added quickly and they were stirred under Argon gas for 48 hours at 80-90 $^o$ C. After 3 hours phase transfer catalyst tetra-n-butylammoniumbromid (TBAB) was added. In order for the reaction to occur at 80 $^o$ C, the temperature of the oil bath was maintained at 90 $^o$ C. At the end of the reaction, there were two phases; one was brown organic layer and the other was colourless and transparent water phase. The solvents of the mixture were evaporated and powder was dissolved in chloroform and dropped into cold deionised water (100 ml). Almost, the entire product precipitated in water. The product was collected via centrifugation at 2500 rpm for 30 min. The orange powder of product was transferred into a vial and dried under vacuum.

**Yield**: 0.28 g (47 %).

**1H NMR** (400 MHz, CDCl$_3$, δ) 8.15 (m, 8H, Ar H), 5.60 (m, 2H, CH), 5.0 (t, 4H, CH$_2$), 2.91 (t, 4H, CH$_2$).

**IR** (KBr, pellet, υmax(cm$^{-1}$)): 3074 (-CH, w), 2918 (-CH, s), 1455 (C=C-, w)

Gel permeation chromatography (GPC) Mw = 2.5 x 10$^3$ g mol$^{-1}$

(Solvent THF, Standard polystyrene)

λ$_{abs}$=317, 447 nm λ$_{em}$= 541 nm (in THF)
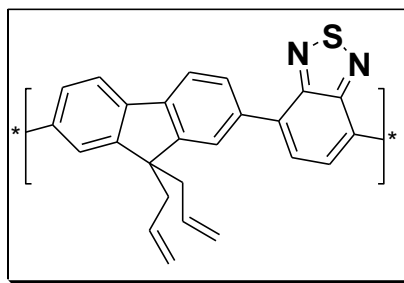


**Scheme 19:** Poly[(9,9- bis{propeny}fluorenyl-2,7-diyl))-co-(1,4-benzo-{2,1,3}-thiodiazole)] (**P3**)

## 4.6 Synthesis of poly[(9,9- bis{carboxymethylsulfonyl-propyl}fluorenyl-2,7-diyl)-co(1,4-benzo-{2,1,3}-thiodiazole)]  (P4)

Poly[(9,9- bis{propeny}fluorenyl-2,7-diyl))-co-(1,4-benzo-{2,1,3}-thiodiazole)] )] (100 mg, 0.24 mmo) was treated with thioglycolic acid (0.106 ml, 1.2 mmol) in chloroform under Argon for 24 h. After the reaction was over, the mixture was precipitated into water. Orange precipitates were collected by centrifugation and the precipitation was repeated twice to get rid off the excess amount of thioglycolic acid. The orange precipitates were dried under vacuum.

Yield: 57 mg 53%

**IR** (KBr, pellet, $\upsilon$max(cm$^{-1}$)): 3040 (-CH, w), 2918 (-CH, s), 1713(C=O, s)

$\lambda_{abs}$= 318, 448 nm, $\lambda_{em}$= 539 nm (in THF)
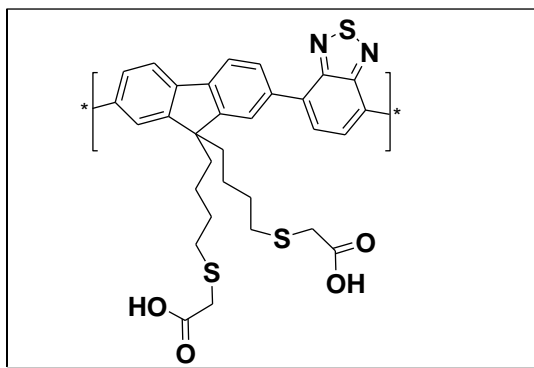


**Scheme 20:** Poly[(9,9- bis{carboxymethylsulfonyl-propyl}fluorenyl-2,7-diyl)-co(1,4-benzo-{2,1,3}-thiodiazole)]  (**P4**)

## 4.7 Synthesis of poly[(9,9-bis{3-bromopropyl}fluorenyl-2,7-diyl)-co-(1,4-benzo-{2,1,3}-thiodiazole)] (P5)

2,1,3-benzothiadiazole-4,7-bis (boronic acid pinocol ester) (411 mg, 1.06 mmol), 2,7-dibromo-9,9-bis-(dibromopropane)-9H-fluorene (566 mg, 1.06 mmol) and K$_2$CO$_3$ (1.47 g, 10.6 mmol) were dried under vacuum and the flask was filled with argon. First the degassed solvents, THF (10 ml), water (10 ml) and toluene (10 ml) were added under Argon gas and then, catalyst tetrakis (triphenylphosphine) palladium (Pd

(PPh$_3$)$_4$) was added quickly. After 3 h stirring of the mixture under argon at 80–90 °C, the phase transfer catalyst, tetra-n-butylammonium bromide (TBAB) was added. The stirring was continued for another 48 h at 80–90 °C to complete the polymerization reaction. The mixture was evaporated under vacuum to obtain a solid residue, which was suspended in water; the water insoluble particles were collected by suction and dissolved in THF (20 ml) and the solution was precipitated into cold methanol (200 ml). The precipitates were collected by suction and dried under vacuum for 5 h.

**Yield:** 0.55 g (56 %)

**1H NMR** (400 MHz, CDCl$_3$, δ) 7.99 (m, 8H, Ar H), 3.26 (q, 4H, CH$_2$Br), 2.41 (q, 4H, CH$_2$), 1.25 (m, 4H, CH$_2$), 0.81 (m, 6H, CH$_3$)

**IR** (KBr, pellet, υmax(cm$^{-1}$)): 3033 (-CH, w), 2918 (-CH, s), 1597 (C=C, s)

λ$_{abs}$= 318, 442 nm, λ$_{em}$= 533 nm (in THF)

Gel permeation chromatography (GPC) M$_w$ = 1.08 x 10$^4$g mol$^{-1}$ (Solvent THF, Standard polystyrene).
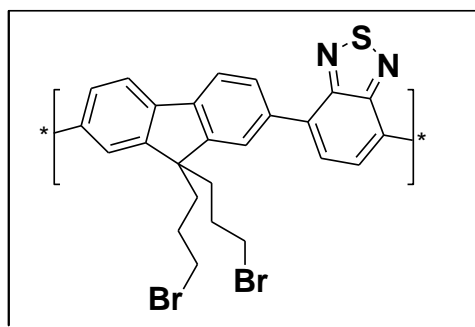


**Scheme 21:** Poly[(9,9-bis{3-bromopropyl}fluorenyl-2,7-diyl)-co-(1,4-benzo-{2,1,3}-thiodiazole)] (**P5**)


**4.8 Synthesis of poly[(9,9-bis{3-azidopropyl}fluorenyl-2,7-diyl)-co-(benzothiadiazole)] (P6)**

Poly[9,9-bis(3-bromopropyl)fluorene)-co-alt-(benzothiadiazole)] (100 mg, 0.185 mmol) and NaN3 (26 mg, 0.400 mmol) were dissolved in DMF (6 ml) and the mixture was refluxed for 24 h. After the reaction was over, the mixture was

precipitated into cold methanol (100 ml). The precipitates were collected by suction and dried under vacuum.

**Yield:** 60 mg (69%)

**1H NMR** (400 MHz, CDCl$_3$, δ) 7.5 (m, 8H, Ar H), 3.21 (q, 4H, CH$_2$N$_3$), 2.40 (q, 4H, CH$_2$), 1.25 (m, 4H, CH$_2$),

**IR** (KBr, pellet, υmax(cm$^{-1}$)): 3033 (-CH, w), 2918 (-CH, s), 2088(C-N$_3$, s)

$\lambda_{abs}$= 319, 440 nm, $\lambda_{em}$= 532 nm (in THF)
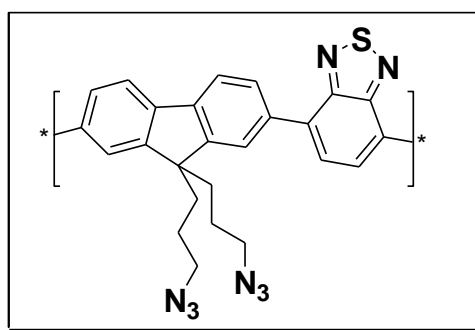


**Scheme 22:** Poly[(9,9-bis{3-azidopropyl}fluorenyl-2,7-diyl)-co-(benzothiadiazole)] (**P6**)

## 4.9 Preparation of poly[(9,9-bis{propenyl}-9H-fluorene)-co-(9,9-dihexyl-9H-fluorene)] nanoparticles P1NPs

2 mg of **P1** polymer was dissolved in 5 ml THF and ultrasonicated for 1 hour. Stock solution was filtrated by 0.45 μm syringe filter and poured into 100 ml Milli-Q water (18.2 MΩ) under stirring and then dispersion was ultasonicated about 30 min. After that, THF was removed by vacuum rotary evaporator at 35$^0$ C.

After preparation of **P1NPs** cross-linking experiment was done. Same volume of dispersant were cross-linked via 254 nm UV light about 15 min, 30 min, 1 h, 2 h, 3 h, 4 h, and 5 h. Characterization of nanoparticles were done by UV-Vis spectrophotometer, fluorescence spectrophotometer. Dynamic light scattering results show no change in the size during cross-linking.

### 4.10 Preparation of poly[(9,9-diallyl-9H-fluorene)-co-(benzothiadiazole)] nanoparticles P2NPs

2 mg of **P2** polymer was dissolved in 5 ml THF and ultrasonicated for 1 hour. Stock solution was filtrated by 0.45 μm syringe filter and poured into 100 ml Milli-Q water (18.2 MΩ) under stirring and then dispersion was ultasonicated about 30 min. After that, THF was removed by vacuum rotary evaporator at $35^0$ C.

After preparation of **P2NPs** cross-linking experiment was done. Same volume of dispersant were cross-linked via 254 nm UV light about 15 min, 30 min, 1 h, 2 h, 3 h, 4 h, and 5 h. Characterization of nanoparticles were done by UV-Vis spectrophotometer, fluorescence spectrophotometer. Dynamic light scattering results show no change in the size during cross-linking.

### 4.11 Preparation of poly[(9,9- bis{propeny}fluorenyl-2,7-diyl))-co-(1,4-benzo-{2,1,3}-thiodiazole)] nanoparticles P3NPs

2 mg of **P3** polymer was dissolved in 5 ml THF and ultrasonicated for 1 hour. Stock solution was filtrated by 0.45 μm syringe filter and poured into 100 ml Milli-Q water (18.2 MΩ) under stirring and then dispersion was ultasonicated about 30 min. After that, THF was removed by vacuum rotary evaporator at $35^0$ C.

### 4.12 Preparation of poly[(9,9- bis{carboxymethylsulfonyl-propyl}fluorenyl-2,7-diyl)-co(1,4-benzo-{2,1,3}-thiodiazole)]  nanoparticles P4NPs

2 mg of **P4** polymer was dissolved in 5 ml THF and ultrasonicated for 1 hour. Stock solution was filtrated by 0.45 μm syringe filter and poured into 100 ml Milli-Q water (18.2 MΩ) under stirring and then dispersion was ultasonicated about 30 min. After that, THF was removed by vacuum rotary evaporator at $35^0$ C.

## 4.13 Preparation of poly[(9,9-bis{3-bromopropyl}fluorenyl-2,7-diyl)-co-(1,4-benzo-{2,1,3}-thiodiazole)] nanoparticles P5NPs

2 mg of **P5** polymer was dissolved in 5 ml THF and ultrasonicated for 1 hour. Stock solution was filtrated by 0.45 µm syringe filter and poured into 100 ml Milli-Q water (18.2 MΩ) under stirring and then dispersion was ultasonicated about 30 min. After that, THF was removed by vacuum rotary evaporator at $35^0$ C.

## 4.14 Preparation of poly[(9,9-bis{3-azidopropyl}fluorenyl-2,7-diyl)-co-(benzothiadiazole)] nanoparticles P6NPs

2 mg of **P6** polymer was dissolved in 5 ml THF and ultrasonicated for 1 hour. Stock solution was filtrated by 0.45 µm syringe filter and poured into 100 ml Milli-Q water (18.2 MΩ) under stirring and then dispersion was ultasonicated about 30 min. After that, THF was removed by vacuum rotary evaporator at $35^0$ C.

## 4.15 Quantum yield (QY) calculations of polymers and nanoparticles

In QY calculation of blue fluorescent polymer P1, quinine sulphate ($\lambda_{abs}$=348 nm, $\lambda_{em}$= 455 nm) was used as a standard (10 mm cuvettes). It has 54% QY in 0.5M $H_2SO_4$ solution. Fluorescein in ethanol ($\lambda_{abs}$=484 nm, $\lambda_{em}$= 520 nm, Q=97%) was used as a standard to calculate quantum yield of P3, P4, P5 and P6 polymers by using equation 1.

$$Q = Q_R \left( \frac{Grad}{Grad_R} \right) \frac{n^2}{n^2_R} \quad (1)$$

In this equation Q is quantum yield, Gred is gradient obtained from the plot of the integrated fluorescent intensity vs. optical density and n is a refractive index Quantum yields of nanoparticles P3NPs, P4NPs, P5NPs and P6NPs were calculated by using P3, P4, P5, P6 polymers, respectively, as a standard according to the equation 2.

$$Q = Q_R \frac{I}{I_R} \frac{OD_R}{OD} \frac{n^2}{n^2_R} \quad (2)$$

In this equation, I- is an integrated intensity, OD- optical density and R refers to the reference fluorophore of known quantum yield.

## 4.16 Isolation and Culture of Mesenchymal Stem Cells (MSCs)

Heterogenous bone marrow cell population is collected from rat femur and tibia by flushing with 5 mL syringe containing 10% FCS in DMEM. Cells were cultured in plastic cell culture dishes with Mesencult Medium with 20% supplement and 1% penicillin/streptomycin solution for 14 days in a 5% $CO_2$ incubator at $37^0$C.[59] On the $13^{th}$ day, MSCs were incubated with P3NPs and P4NPs for 24h in 1:4 ratio. The effect of NPs on the proliferation of MSCs was performed by MTT (3-(4,5-dimethyl-2-thiazolyl)-2,5-diphenyl-2H-tetrazolium bromide) assay.

## **REFERENCES**

**[1]** *Handbook of Conducting Polymers,* 2nd ed., T. A. Shotheim, R. L. Elsenbaumer, J. R. Reynolds., Eds., Marcel Dekker, New York, 1998.

**[2]** http://www.nobelprize.org/nobel_prizes/chemistry/laureates/2000/advanced-chemistryprize2000.pdf

**[3]** Shirakawa, H.; Louis, E.J.; MacDiarmid, A.G.; Chiang, C.K; Heeger, A.J.; *J. Chem. Soc. Chem. Comm.*, 1977, 579.

**[4]** Lakowicz, J. R.; Principles of Fluorescence Spectroscopy, 2nd ed. (Kluwer Academic, Dordrecht/Plenum, New York, 1999).

**[5]** J. H. Burroughes, D. D. C. Bradley, A. R. Brown, R. N. Marks, K. Mackay, R. H. Friend, P. L. Burn, A. B. Holmes, *Nature* (London), 1990, **347**, 539.

**[6]** A. Kraft, A. C. Grimsdale, A. B. Holmes, *Angew. Chem., Int. Ed.,* 1998, **37**, 402.

**[7]** Friend, R. H.; Gymer, R. W.; Holmes, A. B.; Burroughes, J. H.; Marks, R. N.; Taliani, C.; Bradley, D. C. C.; Dos Santos, D. A.; Bredas, J. L.; Lgdlund, M.; Salaneck, W. R.; *Nature*, 1999, 397, 121.

**[8]** http://www.cdtltd.co.uk/technology

**[9]** K. M. Coakley, M. D. McGehee, *Chem. Mater.* 2004**, 16***, 4533.

**[10]** Y. Kim, S. Cook, S. M. Tuladhar, S. A. Choulis, J. Nelson, J. R. Durrant, D. D. C. Bradley, M. Giles, I. McCulloch, C.-S. HA, M. Ree, *Nat. Mater.* 2006, **5**, 197.

**[11]** D.T. McQuade, A.E. Pullen and T. M. Swager, *Chem Rew,* 2000, **100**, 537.

**[12]** a) M. Leclerc, J. Polym. Sci. Part A: *Polym. Chem.* 2001, **39**, 2867; b) M. Leclerc, *J. Polym. Sci.*, 2001, **39**, 2867.

**[13]** K. K. Kanazawa, A. F. Diaz, W. D. Gill, P. M. Grant, G. B. Street, G. P. Gardini, and J. E. Kwak, *Synth. Met.,* 1980, **1**, 329.

**[14]** a) A. F. Diaz, A. Martinez, K. K. Kanazawa, and M. Salmon, *J. Electroanal. Chem., Interfacial Electrochem.,* 1981, **130**, 181. b) A. F. Diaz, K. K. Kanazawa, J. L. Castillo, and J. A. Logan, *Polym. Sci. Technol.,* 1981, **15**, 149.

**[15]** S. Maiti, D. Das and K. Sen, *Journal of Applied Polymer Science*, 2011, **123**, 455.

**[16]** J. Clayden, N. Greeves, S. Warren and P. Whothers, *Organic Chemistry,* Oxford.

**[17]** a) http://www.nobelprize.org/nobel_prizes/chemistry/laureates/2010/; b) http://kva.se/Documents/Priser/Nobel/2010/Kemi/sciback_ke_10.pdf

**[18]** http://www.organic-chemistry.org/namedreactions/heck-reaction.shtm

**[19]** N. Miyaura and A. Suzuki, *Chem. Rev.*, 1995, **95**, 2457.

**[20]** http://www.organic-chemistry.org/namedreactions/suzuki-coupling.shtm

**[21]** http://www.organic-chemistry.org/namedreactions/stille-coupling.shtm

**[22]** S. Ikeda, H. Yamamoto, K. Kondo, Y. Sato, Y., *Organometallics*, 1995, **14**, 5015.

**[23]** K. Sonogashira**,** Y. Tohda and N. Hagihara, *Tetrahedron. Lett.,* 1975 , 50, 4467

**[24]** http://www.organic-chemistry.org/namedreactions/sonogashira-coupling.shtm

**[25]** C. V. Hoven, A. Garcia, G. C. Bazan, T. Q. Nguyen, T. Q, *Adv. Mater.* 2008, **20**, 3793.

**[26]** M. A. Rahman, P. Kumar, D. S. Park and Y. B. Shim, *Sensors,* 2008, **8**, 118.

**[27]** M. Yu, F. He, Y. Tang, S. Wang and Y. Li, D. Zhu, *Macromol. Rapid Commun.*, 2007, **28**, 1333.

**[28]** Z. Mousavi, J. Bobacka, A. Lewenstam and A. Ivaska, *J. Electroanal. Chem.*, 2006, **593**, 219.

**[29]** M. Ocypa, A. Michalska and K. Maksymiuk, *Electrochim. Acta,* 2006, **51**, 2298.

**[30]** H. Zejli, P. Sharrock, H. H. J. L. de Cisneros, I. Naranjo-Rodriguez and K. R. Temsamani, *Talanta,* 2006, **68**, 79.

**[31]** N. H. Kwon, M. A. Rahman, M. S. Won and Y. B. Shim, *Anal. Chem.*, 2006, **78**, 52.

**[32]** Y. M. Uang and T. C. Chou, *Biosens. Bioelectron.,* 2003, **19**, 141.

**[33]** A. Gambhir, M. Gerard, S. K. J. Ain and B. D. Malhotra, *Appl. Biochem. Biotech.*, 2001, **96**, 303.

**[34]** C. A. Traina, R. C. Bakus II and G. C. Bazan, *J. Am. Chem. Soc.,* 2011, **133**, 12600.

**[35]** D. Tuncel and H. V. Demir, *Nanoscale*, 2010, **2**, 484.

**[36]** I. O. Huyal, T. Ozel, D. Tuncel, and H. V. Demir, *Opt. Express*, 2008, **16**, 17.

**[37]** E. Smela, *Advanced Materials*, 2003, **15**, 6.

**[38]** C.T. Adkins, H. Muchalski and E. Harth, *Macromolecules*, 2009, **42**, 5786.

**[39]** B. Baykal, **V. Ibrahimova**, Gizem Er, E. Bengu and D. Tuncel, *Chem. Commun.,* 2010, **46**, 6762.

**[40]** E.J. Park, T. Erdem, **V. Ibrahimova**, S. Nizamoglu, H. V. Demir and D. Tuncel, *ACS Nano*, 2011, **5** (4), 2483.

**[41]** J. Luo, X. Li, Q. Hou, J. Peng, W. Yang and Y. Cao, *Adv. Mater.,* 2007, **19**, 1113.

**[43]** J. H. Park, N. S. Cho, Y. K. Jung, H. J. Cho, H. K. Shim, H. Kim and Y. S. Lee, *Organic Electronics,* 2007, **8**, 272.

**[42]** J. H. Burroughes, D. D. C. Bradley, A. R. Brown, R. N. Marks, K. Mackay, R. H. Friend, P. L. Burns and A. B. Holmes, *Nature*, 1990, **347**, 539.

**[44]** OV Salata, *Journal of Nanobiotechnology*, 2004, **2**, 1.

**[45]** S. Kim, C.K. Lim, J. Na, Y.D. Lee, K. Kim, K. Choi, F.J. Leary and I. C. Kwon, *Chem. Commun*., 2010, **46**, 1617.

**[46]** Z. Jili, H. Zhaorang, S. Qiang, W. Ying and S. Dan, *Front. Chem. China*, 2008, **3**(1), 81.

**[47]** W. Lin, Z. Wenjun, B. O'Donoghue, and T. Weihong, *Bioconjugate Chem.*, 2007, **18**, 297.

**[48]** F. Ye, C. Wu, Y. Jin, Y. H. Chan, X. Zhang and D. T. Chiu, *J. Am. Chem. Soc.* 2011, **133**, 8146.

**[49]** J.H. Moon, P. MacLean, W. McDaniel and F. L. Hancock, *Chem. Commun.,* 2007, **46**, 4910.

**[50]** Y. H. Chan, Y. Jin, C. Wu and D. T. Chiu, *Chem. Commun.,* 2011, **47**, 2820.

**[51]** C. Wu, T. Schneider, M. Zeigler, J. Yu, Pe. G. Schiro, D. R. Burnham, J. D. McNeill and D. T. Chiu, *J. Am. Chem. Soc.*, 2010, **132**, 15410.

**[52]** K. Petkau, A. Kaeser, I. Fischer, L. Brunsveld and A. P. H. J. Schenning, *J. Am. Chem. Soc.* 2011, **133** (42), 17063.

**[53]** P. Howes, M. Green, A. Bowers, D. Parker, G. Varma, M. Kallumadil, M. Hughes, A. Warley, A. Brain and R. Botnar, *J. Am. Chem. Soc.,* 2010, **132**, 9833.

**[54]** P. Howes, M. Green, J. Levitt, K. Suhling and M. Hughes, *J. Am. Chem. Soc.,* 2010, **132**, 3989.

**[55]** C. Wu, Y. Jin, T. Schneider, D. R. Burnham, P. B. Smith and D. T. Chiu, *Angew. Chem. Int. Ed.,* 2010, **49**, 9436.

**[56]** J. Pecher, J. Huber, M. Winterhalder, A. Zumbusch and S. Mecking, *Biomacromolecules,* 2010, **11***,* 2776.

**[57]** N. A. A. Rahim, W. McDaniel, K. Bardon, S. Srinivasan, V. Vickerman, P. T. C. So and J. H. Moon, *Adv. Mater.* 2009, **21**, 1.

**[58]** M. Bernius, M. Inbasekaran, E. Woo, W. Wu and L. Wujkuwski, *J. Mater. Sci.*: *Mater. Electron.*, 2000, **11**, 111.

**[59]** F. Ayaloglu-Butun, E. Terzioglu-Kara, Z. Tokcaer-Keskin and K. C. Akcali, *Stem Cell Rev and Rep*, 2011,  DOI 10.1007/s12015-011-9292-0